Department of Neuroanatomy,
Theoretical Medicine and Biosciences,
Faculty of Medicine
Saarland University, Homburg/Saar
66424, Germany

Isolated rod photoreceptors from mouse retina a useful model system to study ribbon synapses.

A thesis submitted to the Faculty of Medicine in fulfilment of the requirements for the degree of **Doctor of Philosophy (Ph.D.)** at the Saarland University, Germany

May 2015

Submitted by
RASHMI KATIYAR

Supervisor:

Co-supervisor:

Declaration

I hereby declare that the Ph.D. med thesis entitled "**Isolated rod photoreceptors from mouse retina a useful model system to study ribbon synapses**" is a presentation of my original research work. Where other sources of information have been used, they have been acknowledged. No portion of work contained in this thesis has been submitted in support of any application for any other degree or qualification.

Homburg, Germany

29-05-2015

RASHMI KATIYAR

Dedicated to my parent,

husband, sister, brother,

In-laws family

&

Friends

Acknowledgement

It is a pleasure to convey my gratitude to all people who contributed and assisted me in the completion of my doctoral study.

It is with immense gratitude that I acknowledge the encouragement, support and guidance of my supervisor Prof. Dr. Frank Schmitz throughout my thesis work. His valuable advice and scientific discussions have always been of great value for me.

I am thankful to Dr. Karin Schwarz for co-supervising my experiments and translating my summary in German language.

I would like to thank Prof. Dr. Flockerzi for his collaborating project, Dr. Ute Becherer for her help in the initial stage of my Calcium imaging experiment, Dr. Ulf Matti for generating RIBEYE-FP mouse used in my work and Dr. Chad Grabner for his scientific advices.

I would like to express my deepest gratitude to Dr. Andreas Beck for his constant support and valuable advices throughout my imaging experiments.

I also thank Prof. Dr. Jens Rettig, Prof. Dr. Dieter Bruns and all members of synapse club for their critical comments and valuable advice during synapse club seminars.

On professional note, I would like to thank AnneWeinland, Anja Ludes, Daniel Rhode, and Marina Wirth for providing mice for my work.

I am thankful to my colleague and co-authors Dr. Silke Wahl and Mayur Dembla for their friendly behavior.

I am deeply thankful to Dr. Rizwana Anjum for her critical review of my thesis, enduring support and good advices and Shweta Suiwal for her constant support during my thesis writing.

My warm thanks to my former colleagues Dr.Sivaraman Nataranjan & Dr.Jagdeesh Kumar Venkatesan for their help and friendship.

I am also thankful to Sylvia Brundaler for her administrative support. I would sincerely thank to Gabi Kiefer for her excellent technical help for electron microscopy experiments.

I would like to thank Ines Krüger, Gerlinde Kühnreich, Franziska Markwart, Tamara Paul, Jennifer Neumann and Jasmin Messerle for their technical expertise.

I thank to my new colleague Dr. Stephan Maxeiner for exchanging his knowledge with us.

I have been fortunate to come across friends like Ekta Dembla, Sakhi-Jaychandran, Sangita –Saravanan, Anita-Girish, Varsha, Dhanalaxmi and Sawsan Abou Omer without whom life would be bleak as they made my personal life very pleasant in Germany.

I gratefully acknowledge the funding sources that made my Ph.D. work possible. I got financial support from Graduate School (GK1326), LGFG scholarship from Saarland Universty and Sonderforschungsbereichs (SFB 894).

I especially thank my parents, sister, and brother for their great patient and unconditional love. They were always supporting me and encouraging me with their best wishes. I would not have made it this far without them.

I am sincerely thankful to my in-laws for their understanding and support.

Finally, I would like to thank my husband, Jenrthanan Bala Jeganathakurukkal. He is a best gift which I got during my stay in Germany. He has been a good supporter during my work and especially during thesis writing.

I am also grateful to God for his constant blessings and for giving me strength.

Contents

Summary 10

Zusammenfassung 12

1. Introduction 15

1.1. The mammalian eye 15

1.2. Synaptic complexity of retina 16

1.3. Specialized tonically active ribbon synapse with a unique presynaptic structure 22

1.4. Vesicle trafficking at ribbon synapses 26

1.4.1. Exocytosis 27

1.4.2. Endocytosis 28

1.5. Presynaptic Ca2+ dynamics 29

1.5.1. Voltage gated L-type Ca^{2+}-channels 29

1.5.2. Intra-terminal Ca^{2+}-stores 31

1.6. Aim of the study 32

2. Material and Methods 33

2.1. Antibodies used for immunolabeling 33

2.2. Reagents and chemicals 35

2.3. Buffers and Media 37

2.4. Enzymes and Proteins 40

2.5. Laboratory Instruments 41

2.6. Isolation of photoreceptor cells from the mouse retina 41

2.6.1. Coating of coverslips 41

2.6.2. Isolation and dissociation of mouse retina 42

2.6.2.1. Dissociation of retinas using pronase enzyme 42

2.6.2.2. Dissociation of retinas using papain enzyme 43

2.6.2.2.1. Dissociation of adult mice retinas 43

2.6.2.2.2. Dissociation of 16-18 days old mice retina 43

2.6.2.2.3. Dissociation of electroporated retinas 44

2.7. Immnocytochemstistry of isolated retinal cells 44

2.8. Live cells assays of pronase treated retinal cells 45

2.8.1. Loading of lysotracker in rod photoreceptor cells 45

2.8.2. Loading of Dextran in rod photoreceptor cells 45

2.9. Live cell assays of papain treated retinal cells 46

2.9.1. SR101 uptake of isolated rod photoreceptor cells 46

2.9.2. ER tracker uptake of isolated rod photoreceptor cells 46

2.9.3. Endo- and Exo-cytosis assay with FM1-43 47

2.9.3.1. Endocytosis Assay 47

2.9.3.1.1. Endocytosis in isolated retina 47

2.9.3.1.2. Endocytosis in isolated rod photoreceptor cells 47

2.9.3.2. Exocytosis Assay in isolated rod photoreceptor cells 48

2.9.4. Ca+2 imaging of acutely dissociated rod photoreceptor cells 48

2.9.4.1. Fluo4 fluorescence measurement 49

2.9.4.2. Fura-2AM measurement 50

2.10. Electron microscopy of isolated mouse photoreceptor cells 51

3. Results 52

3.1. Dissociation of mouse retina to isolate rod photoreceptor cells 52

3.1.1. Dissociation of mouse retina with pronase 53

3.1.2. Dissociation of mouse retina with papain 53

3.2. Ultrastructure of papain dissociated rod photoreceptors 55

3.3. Characterization of the isolated mouse retinal cells by immunocytochemistry 56

3.3.1. Characterization of isolated rod photoreceptor cells obtained by papain / pronase dissociation by RIBEYE 56

3.3.2. Localization of synaptic proteins in the isolated rod photoreceptor cells obtained by papain/ pronase dissociation 59

3.3.3. Localization of Calcium channels in the isolated rod photoreceptor cells obtained by papain/ pronase dissociation 61

3.3.4. Characterization of tubulin in the papain treated cells 62

3.4. Physiological charaterization of rod photoreceptors 62

3.4.1. Viability assy for pronase dissociated rod photoreceptors 63

3.4.2. Endocytosis of papain dissociated rod photoreceptors 66

3.4.2.1. Sulforhodamine uptake assay 66

3.4.2.2. FM1-43 uptake assay 71

3.4.2.3. Charaterrization of FM1-43 loaded endocytosis vesicles 75

3.4.3. Ca^{2+} imaging in solitary rod photoreceptor of mouse retina 76

3.5. Localisation of Ribeye in dissociated rod photoreceptors of Ribeye-RFP mice 78

3.6. Characterization of Fluo-4AM labeled structure in the synaptic terminals of the Papain dissociated rod photoreceptors 79

3.6.1 Characterization of Fluo-4AM-labeled structure by immunofluorescence with different marker antibodies 80

3.6.2 Confirmation of Fluo-4AM labeled structure as part of ER by using ER tracker dye 83

3.7. Intracellular Ca^{2+} stores and calcium release in the synaptic terminal of the papain dissociated rod photoreceptors from Ribeye-RFP mice 84

3.8. Physiological evidence of more calcium release from internal stores in comparison to the calcium entering through calcium channels in the synaptic terminal of the papain dissociated rod photoreceptors 86

4. Discussion 88

5. References 93

7. Abbreviations 109

8. List of figures 113

9. CurriculumVitae 116

10. Publications 120

SUMMARY

Synapses play a vital role for communication in the nervous system. The neurons are provided with highly focal and fast signalling performances through synaptic transmission. Unlike the conventional synapses, ribbon synapses are specialized continuously active chemical synapses which contain a large electron-dense structure called synaptic ribbon which is anchored at the active zone. The base of the ribbon that is located close to L-type voltage-gated Ca^{2+}-channels is a hotspot of exocytosis. Continuous exocytosis needs to be balanced by compensatory endocytosis. Based on recent studies, the synaptic ribbon complex is also involved in endocytic vesicle retrieval. Both exo- and endocytosis are controlled by changes in presynaptic Ca^{2+}. In photoreceptor a terminal, presynaptic Ca^{2+} is controlled by various mechanisms which include Ca^{2+}-influx through voltage gated calcium channels and Ca^{2+}-induce Ca^{2+}-release from the intracellular calcium source, i.e. the smooth endoplasmic reticulum ER.

To study the synaptic vesicle membrane trafficking and presynaptic calcium dynamics, I established and analyzed isolated mouse rod photoreceptors as a possible model system. For this purpose, immunofluorescence technique, time- lapse microscopy and electron microscopy were used. In the earlier phase of work, conditions to isolate intact and physiologically active solitary rod cells from mouse retina were optimized for animals of different ages and genetically manipulated retinas. I found that photoreceptor cells retained their typical morphology including the integrity of synaptic terminal along with the proper localisation of synaptic protein and calcium channels. Calcium imaging studies with Fura-2AM dye provides evidence that calcium channels of the solitary cells are functional. Endocytic uptake assays were established and successfully applied to analyze the endocytic properties of photoreceptor terminals. A preferential uptake of fluid phase endocytosis marker, sulforhodamine (SR101) and FM1-43 dye was observed in close vicinity to the synaptic ribbon in photoreceptor terminals. In a second part of my studies, by using transgenic RIBEYE-FP mice with fluorescent synaptic ribbon and Ca^{2+}-imaging,

ER-related Ca^{2+}-source localized near the synaptic ribbon of mouse rod photoreceptor terminals has been identified. RIBEYE-FP mice were generated by Ulf Matti in our lab. This intra-terminal calcium source co-localized with antibodies against SERCA2 and co-localized with a marker dye for the endoplasmic reticulum, ER-tracker. Experimental data showed that the Ca^{2+}- signals obtained from this store are considerably bigger than Ca^{2+}-signals via influx of Ca^{2+} through voltage-gated calcium channels (VGCC). With Ca^{2+}-imaging, exo- and endo-cytosis assay, I demonstrated that this ER-related Ca^{2+}-source can be emptied by depolarisation probably via Ca^{2+}-induced Ca^{2+}-released (CICR) and also can be depleted by application of caffeine and thapsigargin.

In conclusion, data from this research work proposed the presence of an ER-related Ca^{2+}-source in the rod ribbon synapse of mouse photoreceptor in close vicinity to the synaptic ribbon. CICR from this Ca^{2+}-source can amplify Ca^{2+}-signals and enhance signal transmission which could be contributing in the tonic release at the rod photoreceptor synapse. Isolated photoreceptor cells obtained by isolation methods in this study can be used as a valuable study tool to understand structural and functional organisation of ribbon synapse.

Zusammenfassung

Synapsen sind für die Kommunikation zwischen Nervenzelen von großer Bedeutung. In chemischen Synapsen erfolgt die synaptische Kommunikation über die Exozytose von Neurotransmitter-enthaltenden synaptischen Vesikeln mit der präsynaptischen Plasmamembran. Ribbon Synapsen sind spezialisierte, kontinuierlich arbeitende chemische Synapsen, die abgestufte Änderungen des Membranpotentials in Modulationen einer kontinuierlichen Vesikelexozytose umsetzen. Um diese dauerhafte Transmitter-freisetzung erfolgreich bewerkstelligen zu können, besitzen die Ribbon Synapsen eine elektron-dichte präsynaptische Spezialisierung, den sogenannten synaptischen Ribbon. Der synaptische Ribbon ist eine plattenartige Struktur, deren unteres Ende an der aktiven Zone der Synapse verankert ist. Durch diese Anordnung befindet sich der Ribbon in unmittelbarer Nähe der spannungsabhängigen L-Typ Kalziumkanäle. Diese Region stellt einen „hot spot“ für die Vesikelexozytose dar. Die kontinuierliche Exozytose von Neurotransmittern muss von einer kompensatorischen Vesikelendozytose begleitet werden, um den Vesikelnachschub zu gewährleisten. Basierend auf neueren Untersuchungen stellt der synaptische Ribbon nicht nur einen Ort für kontinuierlich Exozytose dar, sondern ist viel mehr auch Ort, an dem zahlreiche Endozytoseprozesse ablaufen. Da sowohl Exozytose- als auch Endozytose durch Kalziumionen reguliert werten. ist der Ribbon in unmittelbarer Nähe der L-Typ Kalziumkanäle ideal positioniert, um an den beiden Vorgängen beteiligt zu sein. In den Photorezeptorterminalen wird die intrazelluläre Kalziumkonzentration $[Ca^{2+}]i$ durch verschiedene Mechanismen kontrolliert, unter anderen durch den Einstrom von Kalzium-Ionen durch die spannungsabhängigen L-Typ Kanäle sowie durch die Kalzium-abhängige Freisetzung von Kalzium-Ionen aus intrazellulären Kalziumspeichern wie dem endoplasmatischen Retikulum.

Ziel meiner Arbeit war es, die Dynamik der präsynaptischen Kalziumkonzentration und den Membranverkehr in der Photorezeptorsynapse zu untersuchen. Zu diesem Zweck habe ich Photorezeptoren (Stäbchen) aus der Mausretina isoliert, um ein

Modelsystem für Exozytose- und Endozytoseprozesse sowie die Kalziumdynamik in den Ribbonsynapsen zu etablieren. Die isolierten Stäbchen wurden mit Hilfe von Immunfluoreszenzmarkierungen, Elektronenmikroskopie und intravitale Mikroskopie untersucht. Zu Beginn der Arbeit habe ich zunächst Protokolle etabliert, um einzelne, morphologisch intakte und physiologisch aktive Photorezeptoren zu isolieren. In dieser Phase meiner Arbeit habe ich zunächst die Bedingungen der Isolation von Photorezeptoren aus Netzhäuten von unterschiedlichen Mäusen (verschiedene Alter, verschiedene genetische Hintergründe) optimiert. Es ist mir gelungen, intakte und physiologisch aktive Stäbchen photorezeptoren zu isolieren. In diesen isolierten Zellen war die Verteilung der synaptischen Proteine und auch die Lokalisation der Kalziumkanäle, genauso, wie sie auch im Gewebsverband der Retina beobachtet werden kann. Messung der intrazellulären Kalziumkonzentrationen mit Hilfe des Kalziumsensors Fura-2AM zeigten zudem, dass die Kalziumkanäle nicht nur am richtigen Ort angereichert sind sondern auch funktionell aktiv sind. Mit Hilfe von Endozytose-Assays konnte ich die Endozytoseprozesse der Photorezeptorsynapse analysieren. Diese Untersuchungen zeigten, dass Flüssigphase-endozytose Marker wie Sulphorhodamin (SR101) und FM1-43 bevorzugt in unmittelbarer Nähe des synaptischen Ribbons aufgenommen werden. Im zweiten Teil meiner Arbeit machte ich mir die genetische Manipulation von RIBEYE-FP-Mäusen zunutze. Diese transgenen Mäuse wurden in unserem Labor von Ulf Matti generiert und exprimieren ein fluoreszenzmarkiertes RIBEYE-Protein. Als Konsequenz dieser genetischen Manipulation besitzen die RIBEYE-FP-Mäuse fluoreszierende synaptische Ribbons. Ich habe Photorezeptoren aus den Netzhäuten dieser Mäuse isoliert und Kalzium-Messungen durchgeführt. Es ist mir gelungen in den Synapsen der isolierten Photorezeptoren einen intraterminalen Kalziumspeicher zu identifizieren, der sich in enger Nachbarschaft zuden synaptischen Ribbons befindet. Weitere Untersuchungen haben ergeben, dass es sich bei diesem Speicher um das endoplasmatische Retikulum bzw. ein dem endoplasmatischen Retikulum ähnlichem Kompartiment handelt. Immunfluoreszenzuntersuchen zeigten sowohl eine Kolokalisation des Kalziumsignals mit dem ER-Marker-Protein SERCA2 aus auch mit dem Farbstoff ER- Tracker,

welcher spezifisch vom endoplasmatischen Retikulum aufgenommen wird. In meinen Untersuchungen konnte ich zeigen, dass die Kalziumsignale aus diesem ER ähnlichem-Speicher deutlich größer ausfielen, als die jenigen, die durch den Einstrom von Kalzium-Ionen durch die spannungsabhängigen L-Typ Kalziumkanäle erzeugt wurden. Mit Hilfe von Kalzium-Messungen, Exo- und Endozytose-Assays konnte ich zeigen, dass das Kalzium aus dem ER ähnlichem-Speicher durch Depolarisation der Synapse in die Terminale frigestzt werden kann. Diese geschieht vermutlich durch Kalzium-abhängige Kalzium Freisetzung (Ca^{2+}-induced Ca^{2+}-released (CICR)). Auch eine Behandlung der Synapse mit Koffein und Thapsigargin sind in der Lage, den intraterminalen Kalziumspeicher zur Freisetzung von Kalzium zu bewegen.

Zusammenfassend weisen die Ergebnisse meiner Untersuchungen auf die Existenz eines ER ähnlichen Kalziumspeichers in der Synapse der Stäbchen Photorezptoren hin. Kalzium-abhängige Kalzium Freisetzung aus diesem Kalziumspeicher kann die Kalziumsignale in der Stäbchen-Synapse verstärken und verlängern und könnte auf diese Weise zur kontinuierliche Trasnmitterausschüttung beitragen. Isolierte Photorezeptoren, die nach dem in dieser Arbeit beschriebenem Protokoll isoliert werden, könnten als Modellsystem verwendet werden, um die strukturelle und funktionelle Organisation von Ribbonsynapse

CHAPTER 1

INTRODUCTION

Sense of sight is the most beautiful gift for humans. Vision, a highly complex process, allows us to observe and learn more about the surrounding world then we does with any of the other four senses. It involves several steps of parallel information processing in various areas of the central nervous system. The eye, sensory organ important for vision, can detect a single photon and transmits its signal to higher brain centres. The signals conveyed from retina of the eye are anticipated by brain to build a precise image of the external environment. The retina in the eye offers an excellent source of material for detailed anatomical, physiological and pharmacological analyses of the neural mechanisms underlying basic information processing by the vertebrate brain.

1.1. The mammalian eye

Eye is the vital organ for vision. It receives the light and forms an image on the light-sensitive layer of tissue, retina, lining the inner surface of the eye. Both dim and bright light can be detected by eye. The eye is a fluid-filled sphere enclosed by three layers of tissues or tunicae (Fig.1). The outer fibrous layer consists of sclera and the transparent light-permeant cornea. The middle vascularised tissue layer includes the iris, ciliary body and the choroid.

The neurons of the retina in the eye present in the innermost photosensitive layer are transmitting visual signals to higher brain centre via the optic nerve (Purves et al., 2001). The eye is derived from three types of embryonic tissue: the neural tube (neuroectoderm), from which the proper retina and its associated pigment epithelium arise; the mesoderm of the head region, which produces most of the corneoscleral and uveal tunics; and the surface ectoderm, from which the lens develops. The retina and the optic nerve develop as an out growth of the brain; therefore, it is a part of central nervous system (Purves *et al*., 2001).

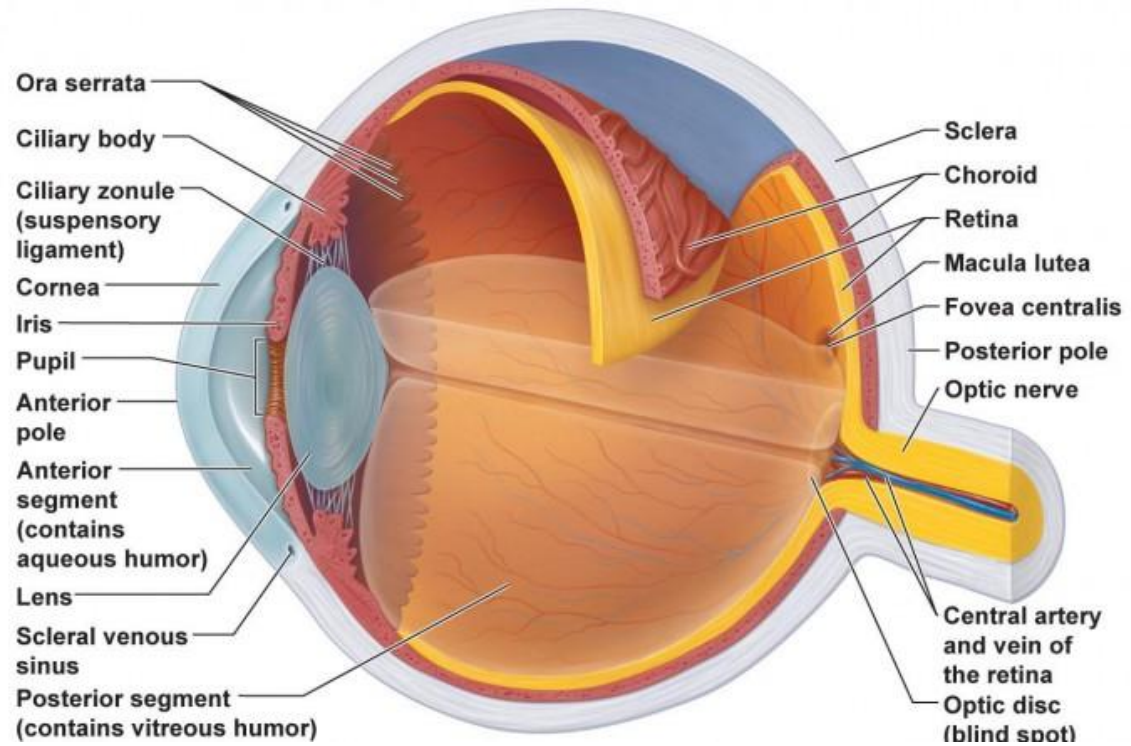

Figure 1. Diagrammatic view of the adult human eye: ©2011 Pearson Education, Inc.

1.2. Synaptic complexity of retina

Retina is a highly organised structure. Similar to the other structures of central nervous system, a large number of higher sensory neurons are present in the retina and make a complex network (Masland, 2001). These neurons are processing wide variety of visual signals side by side by in the retina (Wässle *et al*., 2004). The mature mammalian retina consists of two distinct parts, i.e. neural retina and the single layered retinal pigment epithelium. The outermost layer of retina, retinal pigment epithelium (RPE), is composed of a single layer of hexagonal cells that are densely packed with pigment granules and is situated just internal to the Bruch's membrane. This layer has a close anatomical and functional relation with the retina. It plays a central role in retinal physiology by forming the outer blood-retinal barrier and controls the transportation of ions and metabolites. The RPE cells are indispensible for the maintenance of neural retina as they participate in visual pigment regeneration, phagocytosis and digestion of photoreceptor wastes and maintenance of retinal adhesion.

The neural retina is a highly organized structure and is composed of ten clearly defined cellular layers which contain five main types of neurons: photoreceptors, bipolar cells, horizontal cells, ganglion and amacrine cells. (Figure. 2A, B).

The photoreceptor cells in the vertebrates are specialized and highly photosensitive neurons that are responsible for the transduction of light into an electrical signal. The initial step of vision is initiated when the photoreceptors transmit the electrical signal to other neurons in the retina (Kwok *et al*., 2008). There are two types of photoreceptor cells: rods and cones. Both are contributing information used by the visual system to form a representative of the visual world, sight. The rods are extremely sensitive and responsible for scoptopic or nocturnal vision. The cones are employed for photopic or diurnal colour vision. Cones require significantly higher light in order to produce a signal and have a higher temporal resolution. Both rod and cone photoreceptors consist of five basic principle subcellular regions:

1) outer segment where the process of phototransduction takes place. It filled with an organised stack of more than 1000 discs which contains the visual pigment molecules rhodopsins in higher concentration (Liang et al., 2003; Nickell et al., 2007). The outer segment is connected to the inner segment by a thin cilium. This thin cilium allows for the passage of proteins and other molecules between the inner segment and outer segment of the photoreceptor cells. In rods discs are surrounded by a separate plasma membrane unlike the cones (Kwok *et al*., 2008).

2) an inner segment is packed with cell organelles which are involved in metabolic activities such as mitochondria, ribosomes and membranes where opsin molecules are assembled and passed to be part of the outer segment discs.

3) a cell body or soma which contains the nucleus of the cell.

4) a synaptic region/terminal contains synaptic vesicles and a specialized electron dense structure, ribbon. In synaptic region neurotransmission to second order neurons occur.

Outer and inner segments of rod are generally thinner than of cones in mammalian retina. The photoreceptor membrane protein opsin contains a pigment molecules called retinal. In rod cells these are called as rhodopsin whereas in cone cells there are

different types of opsins that combine with retinal to form pigments called photopsins. Three different classes of photopsins in the cones react to different ranges of light frequency that allows the visual systems to calculate colour. In outer segment a continuous process of regeneration in which addition of new disc membranes occurs at the base and aged discs are shed from the distal end. The shedded discs are phagocytosed by the neighbouring retinal pigment epithelial cells (Young *et al*., 1967; Young *et al*., 1969). The whole process enables the outer segment to be completely renewed over a period of 10 days (Kwok *et al*., 2008) in rod cells, photoactivation of rhodopsin results in the activation of G-protein(transducin)-mediated visual cascade. This results in activation of phosphodiesterase 6 which in turn causes hydrolysis of cGMP and closure of cGMP-gated channels in the plasma membranes, and hyper-polarisation of the cell (Hamer et al., 2005; Kiel et al., 2011). This phototranduction is followed by a series of reactions which involves inactivation of rhodopsin and other protein components of visual cascade, resynthesize of cGMP, and regeneration of rhodopsin from 11-cis-retinal and opsin. After following all these reaction, the rod cells go back to its dark state. The outer segments of cone photoreceptors have almost similar photo excitation and recovery process. However, participating proteins are encoded by different but genes in the cone outer segment (Kwok *et al*., 2008). Photoreceptor outer segments also contain protein that function in other essential cellular processes.

The synaptic region of photoreceptor connects with the dendrites of the bipolar and horizontal cells in the outer plexiform layer and transmits the signals. The bipolar cells make their synaptic contacts with amacrine and ganglion cells in inner segments to transmit signals (tom Dieck et al., 2006). For the initiation of transmitter release, both types of photoreceptor utilize a specialized synaptic apparatus, the ribbon synapse, and voltage dependent L-type calcium channels (Heidelberger et al., 2005).

A chain of three-neuron is involved in the processing of information flow through the retina. Light must travel through the entire layers of the retina before striking and activating the photoreceptors. Photoreceptors detect the light at the outer segments in a process called phototransduction and transforms into a neuronal signal

transmitted to 2nd order neurons know as bipolar cells. Bipolar cells transmit the visual signals from the outer plexiform layer to the inner plexiform layer, where the signal is passed to the dendrites of the 3rd layer of neuron called ganglion cells. Axons of ganglion cells run in the fiber layer of the retina and collect at the optic disk to form the optic nerve. The optic nerve carries all visual information from the eye to the visual fields of the occipital lobe in brain where the signals are translated into what we perceive as light.

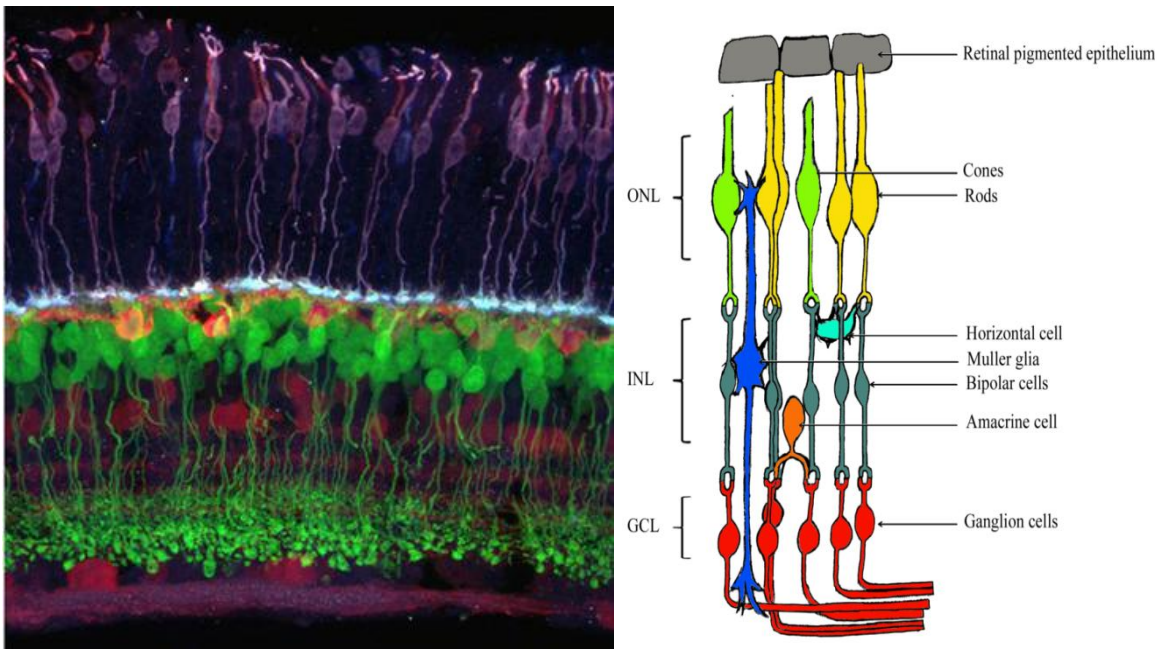

Figure 2. (left) Cross-section through an immunolabeled mature mouse transgenic retina showing lamination of cell bodies and synaptic terminals. This cross-section from a transgenic mouse retina in which ON bipolar cells express GFP (green) under the mGLuR6 promotor. Photoreceptors (purple) immunolabed with anti-cone arrestin, amacrine and ganglion cells immunostained for calbindin (red). (Morgans and Wong et al., Nat.Neuroscience, 2006). **(right) Schematic representation of main retinal neurons.** Abbreviations : ONL, outer plexiform layer; INL, inner nuclear layer; GCL, ganglion cell layer. (Belecky-Adams et al., 2013)

In the inner nuclear layer of the retina the cell bodies of interneurons of amacrine cells and horizontal cells are present and the processes of amacrine cells are projected into the inner plexiform layer (Vigh *et al*., 2000). In the mammalian retina, amacrine cells are important relay stations for rod- mediated signals. They receive synaptic signals from depolarizing and hyperpolarizing bipolar cells and also receive input signals from other amacrine cells (Pang *et al*., 2007). The interaction between

horizontal cells and photoreceptor terminals, known as “lateral elements”, is post-synaptic to photoreceptor terminals (Hirano *et al*., 2011). These lateral interactions between receptors, horizontal cells and bipolar cells in the outer plexiform layer play a vital role in the visual system's sensitivity to luminance contrast over a broad range of light intensities. The neuronal circuits between photoreceptors, ganglionic cells and optic nerve play an organised functional role in neural processing that a message is transmitted to brain along the optic nerve.

The architectural supports for the retina are provided by the inner and outer limiting membranes which are formed by the principal glial cells of the retina called the Müller cells. The cells bodies of müller cells are located in the inner nuclear layer and they project irregularly thick and thin processes in either direction to the outer limiting membrane and inner limiting membrane. The inner limiting membrane is formed by the conical end feet of the Müller cells and a basal lamina/membrane. The junctions forming the outer limiting membrane are between the Müller cells and other Müller cells and photoreceptor cells as zona adherens.

The cell bodies of rods and cone photoreceptors are present in the outer nuclear layer contains. These cell bodies are grouped parallel to each other and spread their light sensitive processes, the outer segments, in the direction of the retinal pigment epithelium.

The first synaptic layer in the retina is outer plexiform layer which interconnects the dendrites of horizontal and bipolar cells with the terminals of photoreceptors forming the first level of intra-retinal information processing.

The inner nuclear layer contains the cell bodies of bipolar, amacrine and horizontal cells for the processing of signals. The neuronal cell bodies of supporting Müller glial cells are also located in INL.

The inner plexiform layer contains the dendrites of the ganglion cells, amacrine cells and the axon terminals of bipolar cells and forms a dense plexus. The bipolar cell, being the second order retinal neuron, occupies a pivotal position in the retina as a major neuron that bridges the gap between the two synaptic layers of retina. Their dendrites reside in the outer plexiform layer and the synaptic terminals are in the inner

plexiform layer. The major task of the bipolar cells is to transmit spatially and temporally filtered signals from the OPL to five anatomically defined strata present in the second synaptic layer (IPL) of the retina (Ghosh *et al*., 2004). Like photoreceptors ribbon the bipolar cells also form synapses. Bipolar cells which are connected to rod and cone photoreceptor are known as rod and cone bipolar cells respectively. There are two basic types of bipolar cells (Dowling et al., 1969): ON bipolar cells and OFF Bipolar cells and the two types can be distinguished both their functions and morphology. Bipolar cells generate ON and OFF light signals based on the differential action of glutamate released from photoreceptors. From the anatomical studies, it is found out that mouse, cat, rat, rabbit and primate retina have almost 10 different types of cone bipolar cell and one type of rod bipolar cells (Haverkamp *et al*., 2008**).** A typical mammalian retina is known to have 9-10 different types of cone driven bipolar cells (Masland, 2001). The bipolar cells respond to light stimulus by relatively slow changes of membrane potential and these responses are unusual in being non-spiking (Heidelberger *et al*., 2005). The bipolar cells transmit the signals of photoreceptors from the outer retinal layers. These signals are modulated by synaptic interactions with amacrine and ganglion cells and finally transferred to the ganglion cells.

The ganglion cell layer (GCL) contains the ganglion cell bodies and it transmits the visual information via optic nerve to the lateral geniculate ganglion in the brain. Almost 10-15 different ganglion cells receive the signals from the bipolar cells (Masland, 2001).

The nerve fibre layer contains axons of the ganglion cells and they receive their myelin sheaths after exit from the eyeball. The fibre density is lowest in the fovea. The optic nerve connects all axons of ganglion cells and this bundle of more than a million fibres (in humans) then passes information to the next relay station in the brain for sorting and integrating into additional information processing channels.

In the retina various synaptic contacts are involved in the transmissions of signals between two neurons. These various synaptic contacts are basal junctions, gap junctions, conventional synapses and ribbon synapses.

1.3. Specialized ribbon synapse and unique presynaptic organelles, the synaptic ribbons

Conventional synapse in the retinal resembles chemical synapse of vertebrate nervous system (Pappas et al., 1972). Unlike most neuronal synapses, hair cells, photoreceptor and bipolar cells are able to manage both tonic and graded release of synaptic vesicles at their synapses and their responses are unusual in being non-spiking (Sterling et al., 2005; Moser et al., 2006; Nouvian et al., 2006; Morgans, 2000; Sterling et al., 1998; Schmitz, 2009). For this purpose, terminals of these cells are equipped with large active zones to which a unique electron-dense presynaptic structure, the synaptic ribbons, are attached (tom Dieck et al., 2006; Schmitz, 2009; Matthews et al., 2010; Mercer et al., 2011; Schmitz et al., 2012). The ribbon synapse is versatile and powerful signal-transducing machinery. Ribbon synapses are capable of maintaining rapid exocytosis of synaptic vesicles for a long period of time (Fuchs, 2005; Heidelberger *et al*., 2005; Prescott et al., 2005; Sterling et al., 2005; Nouvian *et al*., 2006; Singer, 2007). It is assumed that the fast release of synaptic vesicle at ribbon synapse could only be achieved by a very rapid transportation of synaptic vesicles to the active zone of ribbon in a manner that resembles a conveyor belt (Sterling et al., 2005; tom Dieck *et al*., 2006). The ribbon has the capacity to accommodate a large reservoir of primed releasable vesicles. A rapidly releasable pool is formed by the vesicles that are in closest contact with the presynaptic plasma membrane at the base of the ribbon. However, the rest of the vesicles tethered to the ribbon make the large slower releasable pool (von Gersdorff *et al*., 1996; Heidelberger *et al*., 2005; Parson et al., 2003). The synaptic ribbon is a large presynaptic sheet -like structure with a lamellar organisation and associated with the active zone (Sterling et al., 1998; Schmitz, 2009). Synaptic ribbons are surrounded and physically in touch with a large amount of synaptic vesicles which are positioned by the ribbon in close proximity to the active zone. In electron micrographs the ribbons appear mostly as bar shaped (Sjöstrand et al, 1953) (Figure 3A). This appearance was also revealed by 3D reconstructions providing the synaptic ribbon with a large surface area. This surface area is around 0.77µM big in mammalian rods (Sterling et al., 2005) (Figure 3A). The

mammalian rod photoreceptor ribbon is approximately 35nm thick and elongated up to 1µM in deep into presynaptic cytoplasm.

The photoreceptor ribbon is not directly connected with the active zone. It is anchored via the arciform density, which is located within a small evagination of the presynaptic plasma membrane, the synaptic ridge. The ridge contains clusters of presynaptic L-type voltage-gated calcium-channels. Due to an overall invagination of the presynaptic plasma membrane, the arciform density has a curved shape. The synaptic ribbon adopts this shape and attains a horseshoe shaped appearance (Figure 4).

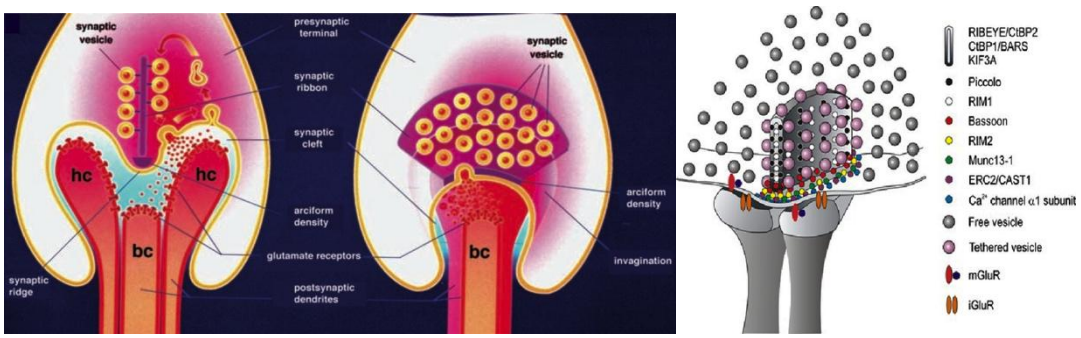

Figure 3. (A) Schematic diagramme of photoreceptor ribbon synapses. *The bar-shaped ribbon (left panel) is actually a cross-section of a plate-like structure that is bended along the invaginated photoreceptor presynaptic plasma membrane in a crescent, horseshoe-shaped manner (right panel). The postsynaptic dendritic profiles of horizontal and bipolar cells are depicted in a simplified manner (Schmitz, 2009).* ***(B) Representation of molecular structure of retinal ribbon synapse.*** *The differential distribution of CAZ proteins defines two presynaptic compartments at the ribbon synapse. The ribbon-associated compartment includes RIBEYE/CtBP2, CtBP1/BARS, KIF3A, Piccolo and RIM1. The active zone compartment includes RIM2, Munc13-1, ERC2/CAST1, and a L-type calcium channel α1 subunit. At the photoreceptor ribbon synapse, Bassoon localizes at the border between the two compartments. Various types of postsynaptic and/or presynaptic metabotropic (mGluR) and ionotropic (iGluR) glutamate receptors mediate the action of glutamate, which is released at the retinal ribbon synapses (tom Dieck et al., 2006).*

Most amazingly, ribbon synapses are equipped with a roughly similar set of synaptic proteins as conventional synapses, although the physiological properties of ribbon synapses are quite distinct (Heidelberger et al., 2005; Thoreson et al., 2007; Zanazzi et al., 2009). Stronger depolarisation at ribbon synapse triggers release of the entire pool of vesicles tethered to the ribbon on a millisecond frame (von Gersdorff *et al*., 1996). Then, the primed vesicles move down the ribbon in a rapid way and reach

the active zone and are readily available for the fusion for exocytosis (Heidelberger *et al*., 2005). The shape of the ribbon and the number of tethered vesicles varies between different types of photoreceptors and bipolar cells in the retina.

The small terminals of the rod photoreceptors usually contain a single large synaptic ribbon, which is several 100nm in height, 1µm in depth and shows a horseshoe shaped structure, which is clearly visible at the light microscopic level. Around 770 synaptic vesicles usually bind to a rod synaptic ribbon (Sterling et al., 2005). 130 of the 770 total vesicles are found in a basal row at the membrane-anchored end of the synaptic ribbon and are considered as ''docked '' vesicles for immediate release. The other remaining synaptic vesicles, the ''tethered '' vesicles, are associated to the ribbon in a more distal row. The terminals of the cone photoreceptors are larger than the rod terminals and contain several ribbons (10-12 ribbons per terminal) with shorter active zones contacted by invaginating postsynaptic elements. By light microscopy, the ribbons in a cone terminal appear like a chain of dots. The individual ribbons are slightly shorter (~ 1µm long; 0.2µm high) as compared them with the one of the rods (~2µm long; 0.4µm high.) The total ribbon surface and the number of ribbon-tethered vesicles are much larger in the cones than in the rods (Sterling et al., 2005; Jackman et al., 2009; Heidelberger et al., 2005).

The terminals of the rod and cone bipolar cells in the IPL contain several small ribbons that are opposed by two non-invaginating postsynaptic processes of amacrine and ganglion cells. Bipolar cell ribbons, like cone photoreceptor ribbons, have a dot-like appearance by light microscopy due to their relative small size (tom Dieck *et al*., 2006). Ribbon synapses of goldfish bipolar cells for example contain 45 to 65 small ribbons. Each of them binds around 110 vesicles from which 22 are docked. In total, they bind approximately 1200 docked vesicles (von Gersdorff, 2001).

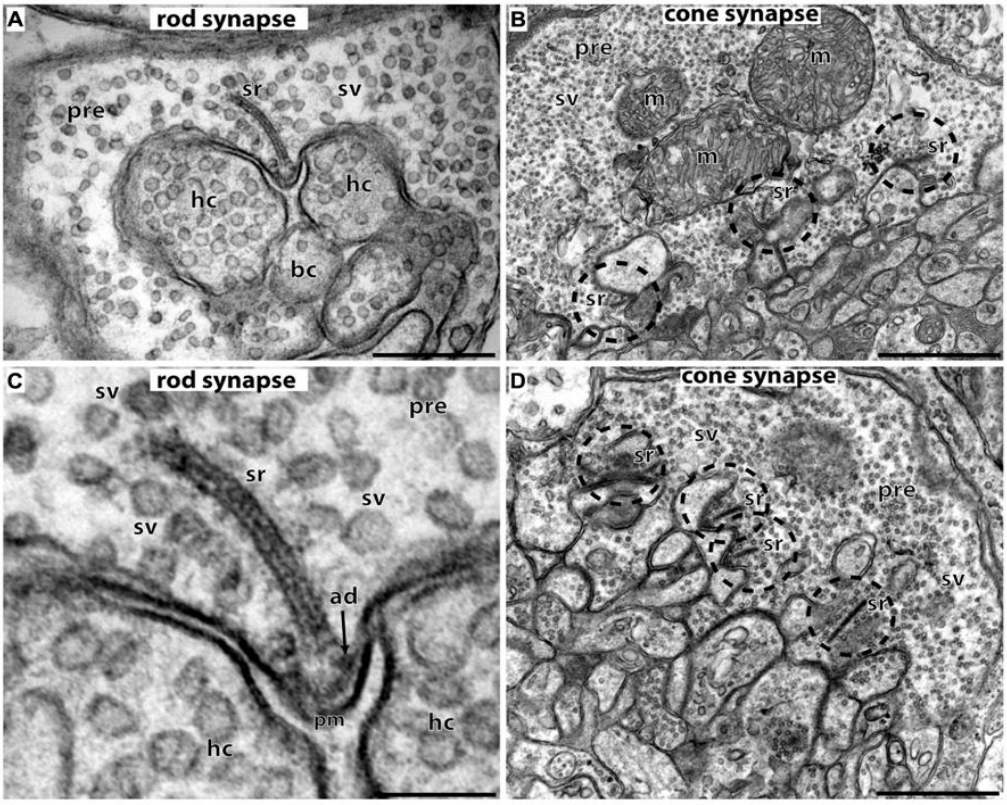

Figure 4. Ultrastucture of photoreceptor ribbon synapses. *In* ***(A, C)*** *rod photoreceptor ribbon synapses are shown by transmission electron microscopy; in* ***(B, D)*** *cone photoreceptor ribbon synapses.* ***(A, B)*** *The large presynaptic terminals are filled with numerous synaptic vesicles (sv). The active zone is characterized by specialized presynaptic densities, the arciform densities (ad). The synaptic ribbon (sr) is anchored to the arciform density. The synaptic ribbon is associated with large numbers of synaptic vesicles. Opposite to the active zones are the dendritic tips of horizontal cells (hc) and bipolar cells (bc) that contain ionotropic and metabotropic glutamate receptors for signaling. The dendritic tips are located within an invagination of the presynaptic terminal. Cone synapses* ***(B, D)*** *are larger in diameter than rod synapses and contain multiple active zones (dashed circles) and multiple synaptic ribbons (sr). sr, synaptic ribbon; sv, synaptic vesicles; ad, arciform density; pre, presynaptic terminal; m, mitochondrium; hc, dendritic tips of horizontal cells; bc, dendritic tips of bipolar cells; pm, presynaptic plasma membrane. Scale bars: 400 nm* ***(A)****, 1 μm* ***(B)****, 150 nm* ***(C)****, 800 nm* ***(D)****. (from Schmitz , 2014)*

RIBEYE is identified as a major component specific for the synaptic ribbons (Schmitz *et al*., 2000; Schmitz *et al*., 2009). In addition to RIBEYE, the photoreceptor ribbons also contain clusters of CtBP1/BARS (tom Dieck *et al*., 2005). RIBEYE consists of an N-terminal A-domain and a C-terminal B-domain. The B-domain is largely identical with the protein CtBP2 and binds NAD (H) (Schmitz *et al*., 2009; Schmitz *et al*., 2012). The A-domain of RIBEYE is not present in D.melanogastor, C.elegans and other lower vertebrates and invertebrates. This is supporting the notion that RIBEYE and retinal synaptic ribbons are an evolutionary innovation of vertebrates (Schmitz *et al*., 2000)

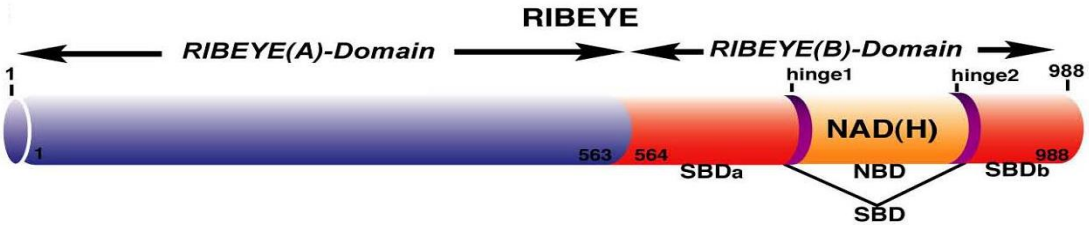

Figure 5. ***Schematic structure of RIBEYE***. RIBEYE contains of a large amino-terminal A-domain and a carboxyterminal B-domain. The B-domain of RIBEYE contains the NADH-binding subdomain (NBD, depicted in yellow) and the substrate-binding subdomain (SBD, denoted in red).

1.4. Vesicle trafficking at ribbon synapse

Presynaptic terminals release neurotransmitter due to action potential which is initiating the synaptic transmission. Opening of calcium channels is induced by the action potential which results in the calcium transient stimulate synaptic vesicle exocytosis. After exocytosis, synaptic vesicles undergo endocytosis, recycling and refilling of neurotransmitter for new round of exocytosis. Photoreceptor terminals contain the glutamate neurotransmitter which is packed into the vesicle by the vesicular glutamate transporter type I (Sherry et al., 2003b; Johnson et al., 2003a). Burger et al., 1989 estimated the concentration of glutamate in the vesicle to be order of 100mM. Synaptic vesicle membrane is derived from the surface membrane by endocytosis (Royle et al., 2003) but is modified by the addition of many proteins implicated in vesicle docking, priming and fusion. Estimated cytoplasmic concentration of vesicles in cone terminal of lizard and turtle retinas (~ 6µm diameter) is approximately 250,000 vesicles (Pierantoni et al., Rea et al.,2004) and assumed similar cytoplasmic concentration of vesicles in mammalian rod (2-3µm diameter) is 8000-27,000 vesicles within the terminal cytoplasm (Heidelberger et al., 2005). It was suggested that synaptic ribbons are important for continuous fusion of synaptic vesicles and for sustained release by providing a large pool of primed release-ready vesicles (von Gersdorff 2001; Sterling et al., 2005; Heidelberger et al., 2005). This suggestion is supported by morphological and electrophysiological data. In various types of ribbon synapses, the total pool of synaptic vesicles associated with the ribbon

matches the size of the pool of the releasable synaptic vesicles. Based on anatomical and physiological data, it has been implicated that at least three vesicle pools exist in ribbon -synapse bearing terminals. These three vesicle pools are cytoplasmic, ribbon related and docked. Based on freeze-fracture and transmission EM pictures, it is estimated that 100-130 docking sites /ribbon in mammalian photoreceptors (Raviola et al., 1975; Rao-Mirotznik et al., 1995). Sterling et al. (2005) have estimated that only lowest row of 20-25 vesicles at the base of the synaptic ribbon is docked in contact with the plasma membrane.

1.4.1. Exocytosis

Imaging data of FM-labelled vesicles confirms that ribbon-associated vesicles undergo exocytosis (LoGiudice et al., 2008). In photoreceptor terminal exocytosis observed at ribbon containing and non -ribbon containing site (Zenisek et al., 2000; Midorikawa et al., 2007; Zenisek, 2008). Weak depolarization causes mild stimulus which results in exocytosis at ribbon sites (Chen et al., 2013) whereas strong stimulation due to longer depolarization results exocytosis at non-ribbon-containing sites (Midorikawa et al., 2007; Zenisek, 2008; Chen et al., 2013) which could contribute to the asynchronous release component (Midorikawa et al., 2007; Zenisek, 2008). These non-ribbon sites are estimated at some distance from the presynaptic Ca^{2+}-channels. At the base of the synaptic ribbon a large number of synaptic vesicles can be fused (Matthews et al., 2010; Mercer et al., 2011; Schmitz et al., 2012) which support coordinated multivesicular vesicle fusion at the synaptic ribbon (Glowatzki et al., 2002; Singer et al., 2004; Khimich et al., 2005). Readlily releasable pool (RRP) is a basal row of synaptic vesicles attached to the synaptic ribbon which can be released immediately in response of stimulus. Based on conveyor belt hypothesis of synaptic ribbon-tethered vesicles could possibly move to the base of the synaptic ribbon prior to the final fuse at the active zone (Lenzi et al., 2001; Parsons et al.,2003). Tethered vesicles are the synaptic vesicles which are attached to the synaptic ribbon in a more distance position and contributes to the slowly releasable pool (SRP) as a result of slow kinetics.

1.4.2. Endocytosis

After exocytosis, endocytosis is important to avoid synaptic depression (Schweizer et al., 2006; Wu et al., 2007; Smith et al., 2008). In ribbon terminals membrane retrieval is a challenging process because of the large membrane turnover (Heidelberger et al., 2005). In photoreceptors endocytotic structure appear at the plasma membrane which are mostly lateral to active zones (Gray et al., 1971). Recent studies proposed the role of synaptic ribbon in replenishment of synaptic vesicles (Jackman et al., 2009; Snellman et al., 2011; Chen et al., 2013). Uptake of endocytosis markers in ribbon synapses showed several modes of endocytosis like convention synapses have been proposed. These include retrieval of coated synaptic vesicles (Heuser et al., 1973), uncoated synaptic vesicles (Ceccarelli et al., 1973) and large uncoated synaptic invaginations (Fried et al., 1978). In retinal photoreceptors because of high vesicular turnover in the dark both coated and uncoated vesicles were labeled with HRP (Townes-Anderson et al., 1985; Cooper et al., 1983; Schacher et al., 1976) and FM (Rea et al., 2004). In retinal bipolar cells, two modes of endocytosis with different kinetics are known from electrophysiological analyses (Smith et al., 2008): one fast retrieval mechanism (with a time constant of τ ~1-2 seconds) and a slow mode (τ ~10-30 seconds) (Wu et al., 2007; Smith and others 2008). Presynaptic Ca^{2+} influx could provide a link between exocytosis and subsequent fast, endocytotic membrane retrieval (Wu et al., 2007). It is the predominant mode of operation in retinal bipolar cells after modest stimulation (LoGiudice et al., 2007). Fast membrane retrieval in ribbon synapses differs from the fast mode of endocytosis in conventional synapses (Paillart et al., 2003; Wu et al., 2007; LoGiudice et al., 2007; Smith et al., 2008). In retinal ribbon synapses, there is no evidence that a “kiss-and run” mechanism operates for fast retrieval (LoGiudice et al., 2007). The molecular mechanisms for fast retrieval are unclear. Slow endocytosis proceeds in a clathrin- and dynamin-dependent but Ca^{2+}-independent manner, particularly after strong stimulation of the presynaptic terminal (Jokusch et al., 2005). Recentaly, Pelasse et al., (2014) demonstrated that the synaptic vesicles are primed for fast mode of endocytosis which is clathrin dependent at the ribbon synapses. Numerous small vesicles detached from the large endocytosed

endosomes and reenter into the synaptic vesicle cycle (Paillart et al., 2003). Bulk endocytosis does not appear to occur in photoreceptor synapses (Rea et al., 2004).

1.5. Presynaptic calcium dynamics

Ca^{2+} is a common second messenger (Campbell, 1983; Carafoli et al., 1999). It functions as a critical and ubiquitous second messenger by regulating a variety of key intracellular processes (Berridge et al., 2000). In excitable cells, Ca^{2+} is a necessary player in multiple processes such as release of neurotransmitter in neurosecretory (Penner et al., 1988; Tse et al., 1997) central neurons (Kuba, 1994) and sensory receptors (Thoresons, 2007). The synaptic vesicle exocytosis at ribbon synapses is highly dependent on changes in membrane potential and influx of Ca^{2+} through voltage-gated calcium channels (VGCC). Ca^{2+} signals generated by influx through VGCC are modulated by various intracellular mechanisms that can subsequently increase or decrease cytosolic Ca^{2+}-concentration. The Ca^{2+}-sensitivity of release is high and exocytosis is triggered by low, submicromolar Ca^{2+}-concentrations (Rieke et al., 1996; Thoreson et al., 2004; Heidelberger et al., 2005; Sheng et al., 2007; Choi et al., 2008). Intraterminal Ca^{2+}- levels regulate synaptic release and somatic calcium levels regulate gene expression and other cell functions (Clapham, 2007). Proper maintenance of intracellular calcium level in the photoreceptors is vital for viability of the cell and to avoid excitotoxic damage to downstream neurons that can be produced by excessive glutamate release (Crosson et al., 1990; Edward et al., 1991; Fox et al., 2003; Sharma et al., 2004; Doonan et al., 2005; Hemara-Wahanui et al., 2005).

1.5.1. Voltage gated L-type Ca^{2+} channels

Synaptic vesicle exocytosis in rod and cone photoreceptor synapses is triggered via Ca^{2+}-influx through L-type voltage-gated calcium channels (LTCCs) at the active zones (Morgans et al., 2005; Striessnig et al., 2010; Catterall, 2011). Unlike conventional synapses which depend on N- and P-type calcium channels (Dunlap et al., 1995), photoreceptors and other ribbon synapses utilize dihydropyridine -sensitive, L-type calcium channels to fluctuate synaptic release in response to change in

membrane potential (Corey et al., 1984; Wilkinson et al., 1996; Thoreson et al., 1997; Schmitz et al., 1997; Juusola et al., 1996). Few voltage-gated L-type calcium channels are localized at the base of the synaptic ribbon (tom Dieck et al., 2005; Heidelberger et al., 2005; Doering et al., 2007; Striessnig et al., 2010; Mercer et al., 2011a; Schmitz et al., 2012) which are sufficient to drive exocytosis (Brandt et al., 2005; Bartoletti et al., 2011). TIRF-microscopic data reveals that the localization site of the L-type channels, synaptic ribbon, is a hot spot of exocytosis (Zenisek et al., 2000) and photodamaged synaptic ribbons analyses showed strongly depressed release (Snellman et al.,2011). The main calcium channels present in photoreceptors are consists of a pore-forming transmembrane α1 subunit (Cav1.4), an auxiliary β2-subunit and the α2δ4-subunit (Ball et al., 2002; Catterall et al., 2005; Morgans et al., 2005vigh; Wycisk et al., 2006; Buraei et al., 2010;Striessnig et al., 2010; Catterall, 2011; Mercer et al., 2011a; Schmitz et al., 2012; Liu et al., 2013). Mutation in Cav1.4 causes variour forms of incomplete congenital stationary night blindness (Bech-Hansen et al., 1998; Hoda et al., 2005, 2006; Hemara-Wahanui et al., 2005). L-type VGCC channels do not show Ca^{2+}-dependent inactivation and little voltage-dependent inactivation in photoreceptors (Singh et al., 2006; Striessnig et al., 2010;Catterall, 2011; Shaltiel et al., 2012) therefore these channels are perfectly suitable to support tonical exocytosis at ribbon synapses. It has been studied that normal physiological activity of the Cav-channel is desirable to convert immature ribbons into mature ribbons (Liu et al., 2013). Several studies demonstrated that Cav-channels are important for the proper development of the synaptic ribbon complex. Knockout models of various proteins which are linked to the Cav 1.4 channels such as β2-subunit of Cav1.4 channels, CaBP4, bassons and laminin β2 displayed absenct, smaller or detached synaptic ribbons (Libby et al., 1999; Ball et al., 2002; Dick et al., 2003; Haeseleer et al., 2004; Nishimune et al., 2004; Nishimune 2012). Zabouri and Haverkamp (2013) have showed that Cav-channels are also necessary for the development of the presynaptic cytoskeleton in photoreceptors.

1.5.2. Internal Calcium stores

The synaptic terminal of photoreceptor and hair cells have voltage -operated Ca^{2+} entry and also release Ca^{2+} from Ca^{2+}–stores which play significant role in Ca^{2+} homeostasis and synaptic signalling (Babai et al., 2010; Cadetti et al., 2006; Lelli et al., 2003; Surynarayanan et al., 2006). Both excessively high intracellular calcium levels (Chang et al., 1993; Doonan et al., 2005; Hara et al., 2007) an excessively low intracellular calcium levels (Woodruff et al., 2003) can cause photoreceptor denegation. Endoplasmic reticulum (ER) is primary intracellular Ca^{2+} storage and release organelle which seems to be the responsible for CICR (Verkhratsky, 2005) and subsequent Ca^{2+} influx through plasma membrane store-opetared channels (SOC channels) in presynaptic terminals (Parekh et al., 2005). The store-operated calcium entry (SOCE) mechanisms can refill the exhausted intracellular Ca^{2+}-stores (Parekh et al., 2005; Lewis, 2011; Gudlur et al., 2013; Soboloff et al., 2012). CICR-mediated amplification of $[Ca^{2+}]_i$ in rods is predominantly prominent with maintained depolarisation and enhance synaptic release in dark (Surynarayanan et al., 2006; Cadetti et al., 2006).Ultra-structural and immunolabeling studies indicate the presence of smooth endoplasmic reticulum in the inner segments and synaptic terminals (Mercurio et al., 1982) that can accumulate Ca^{2+} (Ungar et al.; 1981) in amphibian and mammalian rod photoreceptors (Babai et al., 2010; Shoshan-Barmatz et al., 2005). Electron micrographic studies revealed the presence of ER within ~600nm of the synaptic ribbon in mouse retina (Babai et al., 2010). It has been studied that the Ca^{2+} influx through L-type Ca^{2+} channels can trigger release of Ca^{2+} from intracellular stores to increase synaptic exocytosis in amphibian (Krizaj et al., 1999; Surynarayanan et al., 2006; Cadetti et al., 2006) and mouse rods (Babai et al., 2010). CICR is mediated by the activation of ryanodine receptors (RyR) and IP3 receptors (IP3R) which are located on ER of (Peng et al., 1991; Krizaj et al., 1999; Krizaj, 2003, 2004). Krizaj et al. (2003) demonstrated that the contribution of the ER to kinetics of photoreceptor $[Ca^{2+}]_i$ responses is more prominent in rods than in cones. Synaptic kinetics differences in rod and cone because of ER contribution reflecting the cell type-specific distribution patterns of cisternae of ER (Mercurio et al., 1982) and also

depend on expression of SERCA2 transporters, ryanodine and InsP3 receptors (Krizaj et al., 2004).

1.6. Aim of the study

Ribbon synapses are specialized tonically active synapses involved in the transfer of visual signals in the retina. They are coordinating multi-vesicular release and incomparable sensitivity over a wide dynamic range of signaling. To study vesicles trafficking and calcium signaling at ribbon synapse most of the studies have done in retinal slices, isolated photoreceptor cells and in dissociated bipolar cells of species like salamander and goldfish. In current study, I have focused on ribbon synapse of isolated rod photoreceptor mouse.

The main aim of working with isolated mouse photoreceptor cells instead of retinal slice is provide a clear and convincing data which are not based from feedback responses of secondary neurons (e.g. horizontal cells). In retinal slices, feedback responses of secondary neurons (horizontal cells) could influence signaling at photoreceptor synapses in a way which could be difficult to control. Moreover, in comparison to other species, mouse provides a good genetic model and is genetically close to humans. The results of these studies could also provide a good model system to analyze various retinal diseases in human

Aim 1: Establishment and optimization of the methods to get intact and physiologically active mouse rod photoreceptor cells.

Aim 2: Establishment and optimization of the assays to study calcium signaling and synaptic vesicle trafficking associated with ribbon and at non-ribbon sites in mouse isolated rod photoreceptors.

Aim 3: Identification and characterization of presynaptic calcium internal store in isolated mouse rod photoreceptors.

CHAPTER 2

MATERIALS AND METHODS

2.1. Antibodies used for immunolabeling:

Primary Antibody	**Source**	**Dilution used**	**Secondary Antibody**	**Dilution used**
U2656 (Schmitz *et al*.,2000)	Rabbit polyclonal	1:500	Goat anti-rabbit GAR Cy3 (Invitrogen) Cat. No: A10520 & Alexa Fluor 568 donkey anti- rabbit IgG(Invitrogen) Cat. No: A10042 & Alexa Fluor 568 Donkey anti- rabbit IgG(Invitrogen) Cat. No: A-31573	1:1000
RIBEYE/CtBP2 (BDTransduction Laboratories) Cat.No: 612044	Mouse monoclonal	1:250	Goat anti-mouse Cy3 (Jackson Immuno Research) Cat. No:115-096- 146 & Donkey anti- mouse Alexa Fluor 568 IgG(Invitrogen) Cat. No: A10037 &	1:1000

			Alexa Fluor 647 Donkey anti-mouse IgG(Invitrogen) Cat. No: A-31571	
V216 Synaptotagmin1	Gift of Dr. Thomas C. Sudhof	1:250	Goat anti-rabbit GAR Cy2 (Invitrogen) Cat. No: A11034 & Goat anti-rabbit GAR Cy3 (Invitrogen) Cat. No: A10520	1:1000
Anti-β tubulin (ICN)	Mouse monoclonal	1:250	Donkey anti-mouse Alexa Fluor 568 IgG(Invitrogen) Cat. No: A10042	1:1000
Anti-Synaptophysin (Sigma) Cat. No: S5768	Mouse monoclonal	1:250	Chicken anti-mouse Alexa 488 (Jackson Immuno Research) Cat. No: 115-096-146	1:1000
Anti-Dynamin, Hudy1 (Millipore) Cat. No#05-319	Mouse monoclonal	1:200	Chicken anti-mouse Alexa 488 (Jackson Immuno Research) Cat. No: 115-096-146	1:1000
Anti-SERCA2, clone IID8 (Millipore) Cat. No# MAB2636	Mouse monoclonal	1:25	Donkey anti-mouse Alexa Fluor 568 IgG(Invitrogen) Cat. No: A10042	1:1000

Anti-Cav1.4 clone 4F14 from Hybridoma cells (lab made)	Mouse monoclonal	1:2	Chicken anti-mouse Alexa 488 (JacksonImmuno Research) Cat. No: 115-096-146	
Anti-EEA1 (abcam) Cat. No: ab2900	Rabbit polyclonal	1:10	Alexa Fluor 568 Donkey anti- rabbit IgG(Invitrogen) Cat. No: A10042	
SV2 from Hybridoma cells (lab made)	Mouse monoclonal	1:2	Chicken anti-mouse Alexa 488 (JacksonImmuno Research) Cat. No: 115-096-146 & Donkey anti-mouse Alexa Fluor 568 IgG(Invitrogen) Cat. No: A10042 Cat. No: A10037 & Alexa Fluor 647 Donkey anti-mouse IgG(Invitrogen) Cat. No: A-31571	

2.2. Reagents and Chemicals:

BSA (bovine serum albumin)	Sigma; A7906-100G
FCS (Fetal calf serum)	PAA; A15-151
Saponin	Sigma; S4521-10G

Triton X-100	Sigma; T9284-500mL
NPG (n-Propylgallate)	Sigma; P-3130
PFA (Paraformaldehyde)	Sigma; 158127-500G
EDAC (N-3-Dimethylaminopropyl)-N´-ethylcarbodiimide hydrochloride)	Sigma; E7750-5G
L-Cystein	Roth; Art-Nr.1693.1
Isoflurane	Bexter; HDG9623
Poly-L-lysine (0.01% solution)	Sigma; P4832-50mL
Gelatin	Sigma; G7041
Thapsigargin	Invitrogen ; T7458
Lysotracker Red DND 99	Molecular Probe, L7528
Caffeine	Sigma; C0750-100G
Fura-2AM	Biotium ; Cat: 50034
ER-Tracker™ Red dye	Molecular Probe; E34250
Fluo-4 AM	Invitrogen; F14217
FM1-43FX (Fixable analog of FM 1-43 membrane strain)	Invitrogen; F35355
Texas Red hydrazide	Invitrogen; T6256
Dextran texas Red® 10,000MW	Molecular probe, D-1863
Ionomycin	Sigma; 13909-1mL
Sodium Chloride	Sigma; S5886-500G
Magnesium chloride hexahydrate	Sigma; M2670-500G
Magnesium sulphate	Sigma; M2643-500G
Potassium chloride	Sigma; P4591-500G
HEPES	Sigma; H3375-500G
Calcium Chloride	Roth; Art.Nr.-A119.1
Sodium Pyruvate	Sigma; P5280-25G
Glucose	Sigma; G8270-1KG
Dynasore	Abcam; ab 120192

EGTA (Ethylene glycol tetraacteic acid)	Roth; Art.Nr. - 3054.2
Sodium phosphate dibasic	Sigma; S3264-250G
EGF (Epidermal growth factor)	Sigma; E9644
DMEM/ Ham's F12 (1:1)	PAA; E15-813
Glutaraldehyde	Sigma; G5882
Acetone	PROLABO; 20066.321
Embed-812	Science Services 14120
Propylenoxide	University of Saarland
Uranylacetat	University of Saarland
Ethanol	University of Saarland
PBS	Sigma; D8537
DMEM	PAA; E15-843

2.3. Buffers and Media:

Blocking buffer for immuno cyto-chemistry	1% Bovine serum albumin and 0.1% Saponin / 0.2% TritonX100 in PBS (1x)
Permeablization buffer for immuno cyto-chemistry	0.1% Saponin /0.2% TritonX100 in PBS (1x)
Epon	26g Epon 8-12 11g DDSA 16g NMA 0.4g DMP30
0.05M Maleate buffer	5.53g Maleine acid /L H_2O pH 5.0
100mM Cacodylate buffer	21.4g Cacodylacid /L H_2O pH 7.4

Stimulating Solution (25mM KCl Sol.)	6.428 g NaCl 1.864 g KCl 0.203 g $MgCl_2.6H_2O$ 0.222 g $CaCl_2$ 2.38 g HEPES 1.100 g Sodium Pyruvate 1.80 g Glucose Make up to 1 litre with dd H_2O pH 7.4 & Osmolarity 305-315Osm/L
100mM KCl Sol.	2.0455 g NaCl 7.4551 g KCl 0.203g MgCl2.6H2O 0.222 g CaCl2 2.38 g HEPES 1.100 g Sodium Pyruvate 1.80 g Glucose Make up to 1 litre with dd H2O pH 7.4 & Osmolarity 305-315Osm/L
High K^+ Solution (50mM KCl Sol.)	4.967 g NaCl 3.728 g KCl 0.203g $MgCl_2.6H_2O$ 0.222 g $CaCl_2$ 2.38 g HEPES 1.100 g Sodium Pyruvate 1.80 g Glucose Make up to 1 litre with dd H_2O pH 7.4 & Osmolarity 305-315Osm/L

"Zero" Calcium Solution	7.714 g NaCl 0.223 g KCl 0.203g $MgCl_2.6H_2O$ 2.38 g HEPES 1.100 g Sodium Pyruvate 1.80 g Glucose Make up to 1 litre with dd H_2O pH 7.4 & Osmolarity 305-315Osm/L
4mM Calcium Solution	7.714 g NaCl 0.223 g KCl 0.203g MgCl2.6H2O 0.444 g CaCl2 2.38 g HEPES 1.100 g Sodium Pyruvate 1.80 g Glucose Make up to 1 litre with dd H2O pH 7.4 & Osmolarity 305-315Osm/L
Resting Solution (**RS**, 2mM Ca^{2+} sol.)	7.714 g NaCl 0.223 g KCl 0.203g MgCl2.6H2O 0.222 g CaCl2 2.38 g HEPES 1.100 g Sodium Pyruvate 1.80 g Glucose Make up to 1 litre with dd H_2O pH 7.4 & Osmolarity 305-315Osm/L

Low Calcium Solution (**LCS**, 0.5mM Ca^{2+} sol.)	7.714 g NaCl 0.223 g KCl 0.203g $MgCl_2.6H_2O$ 0.055 g $CaCl_2$ 2.38 g HEPES 1.100 g Sodium Pyruvate 1.80 g Glucose Make up to 1 litre with dd H_2O pH 7.4 & Osmolarity 305-315mOsm
Extracellular Solution (ECS)	8.0063 g NaCl 0.373 g KCl 0.120g $MgSO_4$ 0.222 g $CaCl_2$ 2.38 g HEPES 0.141 g Na_2HPO_4 1.80 g Glucose Make up to 1 litre with dd H_2O pH 7.4 & Osmolarity 305-315mOsm

2.4. Enzymes and Proteins:

Pronase (Protease,Type XIV: Bacterial, from Steptomaces griseus)	Sigma, P5147
Papain (Papain from Carica Papaya)	Sigma, 76220
DNase (Deoxyribonuclease I, from bovine pancreases)	Sigma, DA25
Concanavalin A	Sigma, C7275

2.5. Laboratory Instruments:

Fluorescence inverted Microscope Axiovert 200M Camera Axiocam MRm	Carl Zeiss
Electron Microscope	FEI; Tecnai 12
pH Meter	Inolab
Osmometer	Vapro Osmometer 5520, Wescor Inc, USA)
Shaker	Ika MS3 basic
Confocal microscope; AIR-MP	Nikon
Centrifuge	Ct15RE, Hitachi
Incubator 37c & 25c	Thermo Electron Corporation

2.6. ISOLATION OF PHOTORECEPTOR CELLS FROM THE MOUSE RETINA

2.6.1 Coating of coverslips

Cleaned, autoclaved round coverslips (25mm diameter, Menzel GmbH, Germany) were transferred into a sterile 6 well plate; 200µl coating solutions were added and kept for 1hr incubation to absorb the solution completely. The coverslips were washed thrice with LCS/ECS and used immediately for plating the cells.

a) Poly-L-Lysine: 0.001% solution in H_2O
b) Concanavalin A : 1 mg/ml H_2O

For gelatinisation of coverslips, 1g gelatin was dissolved in 200mL PBS by heating on a shaker. Then, 100ml of the gelatin solution was added to 100 round coverslips (25mm diameter, Menzel GmbH, Germany) in a glass jar for 1hr on shaker.

After three washes with PBS 10ml of 25% glutaraldehyde was added and incubated with gelatin solution for 1hr on a shaker. Afterwards, coverslips were washed three times with PBS and once with 70% ethanol. The coated coverslips were kept in 70% ethanol for storage and washed with PBS before use.

2.6.2 Isolation and dissociation of mouse retina

Mice were euthanized with an overdose of isoflurane, followed by cervical dislocation in ambient light. The eyes were enucleated and kept either in LCS for papain dissociation method or in ECS for pronase dissociation method. In the next step, the eyes were hemisected into anterior and posterior eyecups. From the posterior eyecup, the neural retina was peeled off from pigmented epithelium in LCS/ECS solution, pH 7.4, at room temperature.

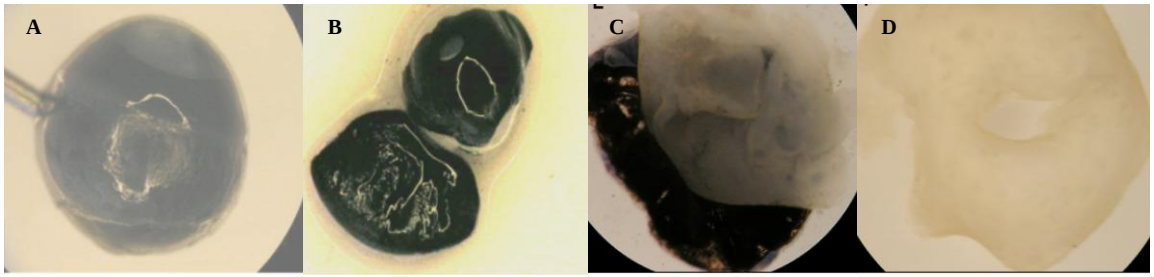

Figure 6. Isolation of mouse retina. *(A-B) Dissected of mouse retina with anterior and posterior portion of eyecup. Posterior eyecup contained sclera and retina. (C) Retina separated from pigment epithelium and (D) isolated retina (images taken by Sivaraman Natarajan).*

2.6.2.1 Dissociation of retinas using pronase enzyme

For mechanical and enzymatic isolation of the photoreceptor cells, freshly isolated retinas were incubated in Extra-Cellular Solution, ECS containing 1mg/L pronase and 2 mM EGTA, for 15 minutes at 37°C. After three washes with ECS containing 0.5% bovine serum albumin (BSA), 2mM EGTA, and 1mg/L DNase, cells were obtained by gentle trituration of enzymatically treated retina with plastic Pasture pipette 4-5 times. Isolated cells were platted on poly-L-lysine coated coverslips and incubated in ECS at 37°Cfor 30 min. The cells were washed once with the ECS to remove unbounded cells and proceeded for further experiments

2.6.2.2 Dissociation of retinas using papain enzyme

2.6.2.2.1 Dissociation of adult mice retinas

Activation of papain (9U/ml) has been done at 37^{o}C for 15 min with 2.7mM L-cystein in Low Calcium Solution, LCS, (LCS was saturated with 5% CO_2/95% O_2 before use). Then, fresh isolated retinas from adult mice (minimum 6 weeks old) were washed once with LCS and transferred to 1ml activated papain solution for 20 min at 25^{o}C. In the next step, papain solution was aspirated and the enzymatic reaction was stopped by washing three times with 1ml of LCS supplemented with 2% fetal calf serum (FCS), and 0.01mg/ml DNase (to eliminate the tissue aggregates). To dissociate the cells, enzymatically treated retinas were gently shaken by hand. The resulting cell suspension was plated on concavalin-A coated coverslips by plastic Pasture pipette and allowed to settle for 30 min at 37^{o}C for strong attachment to the surface. After that, the cells were washed once with the LCS to remove unbounded cells and proceeded for further experiments.

2.6.2.2.2 Dissociation of 16-18 days old mice retina

Rod photoreceptor cells were isolated from the retinas of 16-18 days old mice within 5 min postmortem (in ambient light). The enucleated eyes were bisected at the equatorial plane, and the posterior eyecup was transferred into LCS which was saturated with 5% CO_2/95% O_2 before use. The isolated posterior eyecup was kept at 37^{o}C for minimum 2 hours in oxygenated LCS. From the posterior eyecup, the neural retina was gently peeled off from the pigment epithelium and incubated in 1 ml of cysteine-activated papain solution for 25 min at 25°C. Activation of papain (9 U/ml) was done by preincubation with 2.7mM L-cysteine in LCS at 37°C for 20 min. After removing the papain solution, the retina was gently washed three times with 1ml of LCS solution containing 2% FCS and 0.01 mg/ml DNase. Afterwards, the retinas were dissociated as described before.

2.6.2.2.3 Dissociation of electroporated retinas

Activation of papain (9 U/ml) was done with 2.7mM L-cysteine in LCS at 37°C for 20 min. Then, the electroporated retinas were incubated in the activated papin solution for 10 min at 25^{o}C and proceeded for the isolation of rod photoreceptor cells as described above.

2.7. IMMUNOCYTOCHEMISTRY OF ISOLATED RETINAL CELLS

Acutely dissociated cells were fixed for 15min at room temperature with 4% ice-cold parafarmaldehyde solution (in PBS). Afterwards, cells were rinsed three times (5min each) with PBS and permeabilized with 0.1% saponin (in PBS) for 15 min at room temperature. Unspecific binding sites were blocked with 1% BSA and 0.1% saponin (in PBS) for 30 min at room temperature. The cells were then incubated with the specific primary antibodies, which were diluted in blocking buffer for overnight at 4^{o}C. After overnight incubation, the cells were washed with PBS three to four times (5min each) and then incubated with corresponding secondary antibodies, which were diluted in the blocking buffer for 1hr at room temperature.

For immunocytochemistry of Fluo 4AM loaded cells, the isolated mouse photorceptor cells were fixed with 40mg EDAC for 30 min at room temperature. The EDAC solution (in LCS) was prepared immediately before use because of the instability of EDAC (Tymianski et al., 1996: Beck et al., 2004) in aqueous solutions. After fixation, the cells were washed thrice with PBS (15min each) and permeabilized with 0.2% Triton-X100 (in PBS) for 15 min at room temperature. The cells were blocked for non-specific antibody binding sites with 1% BSA and 0.2% TritonX100 (in PBS) for 30 min at room temperature. The cells were then incubated with primary antibodies for overnight at 4^{o}C. Cells were washed with PBS for 3 times for 5 min and then incubated with corresponding secondary antibodies for 1hr at room temperature.

Finally, the incubated cells on the coated coverslips were washed three times with PBS. Afterwards, the immunolabelled cells were carefully embedded by adding 20µl of NPG a antifade (containing 1.5% w/v n-propylgallate in 60% glycerol in PBS) to retard the photo bleaching. Afterwards, the cells were covered with cover slips without capturing the air bubbles beneath them.

2.8. LIVE CELL ASSAYS OF PRONASE TREATED RETINAL CELLS

2.8.1. Loading of lysotracker in rod photoreceptor cells

The LysoTracker is a fluorescent acidotropic probe that accumulates inside acidic secretory vesicles (Becherer *et al.*, 2003; Giner *et al.*, 2007). In my experiments, I used LysoTracker® Red DND-99 which is a red-fluorescent dye for labeling and tracking acidic organelles in live cells. This probe has several important features, including high selectivity for organelles with acidic pH and effective labeling of live cells at nanomolar concentrations. LysoTracker® Red DND-99 consists of a fluorophore linked to a weak base that is only partially protonated at neutral pH. This allows it to freely permeate cell membranes enabling them to label live cells. LysoTracker® Red DND-99 does not require use of a second antibody for detection and also fluorescence is retained after fixation.

Acute dissociated mouse photoreceptor cells were incubated for 30mins in ECS containing BSA (0.5% w/v) and 500nM LysoTracker at 37^{o}C. For control experiment, cells were incubated with 100µM sodium azide ($NaN_{3,}$ Bagar et al., 2009) for 30 min at 37^{o}C before incubating with Lysotracker and then rapidly washed 3 times with ECS. After staining, the cells were rinsed trice with ECS to remove the extra Lysotracker from the cell surface and then observed under (absorption: 577nm, emission: 590nm) Axiovert 200 (Zeiss GmbH) epifluorescence microscope.

2.8.2. Loading of Dextran in rod photoreceptor cells

Dextran is a hydrophilic polysaccharide which is synthesized by *Leuconostoc* bacteria. It is characterized by its high molecular weight, good water solubility, low toxicity and relative inertness. These properties make dextran effective water-soluble carrier for dyes, indicators, and reactive groups in a wide variety of applications. Florescence- tagged dextran is used as a fluorescent marker of fluid-phase endocytosis. For my experiments, I used a fixable10kDa dextran rhodamine as fluid phase marker to confirm viability of the cells. Isolated mouse photoreceptor cells were kept in condition medium that were taken from 2 days cultured ARPE-19 cells for 4hrs at 37^{o}C. Medium was aspirated and after washing once with PBS, DMEM: F12 (1:1) was

added for 1hr at 37^{o}C.Then medium was removed and 250µg 10KD dextran in DMEM and 100ng EGF was added for 10mins at 37^{o}C.Afterwards, dextran loaded cells were washed three times with PBS (5min each) and fixed with 4%PFA for immunocytochemistry as described before.

2.9. LIVE CELL ASSAYS OF PAPAIN TREATED RETINAL CELLS

2.9.1 SR101 uptake of isolated rod photoreceptor cells

Freshly isolated photoreceptors were incubated for 2 min at RT with 1µM paraformaldehyde- fixable analog Texas Red-hydrazide (in LCS) which resulted in a staining pattern similar to sulforhodamine, SR10, pattern and then rinsed 3 times (5min each) with LCS. SR101 is a fluid phase marker and the resulted labeling allowed assessment of the viability of the tissue.

For control experiments in two separate experiments, either the cell were incubated with 100µM dynamine inhibitor dynasore for 30 min to block dynamine dependent ribbon associated endocytosis or with 1mM Cobalt to block calcium channels for 10 min at 37^{o}C before incubating with sulforhodamin. After uptake, the cells were rapidly washed 3 times with LCS and fixed with 4% PFA for 15 min at RT. For immunolabeling, fixed cells were treated as described before.

2.9.2 ER tracker uptake of isolated rod photoreceptor cells

ER tracker dye is cell-permeable, live-cell stain that is highly selective for the endoplasmic reticulum (ER) and the staining pattern is partially retained after fixation with formaldehyde.

In the experiment for double staining of ER tracker dye and Fluo-4AM, first freshly isolated photoreceptors were incubated for 15 min at 37^{o}Cwith 1µM ER tracker dye (in LCS) and then the cells were incubated for 15 mins in LCS containing BSA (0.1% w/v) and 1µM Fluo4 AM dye at 37^{o}C. The incubated cells were washed thrice with LCS and fixed with 40mg EDAC to retain Fluo-4AM staining for 30 min at room temperature. The EDAC solution (in LCS) was prepared immediately before use because of the instability of EDAC in aqueous solutions. After fixation, the cells were

washed thrice with PBS (15min each) and carefully embedded by adding 20µl of NPG antifade (containing 1.5% w/v n-propylgallate in 60% glycerol in PBS) to retard the photo bleaching. Finally the cells were covered with cover slips without capturing the air bubbles beneath them.

.

2.9.3 Endo- and Exo-cytosis assay with FM1-43

FM1-43 is a modified styryl membrane selective non-toxic fluorescent dye which is much more fluorescent in non-polar solvents (e.g. membrane) than the polar solvents like water. The lipophilic tail region causes easy penetration into one leaflet of a membrane lipid bilayer and the number of double bonds in the bridge connecting the two aromatic rings of middle region of the dye determines the fluorescence spectrum. The positively charged head group of the dye prevents it from flipping across the membrane. Thus, once dye is trapped inside a vesicle, it can escape from the cell only by exocytosis of the vesicle.

2.9.3.1 Endocytosis Assay

2.9.3.1.1 Endocytosis in isolated retina

Freshly isolated retinas were incubated for 15 min in stimulating solution (25mM KCl) containing 10µM FM1-43 at 37^{o}C on orbital shaker (100rpm). After staining, the retinas were rinsed thrice with LCS and proceeded for the papain treatment for the isolation of photoreceptor cells as described before.

2.9.3.1.2 Endocytosis in isolated rod photoreceptor cells

Freshly isolated rod photoreceptor cells were incubated for either 5 min or 20 min in LCS containing 1µM FM1-43 at 37^{o}C. After staining, the cells were rinsed thrice with LCS and fixed with 4% PFA for 15 min at RT. For immunolabeling, fixed cells were treated as before described

For control experiments in two separate experiments, either the cell were incubated with 100µM dynamine inhibitor dynasore for 30 min to block dynamine dependent

ribbon associated endocytosis or with 1mM Cobalt to block calcium channels for 10 mins at 37^{o}C before incubating with FM1-43. After uptake, cells were rapidly washed 3 times with LCS and fixed with 4% PFA for 15 min at RT. For immunolabeling, fixed cells were treated as described before.

2.9.3.2 Exocytosis assays with FM1-43 using isolated rod photoreceptor cells

Freshly isolated rod photoreceptor cells were incubated for 20 min in LCS sol. containing 1µM FM1-43 at 37^{o}C. After staining, the cells were rinsed thrice with LCS. For imaging, the coverslips were placed into a circular open-bottom chamber supplemented with 500µl Resting solution (RS) and mounted on the Zeiss Axiovert200 microscope at RT. Every 10s (0.1Hz), FM1-43 was excited at 488nm for 50ms and the emitted fluorescence was recorded with a cooled charged coupled device (CCD) camera. Synaptic terminal of rod photoreceptors were marked as region of interest (ROI). Data acquisition and analysis were accomplished with the Live Acquisition (LA) imaging software vs.2.4 (TILL Photonics) and ImageJ has been used to re-analysis of the data.

Experiments were started with 500µl Resting solution (RS). After 60sec, the cells were stimulated either with 500µl of 100mM KCl to get final concentration (50mM KCl) or treated with 500µl of 30mM Caffeine in RS to get final concentration (15mM Caffeine).

The control experiments were started with 300µl Resting solution (RS). After 60sec, the cells were treated with 300µl of 2mM Cobalt in RS to get final concentration (1mM Co^{2+}) for up to 2min and then stimulated with 600µl of 100mM KCl to get a final concentration (50mM KCl).

2.9.4 Ca^{2+} imaging of acutely dissociated rod photoreceptor cells

Calcium imaging experiments were performed with an inverted Zeiss Axiovert200 microscope set up using 60x oil immersion objective (N.A.1.4) and a camera based imaging system from Till Photonics (Oligochrome,Martinised, Germany), equipped with fast wavelength switcher. For imaging, the coverslips were

placed into a circular open-bottom chamber supplemented with 500µl of required solution (LCS/RS/Zero calcium sol.) and mounted on the Zeiss Axiovert200 microscopeat RT. Region of interest (ROI) was marked in synaptic terminal of rod photoreceptors based on requirements. Data acquisition and analysis were accomplished with the Live Acquisition (LA) imaging software vs.2.4 (TILL Photonics) and for re-analysis of data ImageJ has been used.

2.9.4.1 Fluo4 fluorescence measurement

In this experiment, Fluo4 AM has been used. Fluo4 available as a cell-permeant acetoxymethyl (AM) ester which is a fluorescent indicator that provides brighter images of intracellular Ca^{2+} dynamics and calcium influxes inside living cells. It is commonly used as the non-fluorescent acetoxymethyl ester (Fluo-4 AM) which is cleaved inside the cell to give the free, fluorescent Fluo-4. Excitation of Fluo-4 at 488 nm by oligochrome light source increases high Ca^{2+} binding affinity which increase fluorescence intensity in response to Ca^{2+} -binding.

Acutely isolated rod photoreceptor cells were incubated for 15 mins in LCS containing BSA (0.1% w/v) and 1µM Fluo4 AM dye at 37^{o}C. The incubated cells were washed thrice with LCS to remove unbound dye from the surface of the cells. Fluo-4AM loaded cells fixed either with EDAC for immunocytochemistry or kept in LCS for imaging experiments.

Fluo-4AM measurements of the rod photorecptors have been done in following 3 ways:

a) **Fluo-4AM & Ionomycin:**

   Experiments were started with 500µl LCS at a rate of 0.2Hz (5s). After 2 min, the cells were treated with 500µl of 2µM Ionomycin in LCS to get the final concentration (1µM).

b) Fluo-4AM & Thapsigargin:

Experiments were started with 300µl Zero calcium solution at a rate of 0.1Hz (10s). After 60sec, the cells were treated with 300µl of 2mM Thapsigargin in Zero calcium sol. to get the final concentration (1mM) for upto 5min and then 600µl of 4mM Ca^{+2} solution was added to get the final concentration (2mM $CaCl_2$).

c) Fluo-4AM & High K^+ sol.

Experiments were started with 500µl Resting solution (RS) at a rate of 40Hz (25ms). After millisecond, the cells were stimulated with 500µl of 100mM KCl to get final the concentration (50mM KCl).

2.9.4.2 Fura-2AM measurement

Fura-2AM is a membrane-permeable derivative of the ratiometric calcium indicator Fura-2. It diffuses along its concentration gradient into the cytosol where intracellular esterases cleave the ester bound. The remaining polar Fura-2 is trapped within the cell where it binds $Ca^{2+.}$ The peak excitation wavelength of fura-2AM shifts from 340nm in the Ca^{2+} -bound state to about 380nm in the Ca^{2+} -free state but its maximum emission stays at 510nm. Fluorescence emission at 340nm excitation wavelength increases, while it decreases at 380nm excitation wavelength with a rising calcium concentration. Reciprocally, 340nm excitation decreases, while it increases at 380nm excitation with the decreasing calcium concentrations. These properties in excitation and emission wavelengths enable Fura-2AM to be used as dual excitation (340nm and 380nm) Ca^{+2} radiometric dyes. Measurements of fluorescence at two-excitation wavelength are used to estimate the intracellular calcium concentration independent of dye concentration and excitation light intensity. Values of intracellular calcium concentration are the results of the ratio of 340nm to 380nm wavelength.

For Fura-2 based Ca^{2+} imaging, freshly isolated rod photoreceptor cells were incubated for 30 min in LCS sol. containing 5µM Fura-2AM with BSA (0.5w/v) at 37^oC. After staining, the cells were washed for 10 min with LCS to remove the excess

dye. Experiments were started with 300µl LCS. After 2min, 300µl of 4mM Ca^{+2} solution was added to get final concentration (2mM CaCl2) and then after 2 min 600µl of 100mM KCl was added to get final concentration (50mM KCl).

2.10. ELECTRON MICROSCOPY OF ISOLATED MOUSE PHOTORECEPTOR CELLS

For electron microscopy, I used the process, described by Schmitz and Drenckhahn (1996) with some modification. The isolated mouse photoreceptor cells obtained from papain treatment of the mouse retinas were fixed with 2.5% glutaraldehyde and 2% PFA (in 100mM Cacodylate buffer pH7.4) for overnight at 4^{o}C. The fixed cells after several washes with PBS were post- fixed for osmification with 2% OsO4 in 100mM Cacoaldehyde buffer pH7.4 for 1hr at RT. The samples were washed with PBS and then with 0.05M Maleate buffer pH5.0. Afterwards, the cells were block-contrasted with 2% uranyl acetate in 0.05M Maleatebuffer pH5.0 for 1hr at 4^{0}C in dark. In the next step, the cells were washed three times with 0.05M Maleatebuffer and dehydrated with an ascending ethanol concentration series and embedded in a resin mixture. The resin was polymerized at 60^{o}C for 12-24 hours. Sections were obtained with Ultracut Microtome (UltraCut R, Leica) and were analyzed with a digital transmission electron microscope (FEI, Tecnai 12) and digitally documented with Analysis software.

CHAPTER 3

RESULTS

3.1 Dissociation of mouse retina to isolate rod photoreceptor cells

In the first step of my work, I standardized a method to get a good number of well morphological preserved intact mouse rod photoreceptors via enzymatic and mechanical trituration from the mouse retina. For this purpose, I tested two different enzymes, pronase and papain, to digest mouse retina.

Furthermore, I investigated different coatings to optimize the adherence of isolated rod photoreceptor cells on the glass coverslips. Initially, I used pronase dissociated retinal cells for plating on gelatin-coated coverslips but very few retinal cells were retained on the coverslips. However, poly-L- Lysin coated coverslips resulted to retain much more cells (Fig.7). The rod photoreceptors obtained by papain treated retinas have good adherence on Concanavalin- A coated coverslips.

All the experiments were performed under dim ambient light condition. The rod photoreceptor cells having long outer -, inner-segment which are attached to soma (5µm) and having a synaptic terminal (2µm) were considered as intact and well morphological preserved.

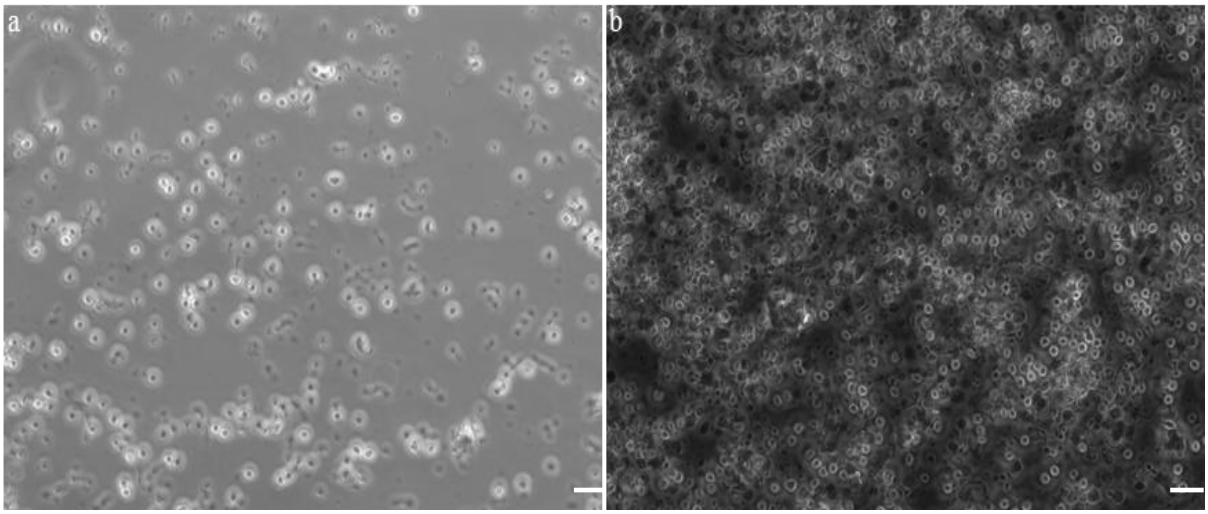

***Figure 7. Pronase dissociated retinal cells**. **(a)**, Dissociated retinal cells obtained by pronase digestion on gelatinized coated coverslip and **(b)** on Poly-L-Lysin coated coverslip at low magnification before fixation. Scale bars: 10µm*

3.1.1 Dissociation of mouse retina with pronase

Dissociation of retina with pronase followed by mechanical trituration yielded a good number of photoreceptor cells. However, at higher magnification, I observed that most of the dissociated rod photoreceptors were morphological not well preserved. Outer and inner segments were absent and only synaptic terminal was attached to the soma (as shown by arrows in figure 8).

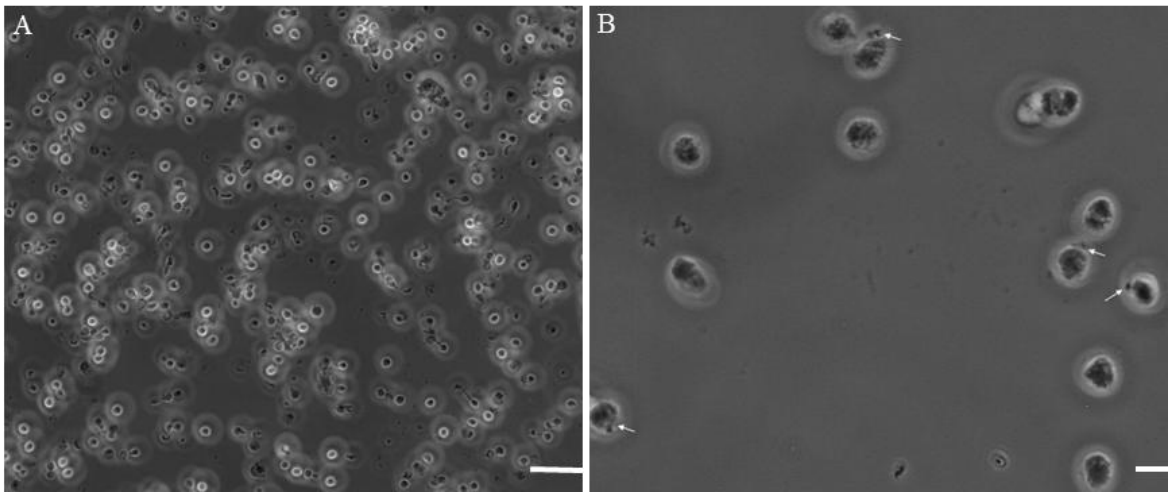

Figure 8. ***Pronase treated retinal cells****. Dissociated retinal cells obtained by pronase digestion at low magnification* ***(A)*** *and* ***(B)*** *high magnification after fixation.* ***(B)****Arrows indicate the terminals of the dissociated photoreceptors. Scale bars: 5µm*

3.1.2 Dissociation of mouse retina with papain

In this method, retinas were enzymatically treated with papain which was followed by mechanical trituration (Fig. 3). The resulted suspension rich in rod photoreceptors showed good adherence on concavalin-A coated coverslips. At high magnification, I observed that the solitary rod photoreceptors were well morphologically well preserved. The isolated cells were having soma, synaptic terminal, outer segment and inner segment (Figure 9)

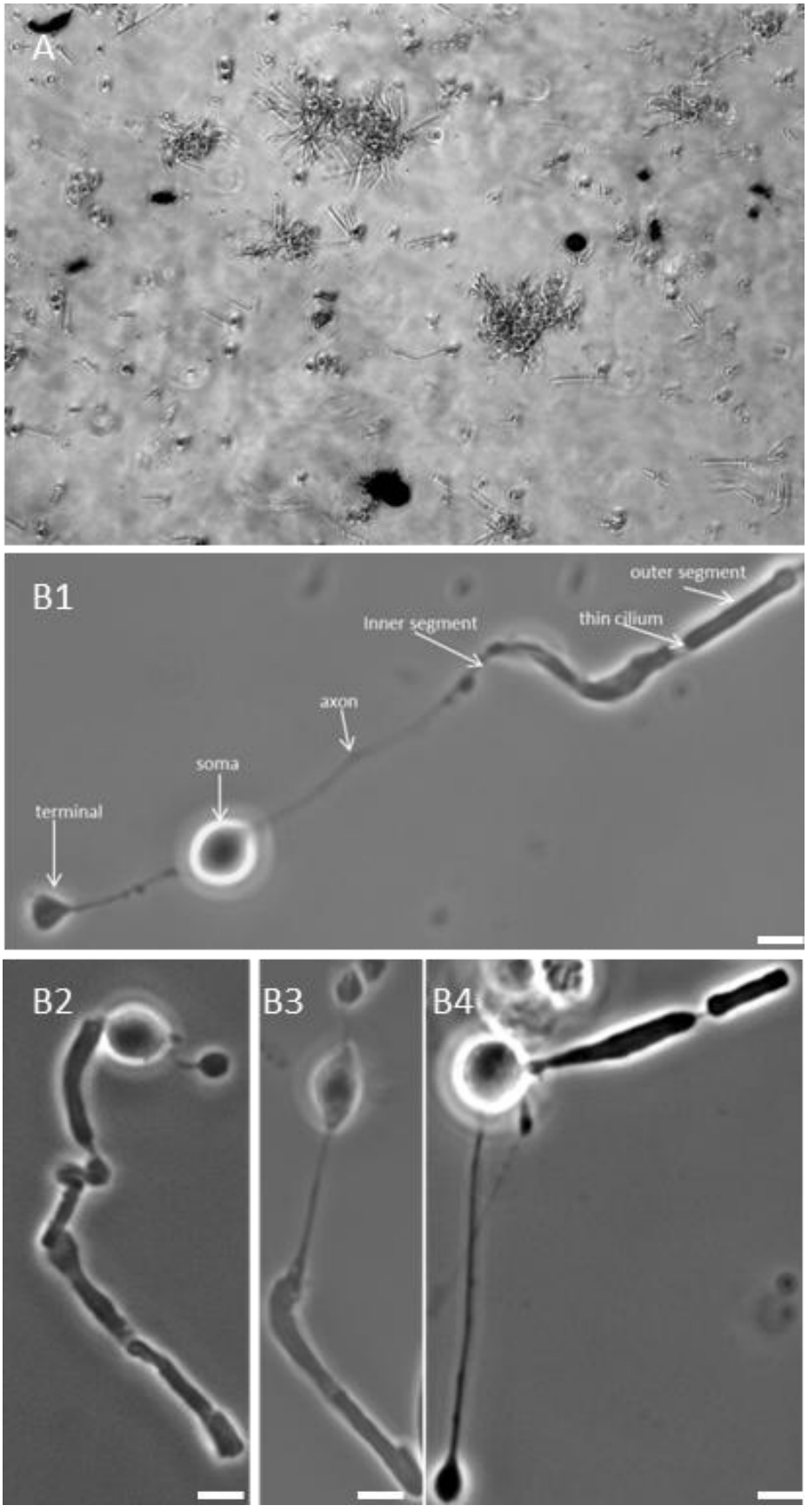

Figure ***9. Papain treated retinal cells****. Dissociated retinal cells obtained by papain digestion at low magnification* ***(A)*** *before fixation and (****B1, B2, B3 & B4)*** *high magnification after fixation. Scale bars: 5µm*

3.2 Ultrastructure of papain dissociated rod photoreceptors

I performed post-embedding electron microscopy to determine the ultrastructural morphology of the synaptic terminal from isolated mouse rod photoreceptors.

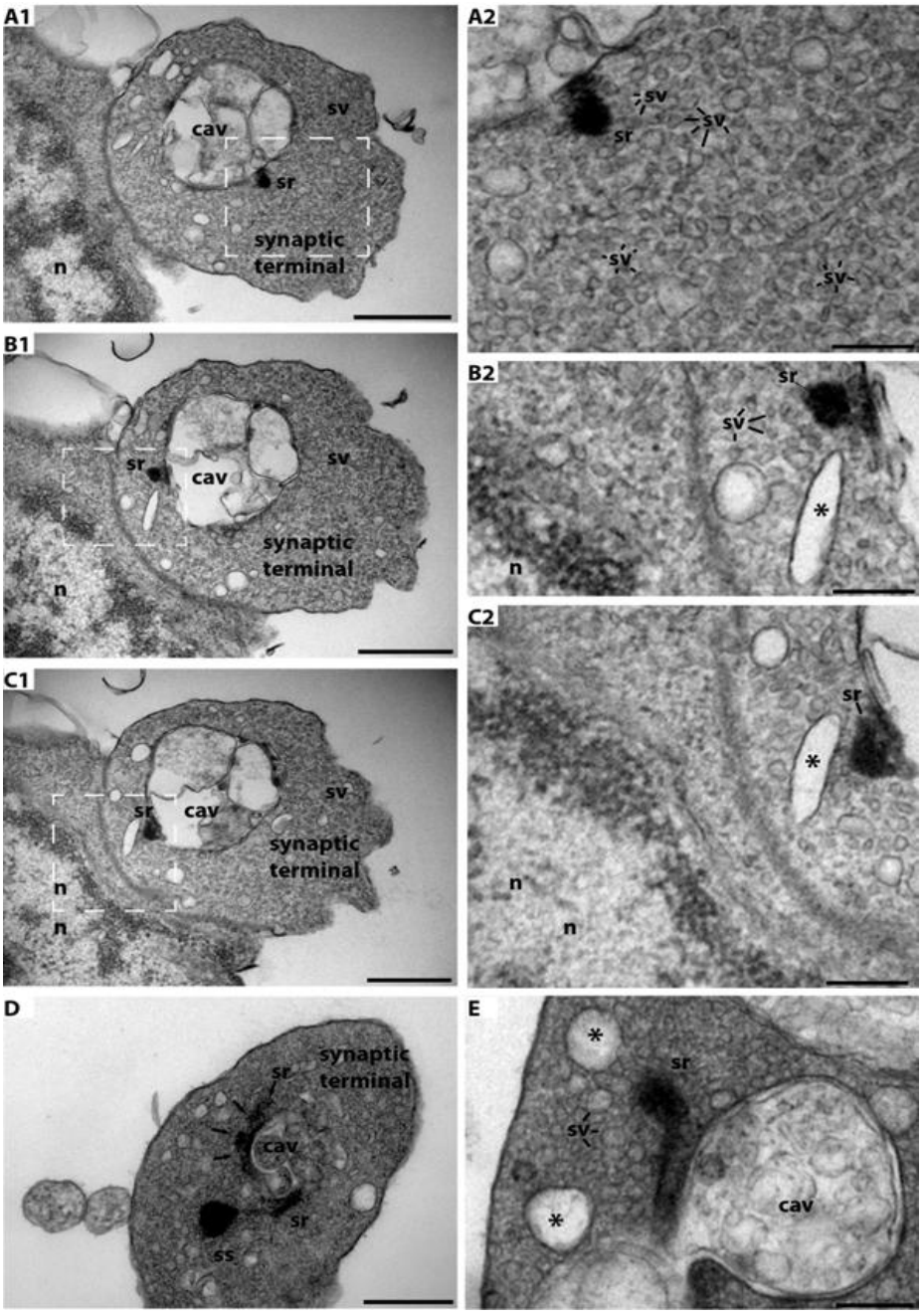

Figure ***10. Ultrastructure of papain isolated rod photoreceptors. (A-E)*** *Synaptic terminals with large number of synaptic vesicles together with a synaptic ribbon anchored to the active zone of isolated rod photoreceptors obtained from papain.* ***(A2, B2& C2)*** *show enlarged view of the respective terminals. Abbreviations: n, nucleus; sr, synaptic ribbon; sv, synaptic vesicles; cav, synaptic invagination of the photoreceptor synaptic complex that contains the tips of the postsynaptic dendrites from bipolar and horizontal cells.*

Figure 10 shows a typical large presynaptic terminal with large numbers of synaptic vesicles together with a synaptic ribbon anchored to the active zone.
In figure A1, B1&C1, the center of the presynaptic terminals contains the postsynaptic cavity with tips of the postsynaptic dendrites from horizontal cells and bipolar cells. These postsynaptic tips were separated from the soma of the presynaptic cells during the isolation procedure. At ultrastructural level, I found that the isolated rod photoreceptors retained a typical similar morphology as present in intact retina.

3.3 Characterization of the isolated mouse retinal cells by immunocytochemistry

Furthermore in the next step**,** I characterized the isolated rod photoreceptors by immunocytochemistry using various antibodies. These experiments determined whether enzymatic treatment of retinal cells retained the proper distribution of synaptic proteins, channel proteins and receptor molecules in the cells.

3.3.1 Characterization of isolated rod photoreceptor cells obtained by papain/ pronase dissociation by RIBEYE

In these experiments, I did immunolabeling on the pronase/papin treated retinal cells. These cells were labeled with anti-RIBEYE to determine whether the cells were rod photoreceptor. The dissociated cells were showing a single ribbon in the synaptic terminal of the cell as shown in figures 11 and 12. The presence of a single ribbon in the synaptic terminal of the cells confirms the presence of rod photoreceptor on the coverslips.

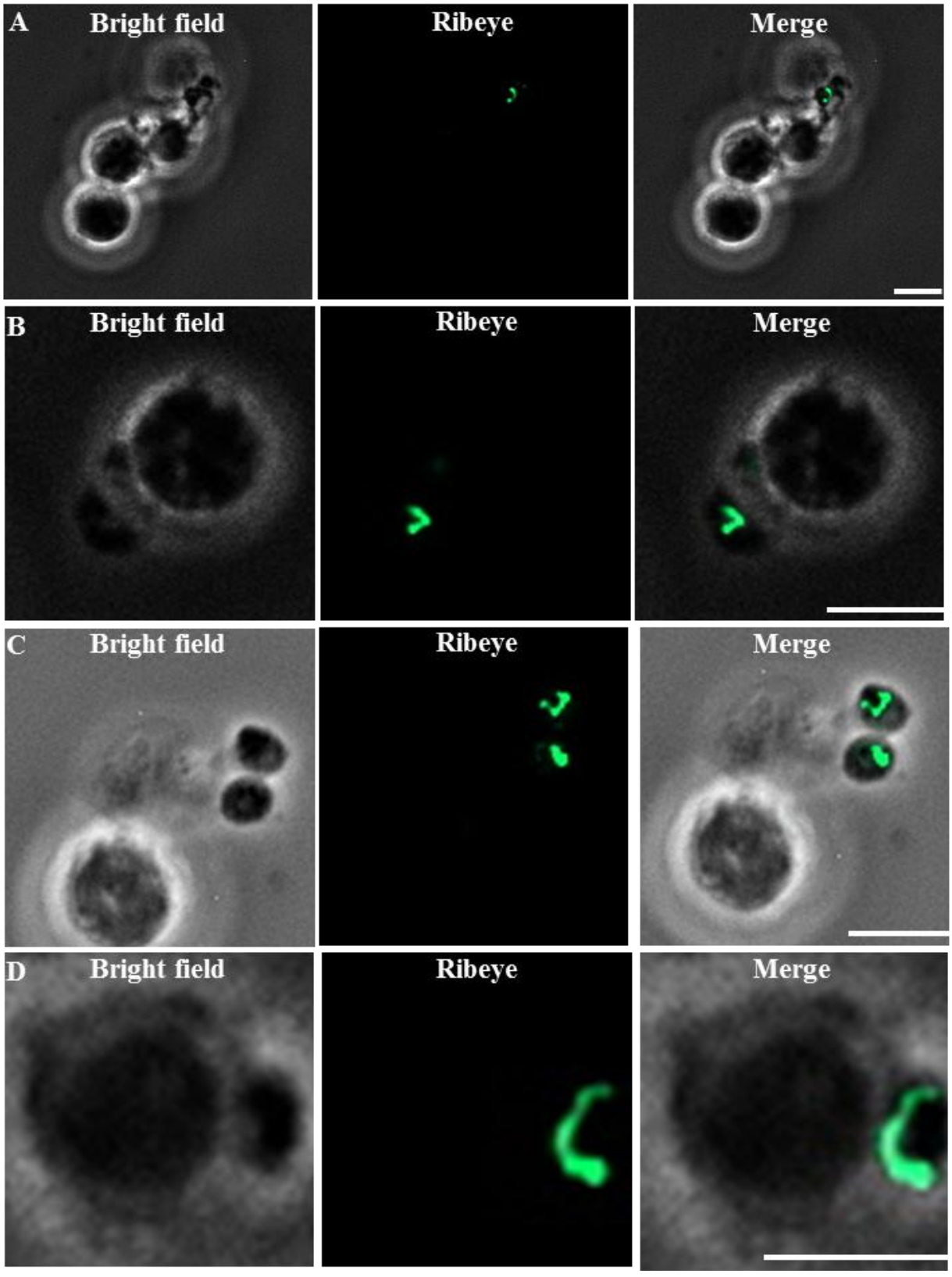

Figure ***11. Immunofluorescence labeling of acutely dissociated rod photoreceptor by pronase.*** *Isolated rod photoreceptors were labeled by RIBEYE.* ***A, B, C & D*** *show synaptic terminals of the acutely isolated rod photoreceptors with a single synaptic ribbon labeled with RIBEYE (green). Scale bars: 5µm*

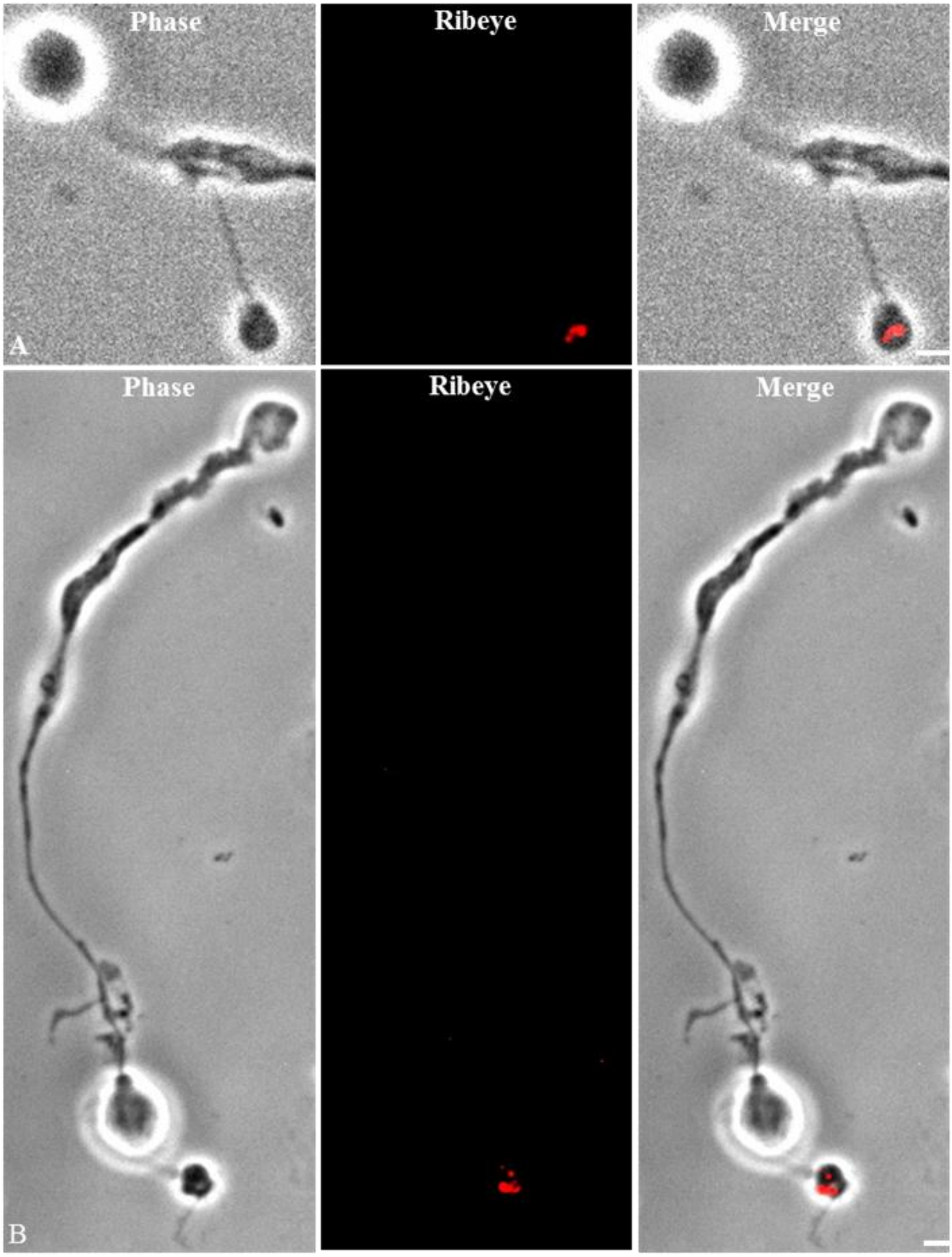

Figure ***12. Immunofluorescence labeling of acutely dissociated rod photoreceptor by papain.****. A &B show synaptic terminals of the acutely isolated rod photoreceptors with a single synaptic ribbon labeled with anti-RIBEYE (red). Scale bars: 1µm* ***(A &B)***

3.3.2 Localization of synaptic proteins in the isolated rod photoreceptor cells obtained by papain/ pronase dissociation

I labeled the cells with antibodies against synaptophysin and synaptotagmin to determine whether the synaptic proteins retained their localization in the dissociated cells. I found the proper localization of the synaptic proteins in the synaptic terminal of the isolated cells as shown in figures 13 and 14.

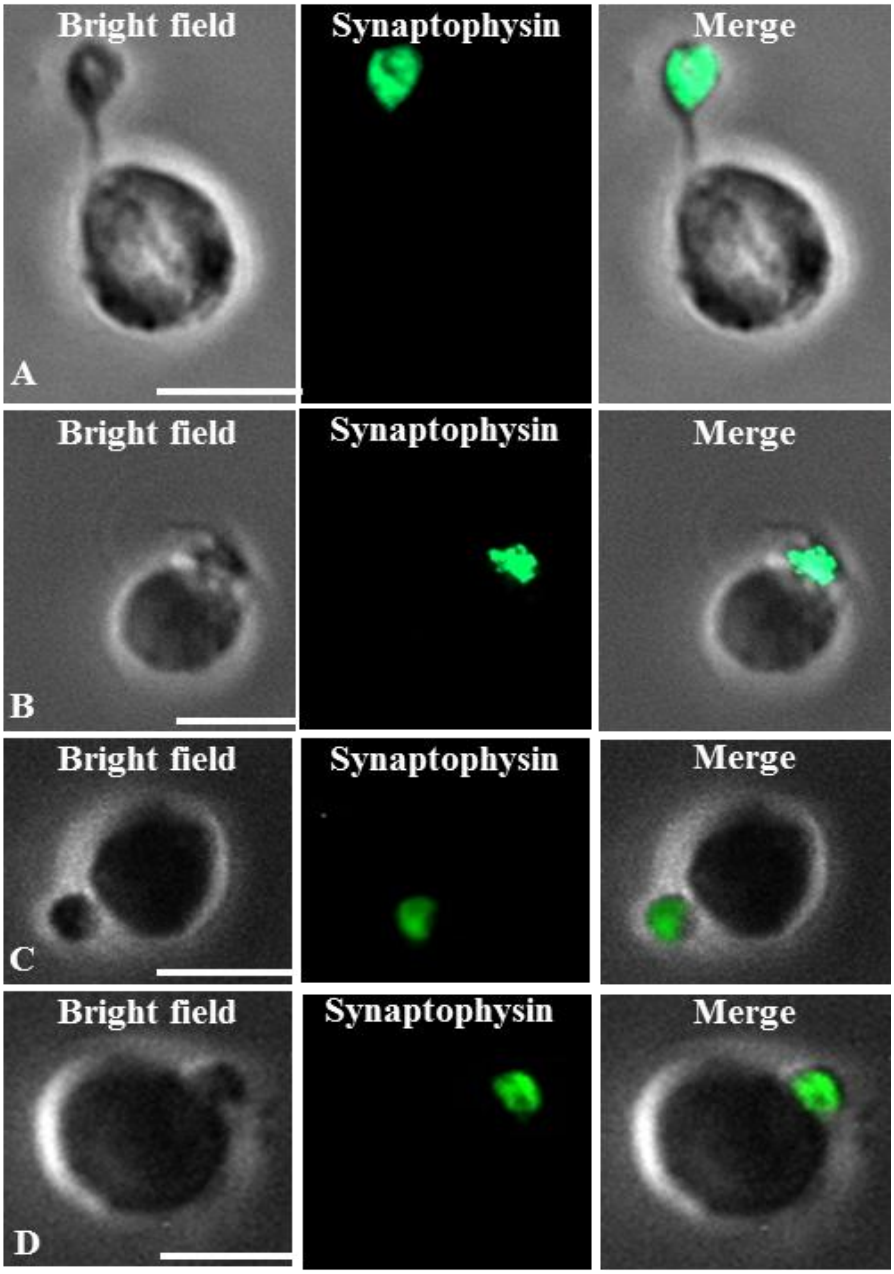

Figure *13*. *Immunofluorescence labeling of acutely dissociated rod photoreceptors by pronase. (A-D)* *Synaptic vesicles were labeled with antibodies against synaptophysin/synaptotagmin (green) in isolated rod photoreceptors. Scale bars: 5µm*

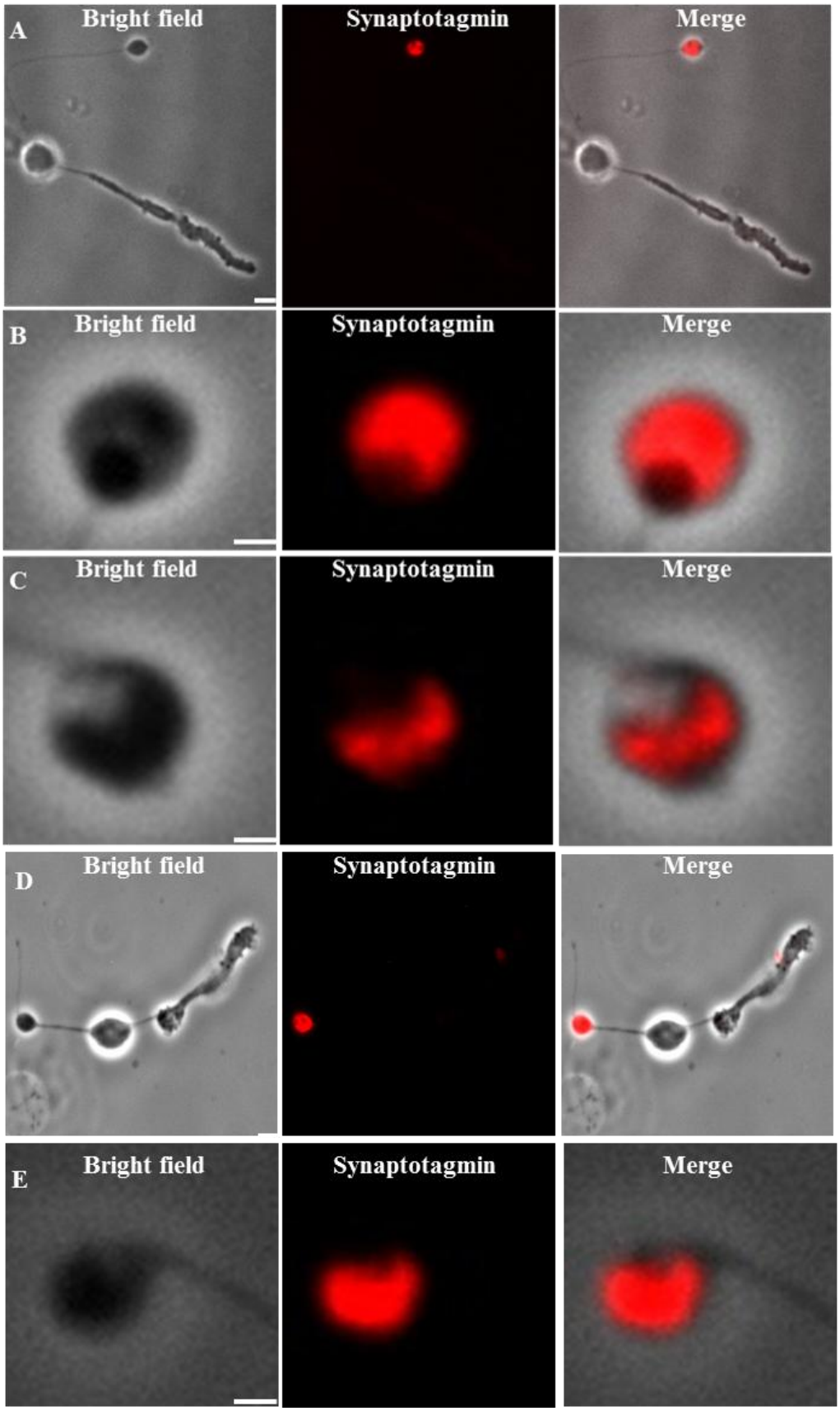

Figure ***14. Immunofluorescence labeling of acutely dissociated rod photoreceptor by papain.*** *Synaptic vesicles were labeled with antibody against synaptotagmin (red) in* ***A- E*** *isolated rod photoreceptors. Scale bars: 1µM*

3.3.3 Localization of Calcium channels in the isolated rod photoreceptor cells obtained by papain dissociation

To confirm the proper localization of calcium channels after isolation process, the cells were immunolabelled with antibodies against calcium channels and synaptic ribbon. I found that calcium channels were located at their respective position in the isolated cells as shown in figures 15.

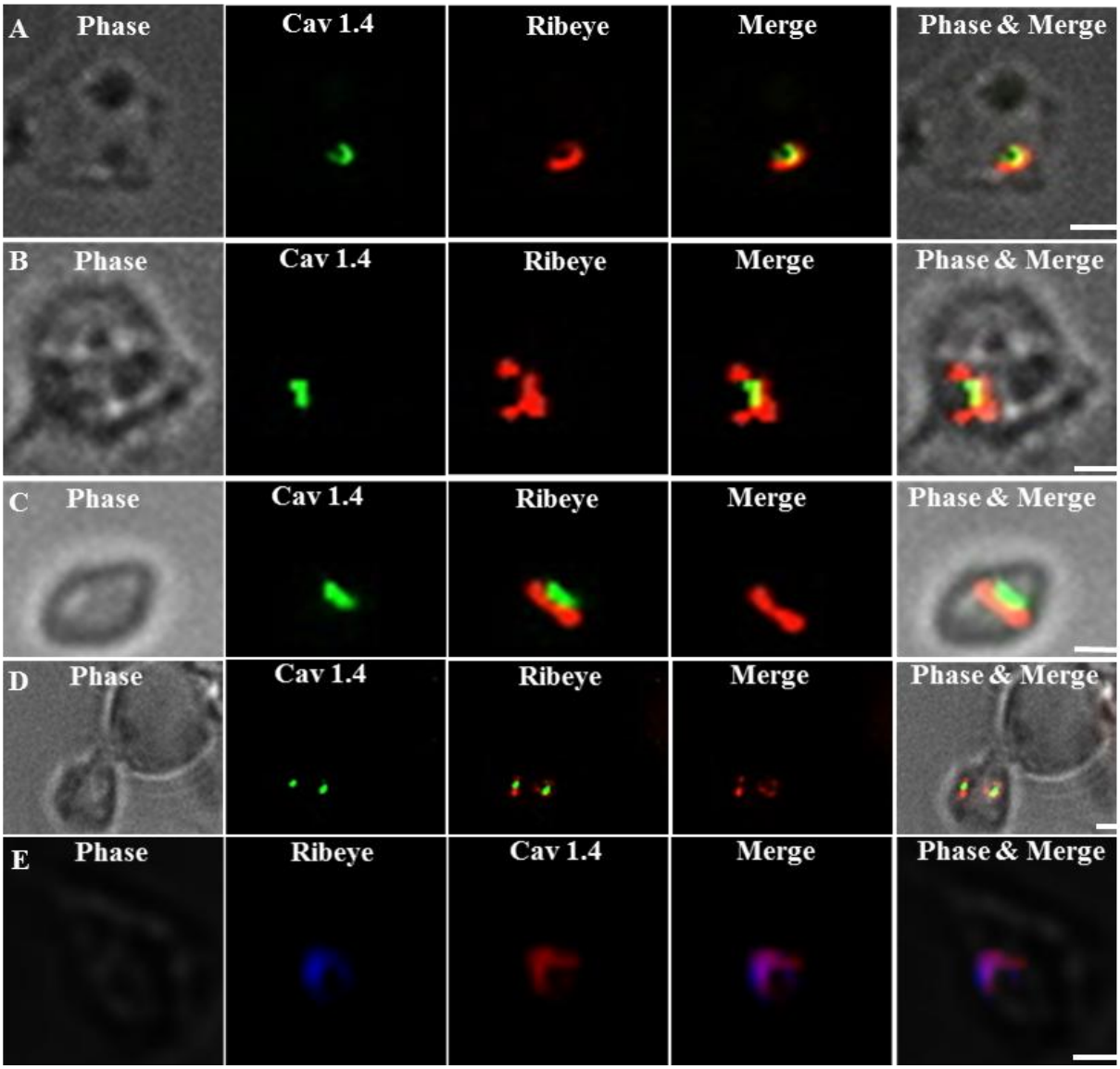

Figure ***15. Immunofluorescence labeling of acutely dissociated rod photoreceptors obtained by papain. (A & B)*** *Calcium channels were labeled with antibody against mouse monoclonal anti-Cav1.4 clone 4F14 (green) and ribbon was labeled with anti-RIBEYE (red).* ***(E)*** *was obtained by confocal imaging, showing labeling of calcium channels with antibodies against Cav1.4 (red) and ribbon labeling with anti- RIBEYE (blue) in the isolated rod photoreceptors.* ***(A- D)*** *obtained by conventional imaging. Scale bars: 1µm* ***(A-E)***

3.3.4 Characterization of tubulin in the papain treated cells

Immunofluorescence labeling experiment was done using antibodies against tubulin to demonstrate the region where axon connected with the synaptic terminal. The FM1-43 loaded cells were fixed and proceeded for labeling with antibody against β-tubulin. (Figure 16)

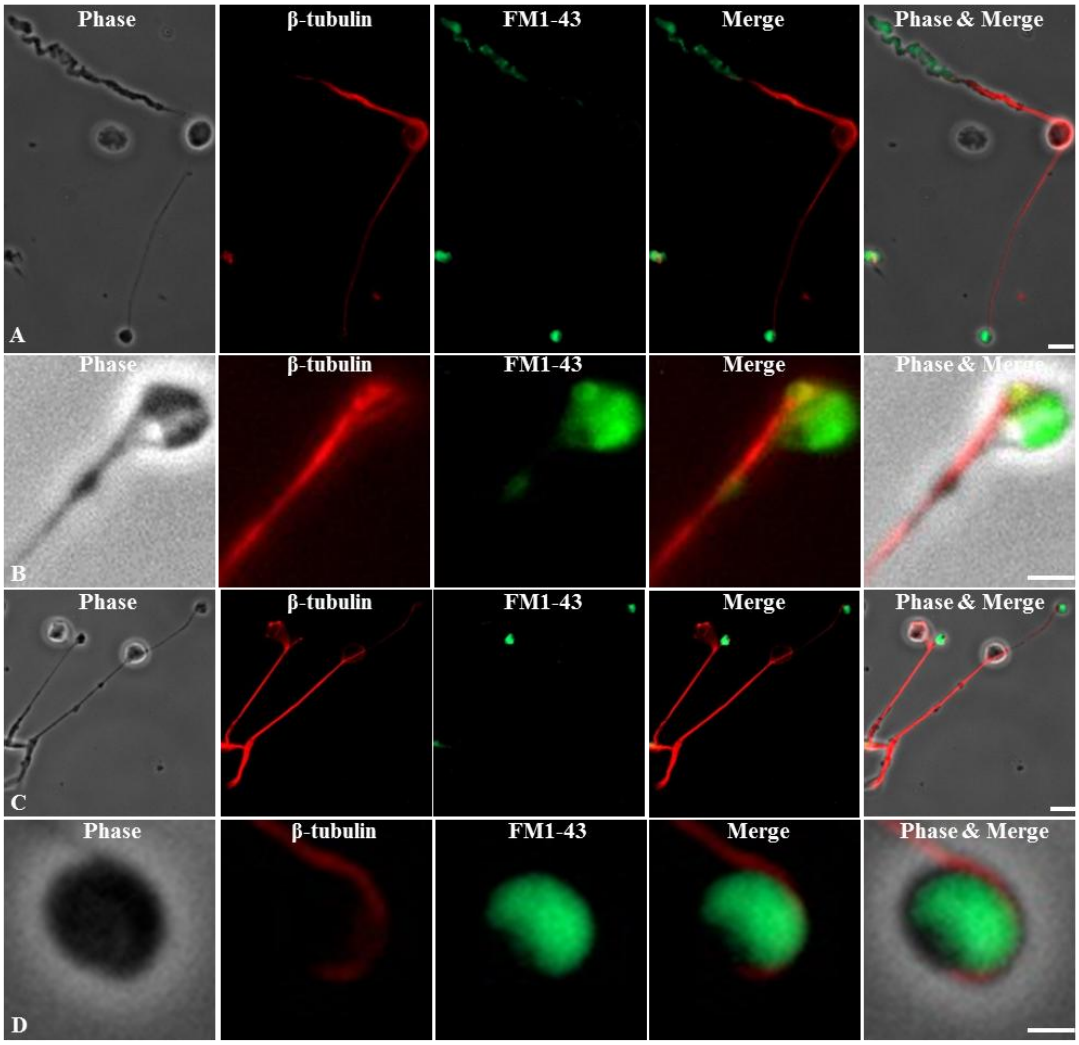

Figure ***16. Immunofluorescence labeling of acutely dissociated rod photoreceptors by papain. (A-D)*** *FM1-43(green) loaded rod photoreceptors were labeled with anti-tubulin (red).Scale bars: 5µm* ***(A&C)*** *and 1µm* ***(B &D)***

3.4 Physiological characterization of rod photoreceptors

Furthermore, I analysed the physiological activity of the isolated cells. To determine that whether dissociation processes were not affecting the physiological conditions of the isolated rod photoreceptor.

3.4.1 Viability assay for pronase dissociated rod photoreceptors

To evaluate viability and vitality of pronase dissociated rod photoreceptor cells, I have used lysotracker and 10KDa dextran rhodamine. The terminals of the cells were strongly and selectively filled with lysotracker and dextran as compared to cell body.

The staining pattern of the dextran confirmed that the cells are physiologically active and have normal exo-and endo-cytosis (Figure 17).

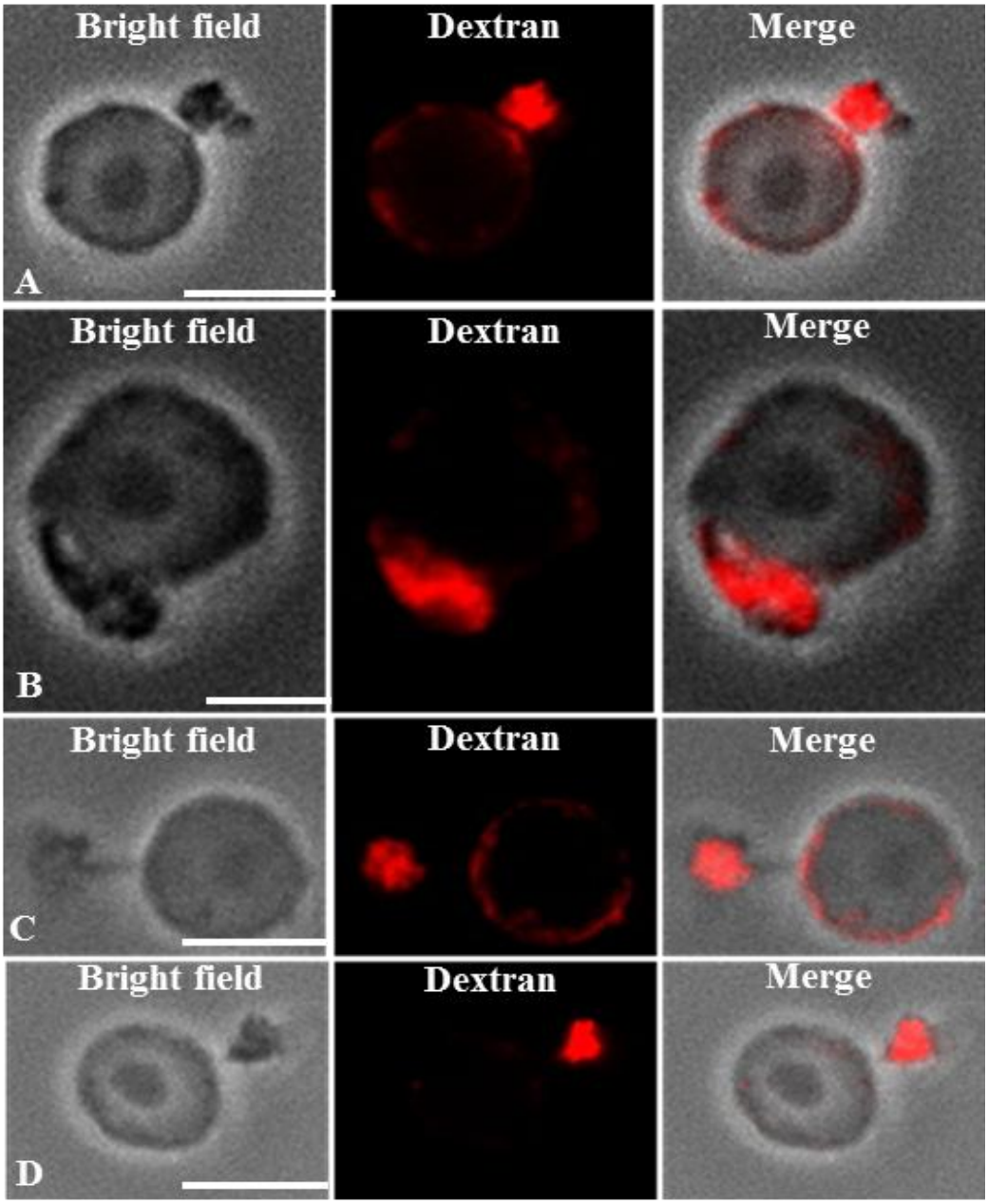

Figure ***17. Dextran uptake assay in pronase treated rod photoreceptors. (A-D)*** *Synaptic terminals were loaded with dextran (red) in isolated rod photoreceptors. Scale bars: 5µm*

After uptake of dextran, the cells were fixed and proceeded for the synaptotagmin immunolabeling. Results of sequential staining of dextran and synaptotagmin confirm the specificity of dextran uptake. This experiments proofs that the dextran has been taken up by the vesicle cycling at the synaptic terminals of the dissociated mouse rod photoreceptors. (Figure 18)

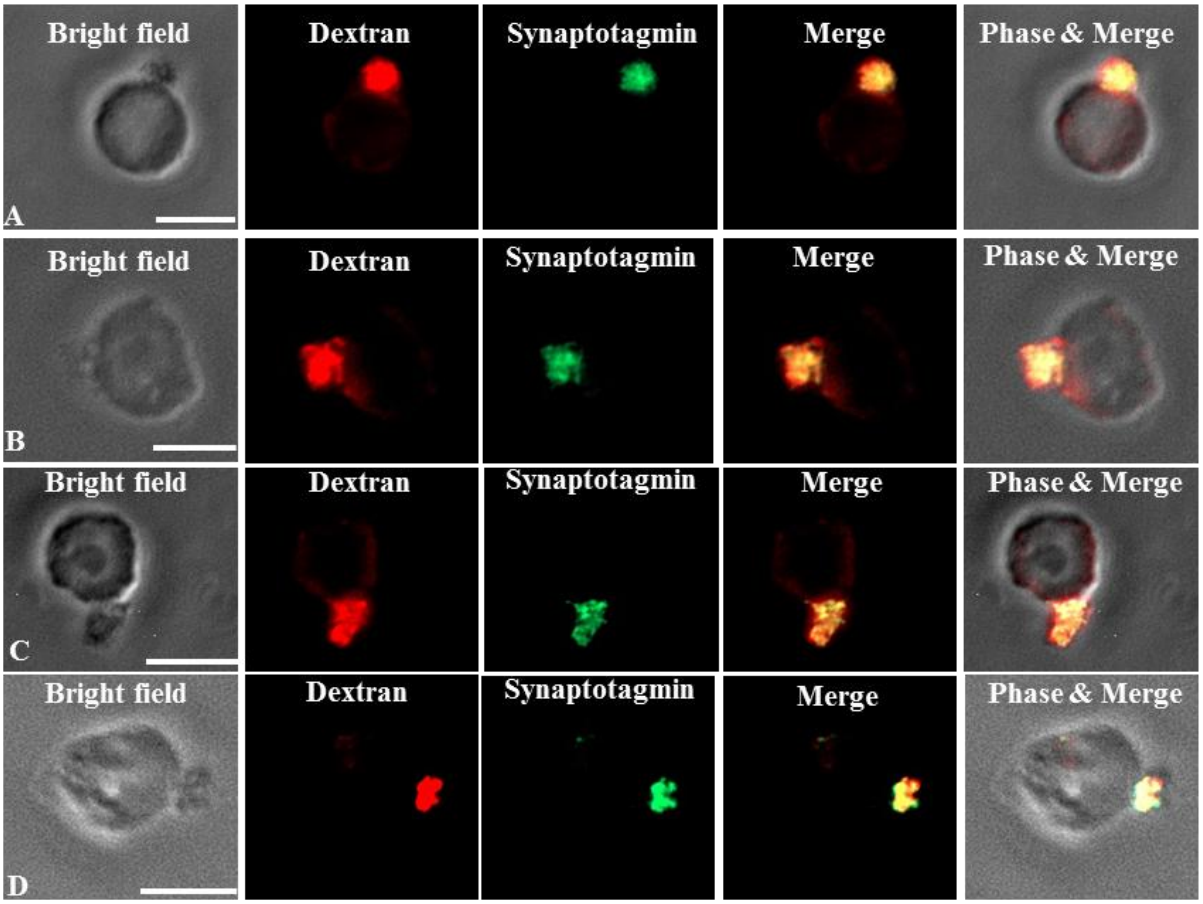

Figure 18. Immunofluorescence labeling of dextran loaded cells. (A-D) *Dextran (red) loaded synaptic vesicales were labeled with antibody against synaptotagmin (green) in the synaptic terminals of the isolated rod photoreceptors. Scale bars: 5µm*

The staining of lysotracker indicated presence of acidic compartment in the synaptic terminals of dissociated rod photoreceptor cells (Figure 19). In the control experiment of lysotracker assay, there was no uptake in the synaptic terminal of the cells which confirmed the specificity of the lysotracker uptake in the cells (Figure 20).

Dextran and Lysotracker uptake in the isolated mouse rod photoreceptors indicated that the cells were not well morphologically intact but physiologically they are active. The enzymatical and mechanical isolation of the mouse rod photoreceptors were not affecting the viability and vitality of the cells.

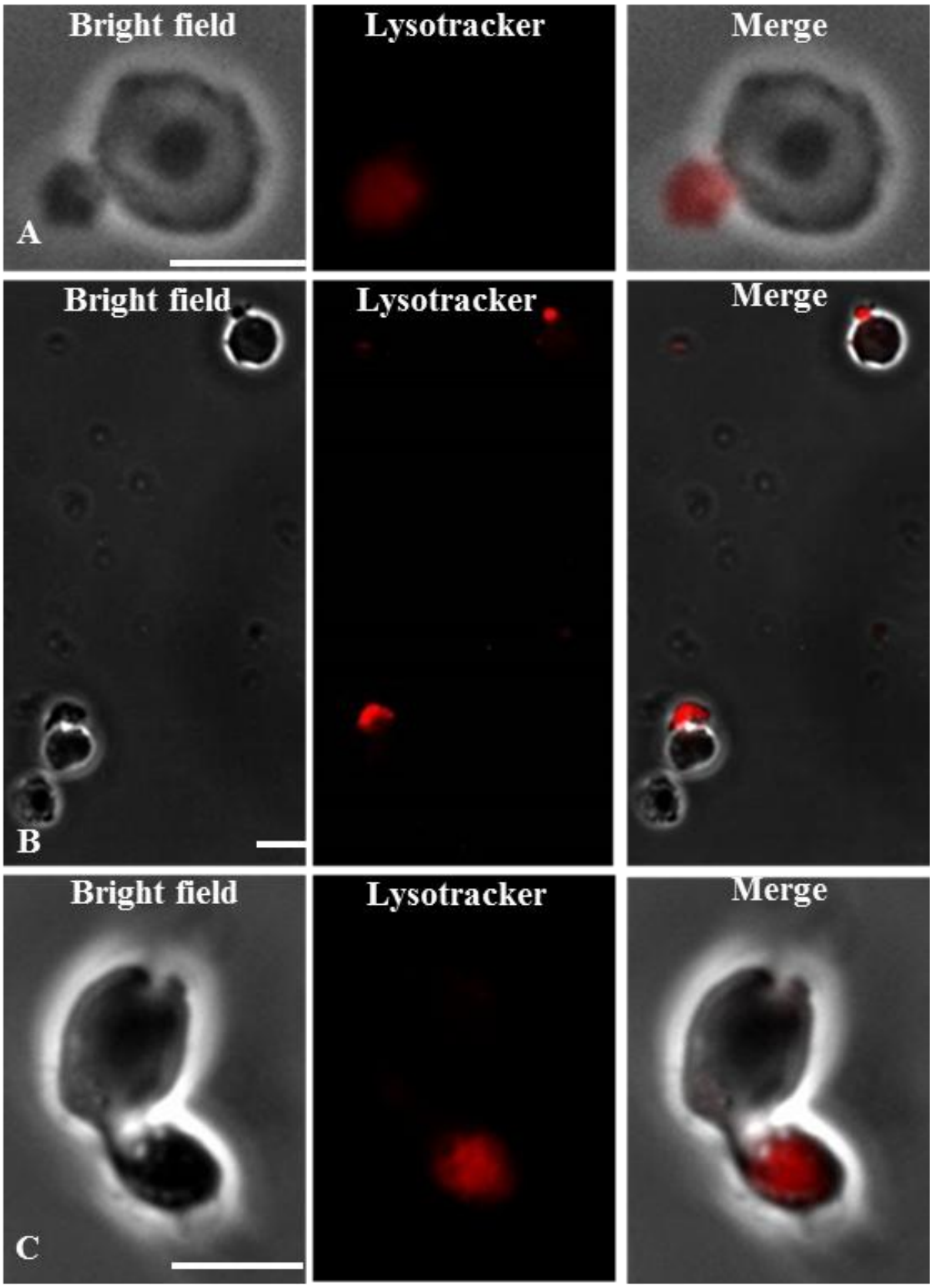

Figure 19 . Lysotracker uptake in rod photoreceptors obtained by pronase isolation method. (A-C) *Synaptic vesicles were labeled with lysotracker (red) in the synaptic terminal of the isolated rod photoreceptors. Scale bars: 5µm*

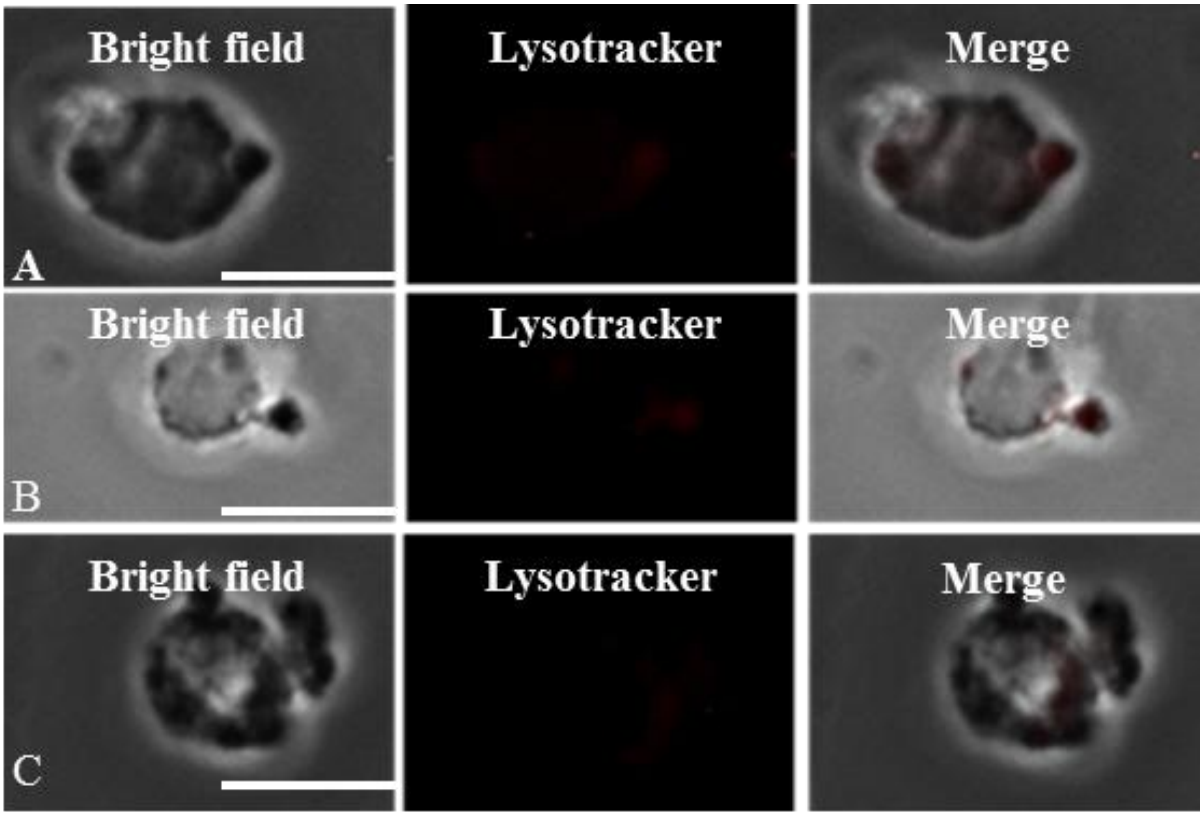

Figure 20. Lysotracker uptake in sodium azide treated rod photoreceptors obtained by pronase isolation method. (A-C) *Uptake of lysotracker is completely abolished in sodium azide pre-treated cells. Scale bars: 5µm*

3.4.2 Endocytosis of papain dissociated rod photoreceptors

Further, I did endocytosis assay by using sulforhodamine (SR101) and FM1-43. This experiments determined that the papain obtained isolated rod photoreceptors are able to retained their physiological activity and synaptic ribbon complex is a hot spot of endocytic activity.

3.4.2.1 Sulforhodamine uptake assay

I performed endocytotic assay by using a fluid phase marker SR101 as described in material and methods. The terminals of the cells were filled with sulforhodamine (SR101) as compared to cell body. This experiment confirmed that the cells are physiologically active. If the cells were incubated with the sulforhodamine (SR101) for long time (20 min) at 37^{o}C, SR101 labeled full terminal in a diffuse manner (Figure 21).

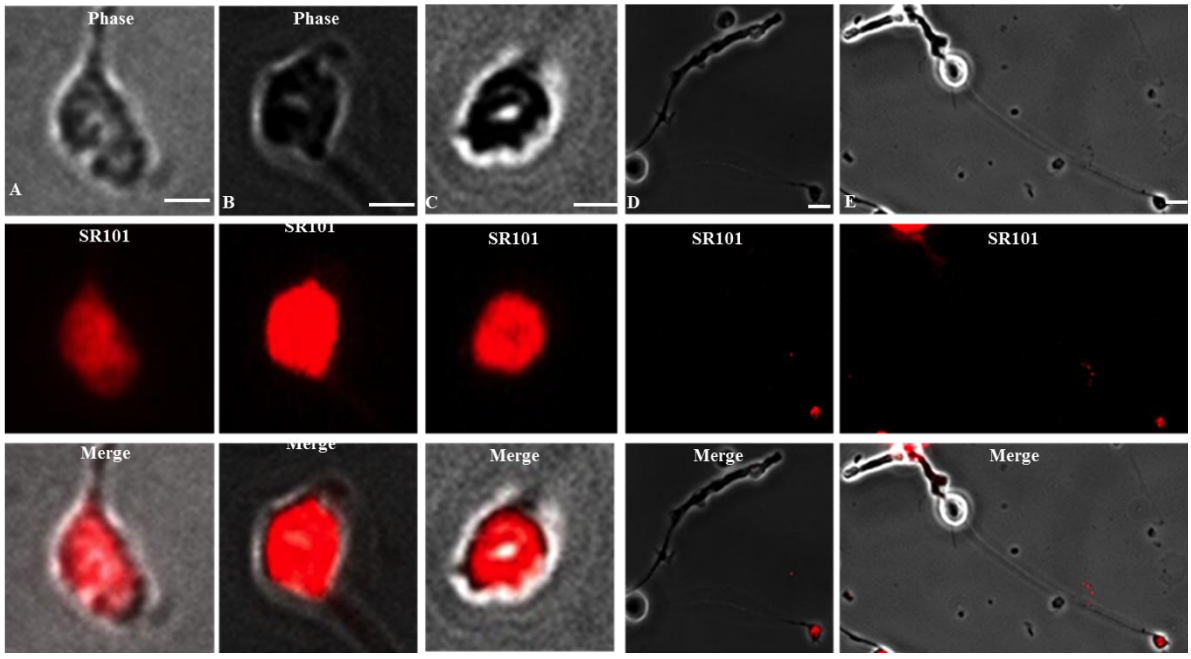

Figure ***21. Long incubation of sulforhodamine (SR101) in papain treated rod photoreceptors. (A-E)*** *Synaptic terminal were completely labeled with SR101 (red) of the isolated rod photoreceptors obtained by papain. Scale bars: 1µm* ***(A-C)*** *and 5µm* ***(E & F)***

In the case of the isolated rod photoreceptors obtained by papain were incubated with SR101 for 2 min. SR101 was taken up by fluid phase endocytosis and a hot spot of SR101 were found in the synaptic terminal of the cells. (Figure 22) To demonstrate the localization of hot spot of SR101, fixed cells were labeled against RIBEYE to label synaptic ribbon (Figure 24). I found that hot spot of SR101 was present in close vicinity of the synaptic ribbon which indicated ribbon-associated endocytosis in the isolated rod photoreceptors (Wahl et al., 2013).

In control experiments, dynasore pre-treated cells showed a complete inhibition of SR101 uptake. (Figure 24)

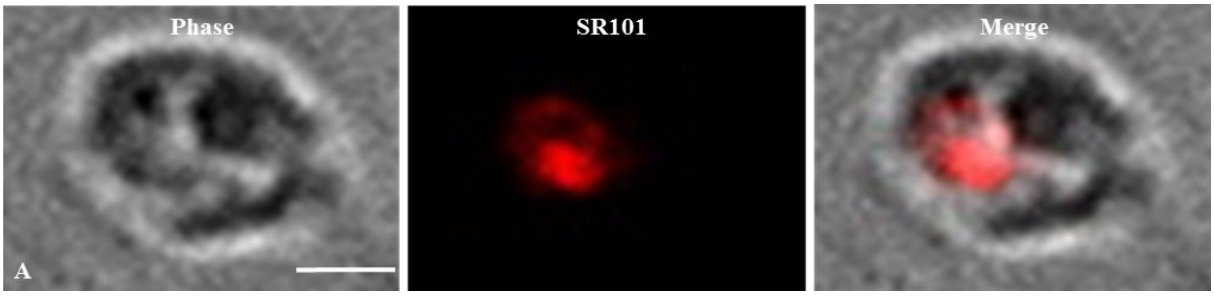

Figure ***22. Short pulse of sulforhodamine (SR101) in papain treated rod photoreceptors. (A)*** *The isolated rod photoreceptors obtained by papain were incubated with SR101 for 2 min. SR101 is taken up by fluid phase endocytosis and presented as a hot spot in the synaptic terminal of the cells. Scale bars: 1µm*

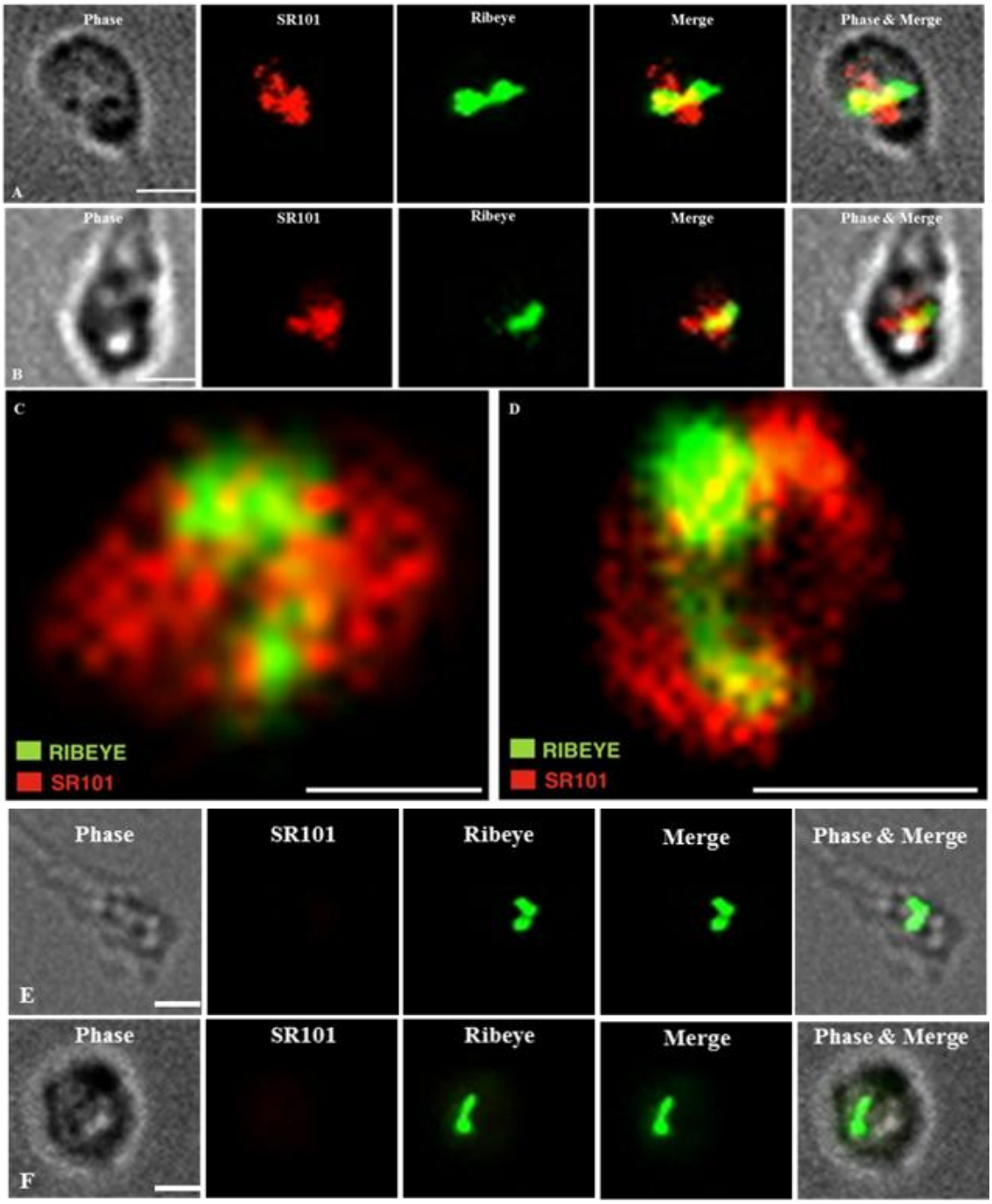

Figure ***23. Ribbon-associated endocytosis and localization of the SR101. (A-F)*** *Sulforhodamine (red) loaded cells were fixed and the synaptic ribbon labeled with RIBEYE (green).* ***(A-D)*** *A hot spot of SR101 uptake is found in close association to the synaptic ribbon.* **(A, B, E&F)** *obtained by conventional imaging;* ***C*** *and* ***D*** *are maximum projections of z-stacks from confocal imaging. In* ***(E-F),*** *synaptic ribbon-associated uptake of SR101 was completely inhibited in the dynasore treated isolated rod photoreceptors. Scale bars: 1µm* ***(A- F) (Wahl et al., 2013).***

Furthermore, I did double immunolabeling of the isolated rod photoreceptors with antibodies against dynamin and ribeye to check localization of dynamin in the synaptic terminals of the solitary cells (Wahl et al., 2013). This is shown in Figure 24.

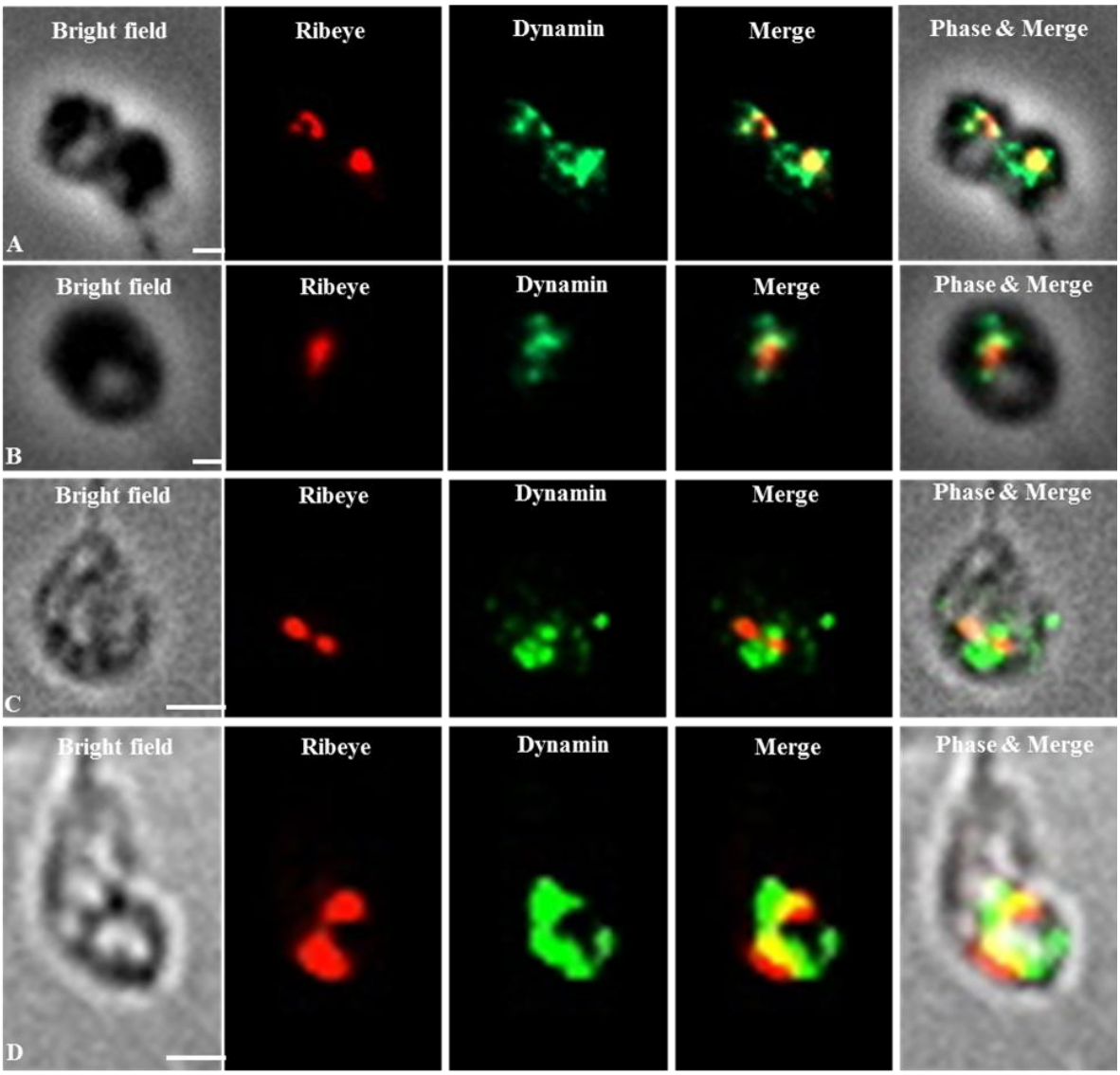

Figure ***24. Localization of Dynamin in synaptic terminal of isolated rod photoreceptors. (A-D)*** *Isolated photoreceptors from the mouse retina were double-immunolabelled with antibody against dynamin (green) and RIBEYE (red).Dynamin is highly enriched in close vicinity to the synaptic ribbon. Scale bars: 1µm*

I performed sulforhodamine (SR101) uptake assay in the isolated rod photoreceptors of Tulp1 mice (control and KO). Cells were isolated at p16 age of the mice (Tulp1 Knockout and littermate control mice) by papain isolation methods as described in material and methods. These experiments showed that isolated rod photoreceptors are a good system to study endocytosis in isolated conditions (Figure 25).

In two separate control experiments, cells were pre-treated with dynasore to inhibit dynamin dependent endocytosis and pre-incubated with cobalt to block the Ca^{2+}

entry through voltage gated calcium channels to inhibite uptake of SR101 in the synaptic terminal of the cells. (Figure 25)

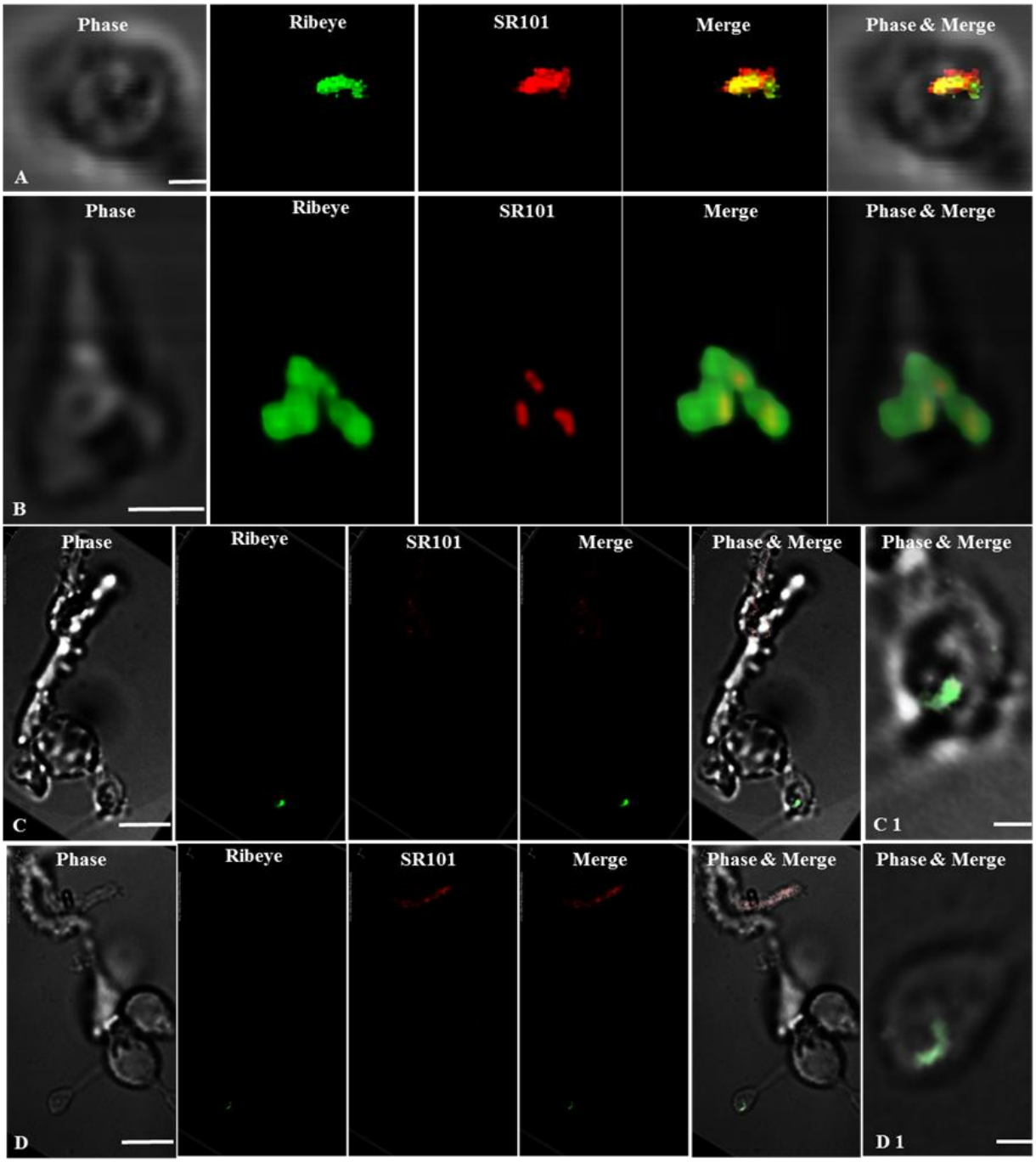

Figure ***25. Sulforhodamin uptake assay in Tulp1 Knockout mice and in littermate control mice.*** *Sulforhodamin(SR101)was shortly incubated in rod photoreceptors isolated from P16 day old control and Tulp1 knockout mice (from the same litter).* ***(A)*** *Intense uptake of SR101 (red) in control cells was found in close vicinity of the synaptic ribbon. The synaptic ribbon was labeled with anti-RIBEYE (green) antibody. Uptake of SR101 is completely abolished in rod photoreceptors isolated from Tulp1 knockout mice* ***(B).*** *Uptake of SR101 was inhibited by using dynasore, a specific dynamin inhibitor* ***(C)*** *and calcium channel blocker* Co^{2+} ***(D).*** *Scale bars: 1µm* ***(A&B)*** *and 5µm* ***(C&D). (B)*** *is volume view of 3D image of confocal microscopy.*

3.4.2.2 FM1-43 uptake assay

In these experiments, I dissociated mouse retina with papain to obtain isolated rod photoreceptor. In the first step, I determined that the isolated cells are physiologically active and retain endo- and exo-cytosis. In one set of experiments, I loaded isolated retina with FM1-43 as described in material and methods and then dissociated the retina to get isolated rod photoreceptors. In other experiment, I incubated isolated cells for 20 min with FM1-43. In both methods, I got approximately same kind of specific labelling of the dye in the synaptic terminals of the isolated rod photoreceptors. This revealed that isolated rod photoreceptors obtained by papain retained vesicle recycling. I found that longer incubation with FM1-43 resulted in diffuse localizations of the dye in the whole terminal of the cells (Rea et al., 2004). This is probably based on the high mobility (Figure 26)

In contrast to long incubation (20min), short incubation (5min) of FM1-43 in isolated rod photoreceptors resulted in a hot spot of the dye in the synaptic terminal. Short pulse of FM1-43 indicated that FM1-43 predominantly taken up in immediate vicinity to the synaptic ribbon in the synaptic terminal of the cells. (Figure 27)

Solitary rod photoreceptors could also be used from electroporated retinas. This is an important tool to measure the consequences of protein overexpression or knockdown. This was exemplified in retinas that were electroporated with ArfGAP3-mcherry (or control m-cherry). ArfGAP3 is an interacting partner of RIBEYE (B).
Using solitary rod photoreceptors from ArfGAP3-mcherry retinas, we could show how ArfGAP3 regulate endocytic vesicle trafficking. This is shown in Figure 28. In this experiment, FM1-43 was incubated as described in the material and methods and cells were isolated by papain dissociation method (Dembla et al. 2014).

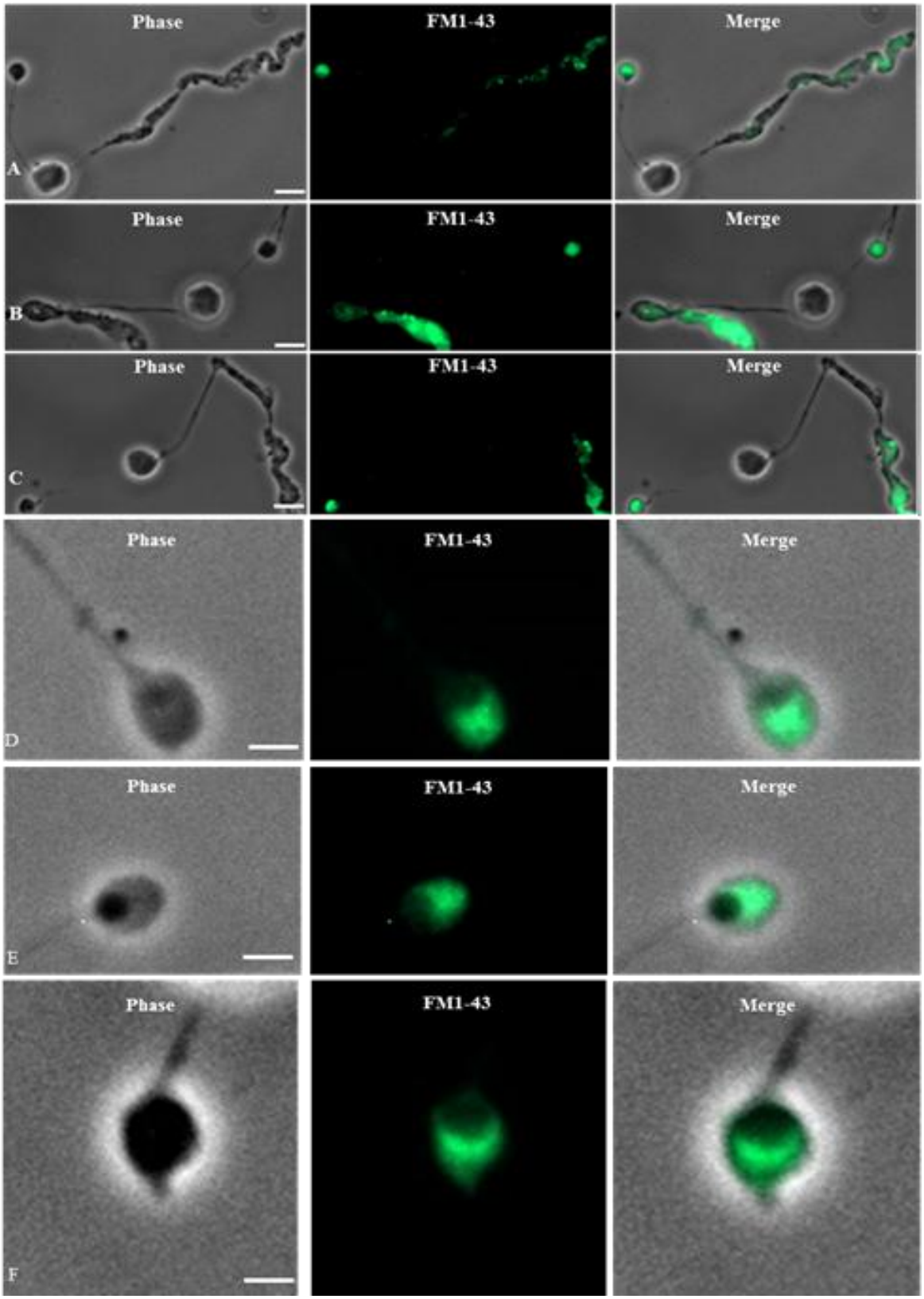

Figure ***26.*** ***Endocytosis in papain treated rod photoreceptors.*** *FM1-43 (green) as endocytosis marker in the synaptic terminal of the rod photoreceptors.* ***(A-B)*** *FM1-43 uptake in isolated rod photoreceptors of preloaded retina with the dye and* ***(B-F)*** *FM1-43 labeling in isolated rod photoreceptors. Scale bars: 5µm* ***(A - C)*** *and 1µm* ***(A1 – C1)***

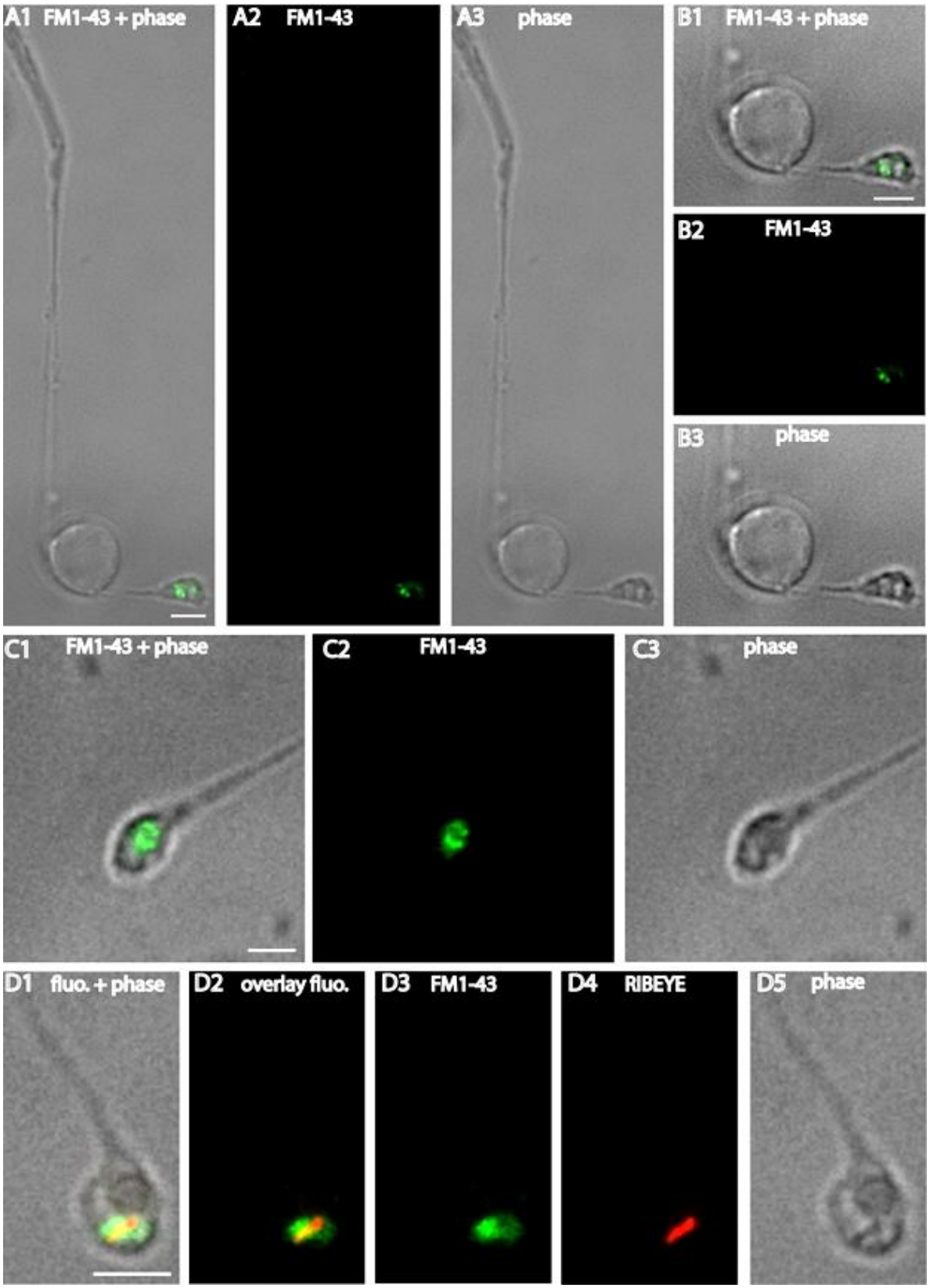

Figure ***27. Focal endocytic uptake of FM1-43. (A-D)*** *Short incubation with FM1-43 (green) in isolated photoreceptors resulted in focal uptake close to synaptic ribbon.* ***(D)*** *Isolated rod photoreceptor showing uptake of FM1-43(green) and synaptic ribbon labeled with anti-RIBEYE (red). Scale bars: 5µm*

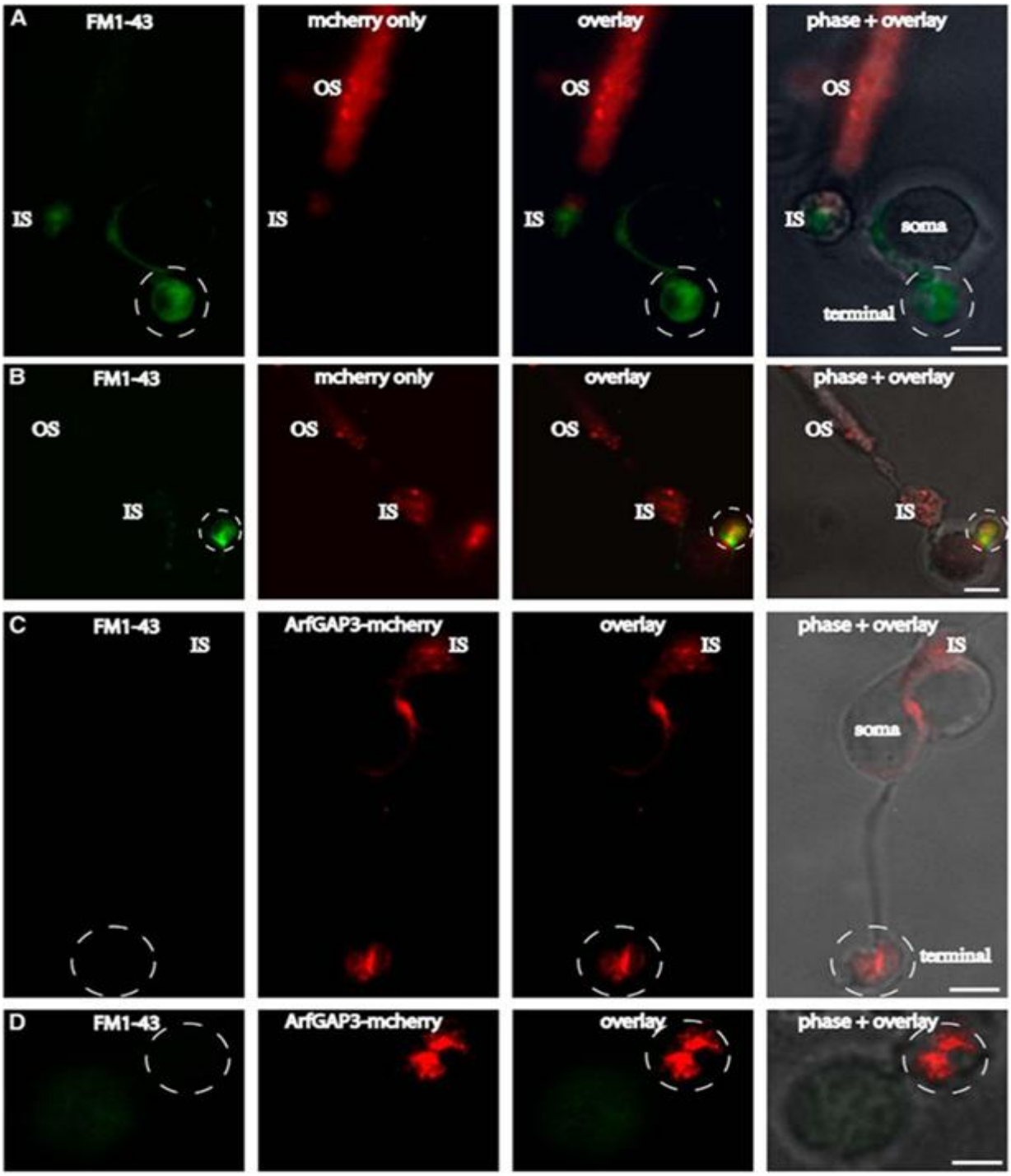

Figure 28. FM1-43 uptake in electroporated retina*. FM1–43 was used to compare endocytic uptake in isolated rod photoreceptors obtained by papain dissociation of electroporated retina. Retinas were electroporated either with mcherry alone* ***(A, B)*** *or ArfGAP3-mcherry* ***(C, D)****. In rod photoreceptors from mcherry-electroporated retinas, there was an intense uptake of FM1–43 in the synaptic terminals* ***(A, B)****. In contrast, rod photoreceptors from ArfGAP3-mcherry-overexpressing showed a strong inhibition of FM1–43 uptake in the synaptic terminals* ***(C, D)****. OS, Outer segment; IS, inner segment; Scale bars:* ***A–C****, 1 μm;* ***D****, 0.75 μm.* ***(Dembla et al. 2014).***

3.4.2.3. Characterization of FM1-43 loaded endocytotic vesicles

In this experiment, I have checked localization of endocytotic vesicles labeled with FM1-43 in the synaptic terminal of the isolated rod photoreceptors obtained by papain. Further, I did immunolabelling in the dye-loaded cells with anti-synaptotagmin to label synaptic vesicles. I found that 90-95% of the synaptotagmin labeled vesicles co-localized with FM1-43 labeled endocytosed vesicles. (Figure 29)

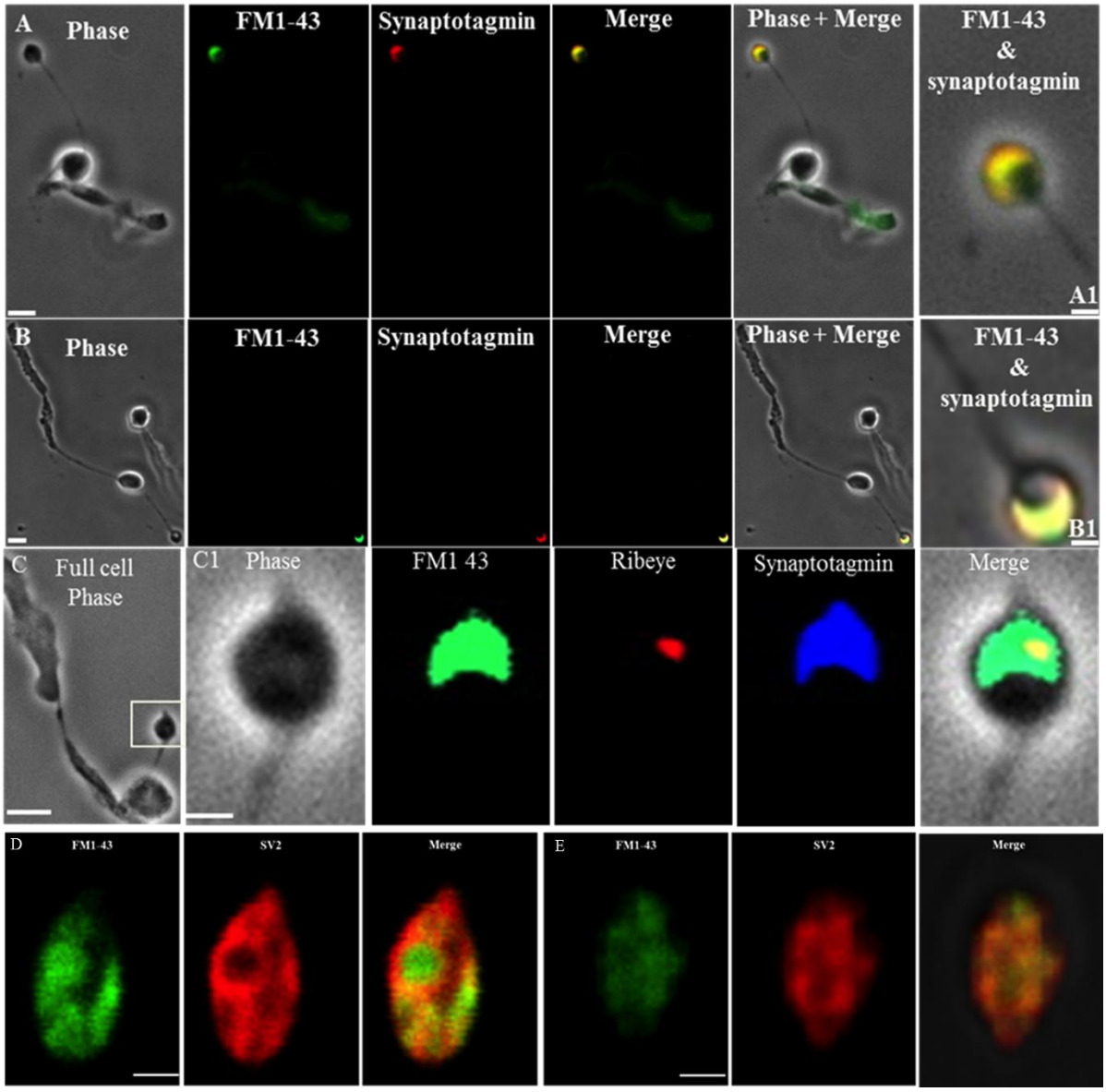

Figure ***29. Localization of endocytosed vesicles in papain treated rod photoreceptors. A,B,D&E*** *show that FM1-43 loaded endocytosed vesicles (green) were co-localized with the synaptic vesicles (red) in synaptic terminal of the isolated rod photoreceptors.* ***(C)*** *Shows co-localization of synaptic vesicles labeled with antibody against synaptotagmin (blue) and FM1-43(green), synaptic ribbon is labeled with anti-RIBEYE (red).* ***A-C*** *was obtained by conventional imaging and* ***D-E*** *was obtained by confocal imaging. Scale bars: 1µm* ***(A-E)*** *and 5µm* ***(C1)***

3.4.3 Ca^{2+} imaging in solitary rod photoreceptor of mouse retina

In order to further evaluate the viability of solitary mouse rod photoreceptors, I performed Ca^{2+} -imaging analyses with Fura-2AM as described in the material and methods. Cells were depolarized with 50mM KCl that resulted in an increase in depolarized calcium influx in the synaptic terminal of the cells. This indicated that in isolated rod photoreceptors there is no disruption of the channels during isolation process. Figure 30 shows a data from a single isolated rod photoreceptor.

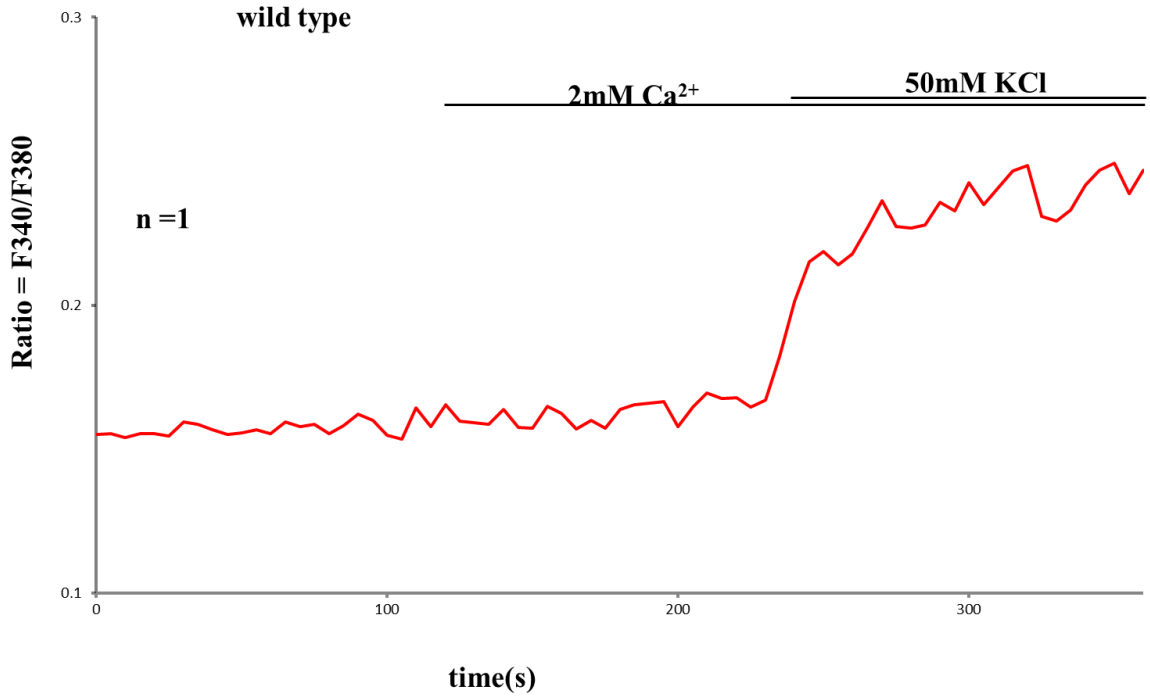

Figure *30.* *Fura-2AM measurement of papain treated rod photoreceptors. (A)* *Radiometric Ca^{2+} imaging of synaptic terminal from a single isolated rod photoreceptor cell. Graph shows F340/F380 (i.e. intracellular calcium) at external low Ca^{2+} and depolarization- evoked Ca^{2+} increase in the synaptic terminal of the cell.*

The usefulness of isolated mouse photoreceptors for characterization of synaptic function was analysed in collaboration with the lab of Prof. Dr. Veit Flockerzi in analyzing Cavβ2-deficient mice (Katiyar et al., 2015). To evaluate the physiological significance of isolated rod photoreceptor cells, I did Fura-2AM imaging in the isolated rod photoreceptors from β2 deficient mice. I found that basic calcium levels (Fura2 F_{340}/F_{380} ratio) were not different in the cells isolated from wild type and ecmβ2knockout mice, but a major reduction of depolarized-induced Ca^{2+} influx

indicating disruption of functional voltage gated calcium channels.

This experiment also revealed that the isolated rod photoreceptors provided a clear and convincing data at higher resolution which are not based from feedback responses of secondary neurons. (Figure 31)

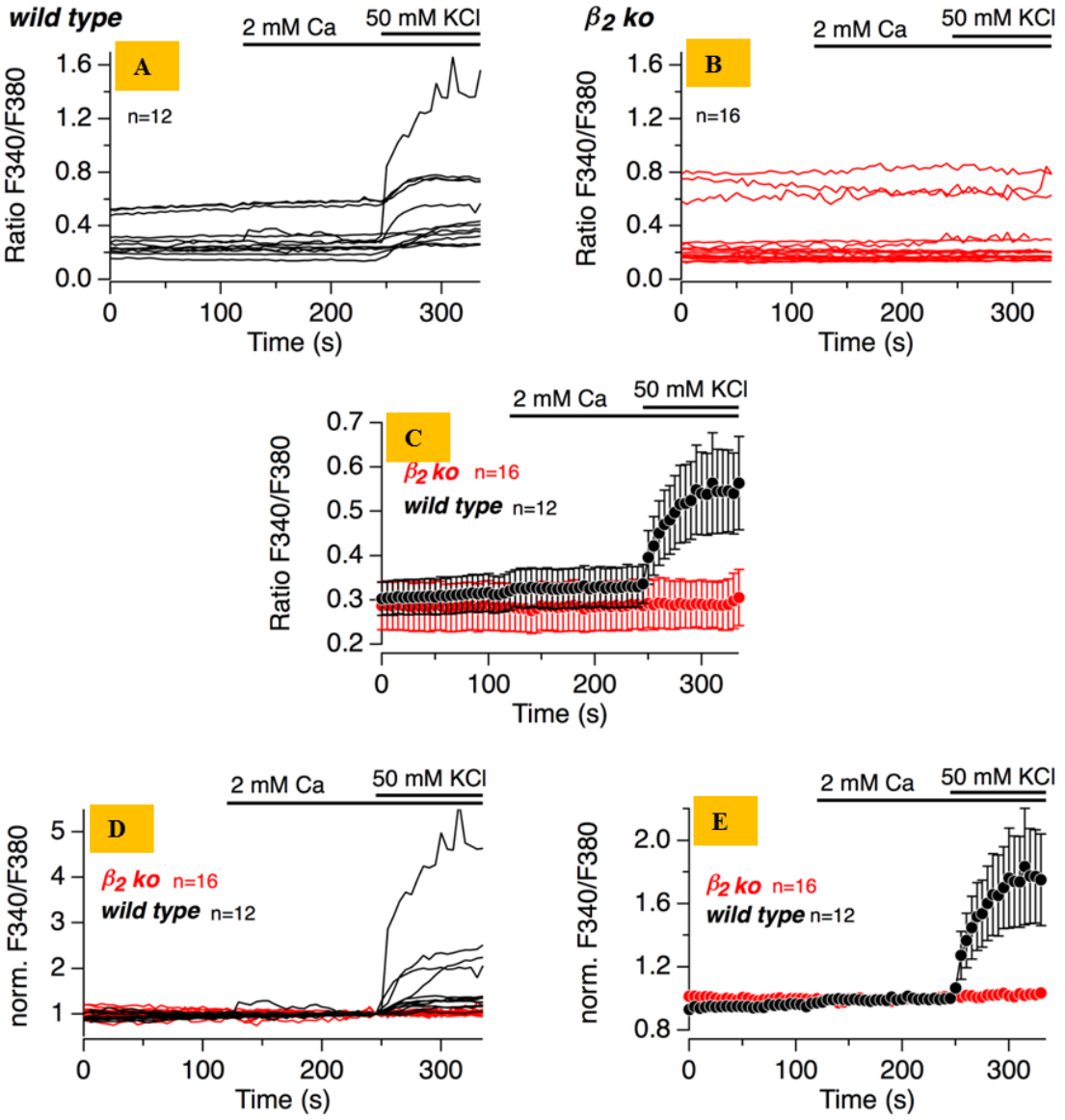

Figure ***31. Radiometric Ca^{2+} imaging from Fura-2AM loaded synaptic terminals of isolated rod photoreceptors of wild type and ecβ2 KO. (A-D)****Cells were bathed in low Ca^{2+} solution and then 2mM Ca^{2+} and 50mM KCl were added as indicated. Graphs show F340/F380 (i.e. intracellular calcium) at external low Ca^{2+} and depolarization- evoked Ca^{2+} increase in the synaptic terminal of the cells.* ***(A)*** *Single traces of measurement of cells isolated from wild type mice and ecβ2 KO mice* ***(B). (C)*** *Average of all single cell Fura-2 measurement graph from wild type and ecβ2 KO cells.* ***(D)****Changes of Fura-2 F340/F380 ratio normalized to the ratio right before application of 50mM KCl and* ***(E)*** *Average of normalized value. (*Katiyar et al., 2015)

3.5 Localisation of Ribeye in dissociated rod photoreceptors of Ribeye- RFP mice

I isolated rod photoreceptors from retinas of Ribeye-RFP mice via papain isolation method. To confirm the localization of Ribeye –RFP, I labelled the cells with anti-RIBEYE. Figure 32 show a proper co-localization of the endogenous Ribeye protein with expressed transgenic RFP-tagged Ribeye protein.

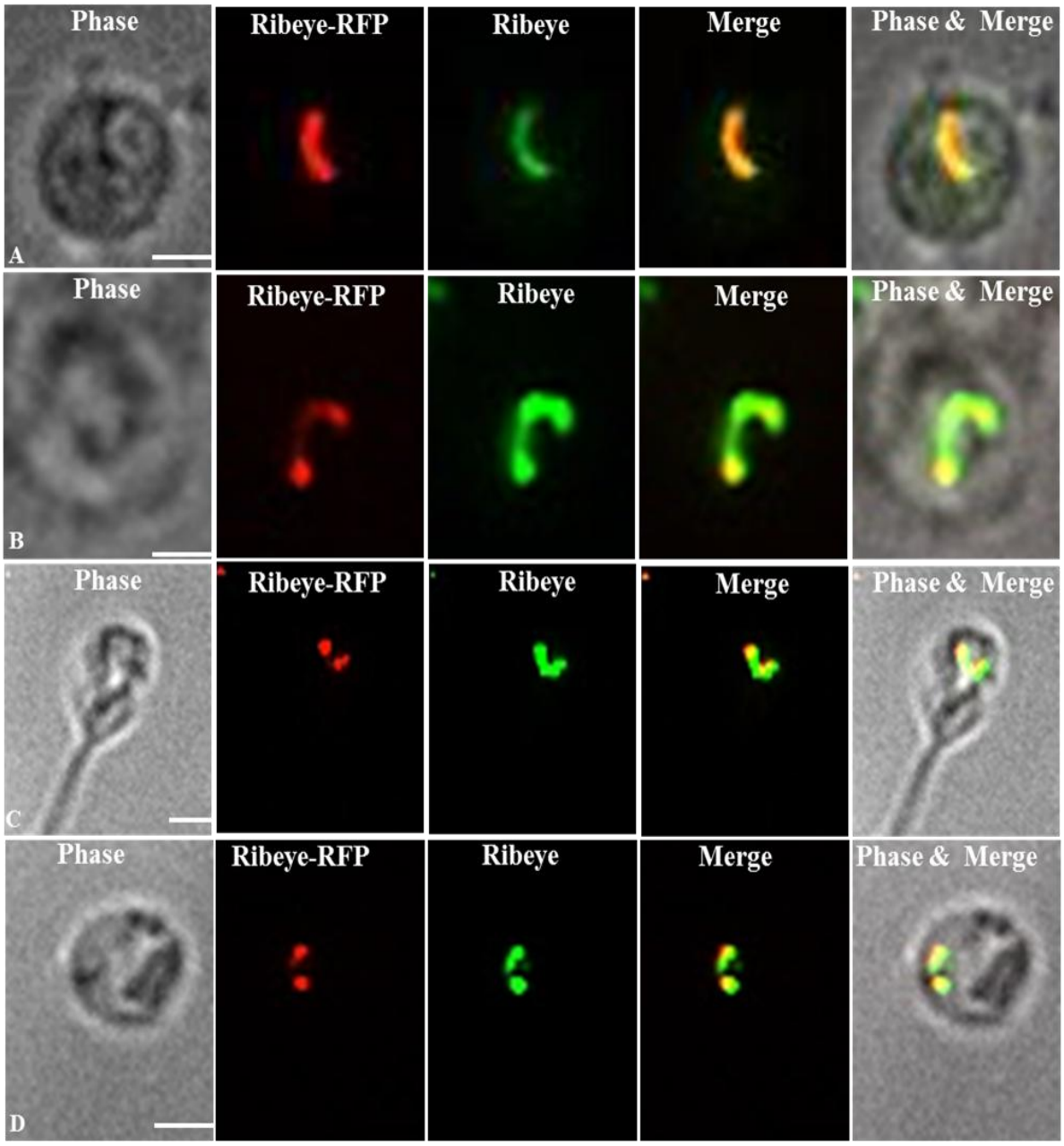

Figure *32.* ***Localization of endogenous RIBEYE with transgenically expressed RIBEYE with RFP- tag in papain treated rod photoreceptors. A-D*** *show co-localization of endogenous RIBEYE (green) with expressed rfp tagged transgenic RIBEYE (red) in the isolated rod photoreceptors obtained by papain.Scale bars: 1µm*

3.6 Characterization of Fluo-4AM labeled structure in the synaptic terminals of the papain dissociated rod photoreceptors

Solitary rod photoreceptors are useful to study intracellular Ca^{2+} - stores (not only VGCC) as I demonstrated in the subsequent analysis. The Fluo-4AM loaded (as described in material & methods) cells were fixed with EDAC to characterize the structure which is intensely labeled with the dye in the synaptic terminal of the cells (Figure 33).

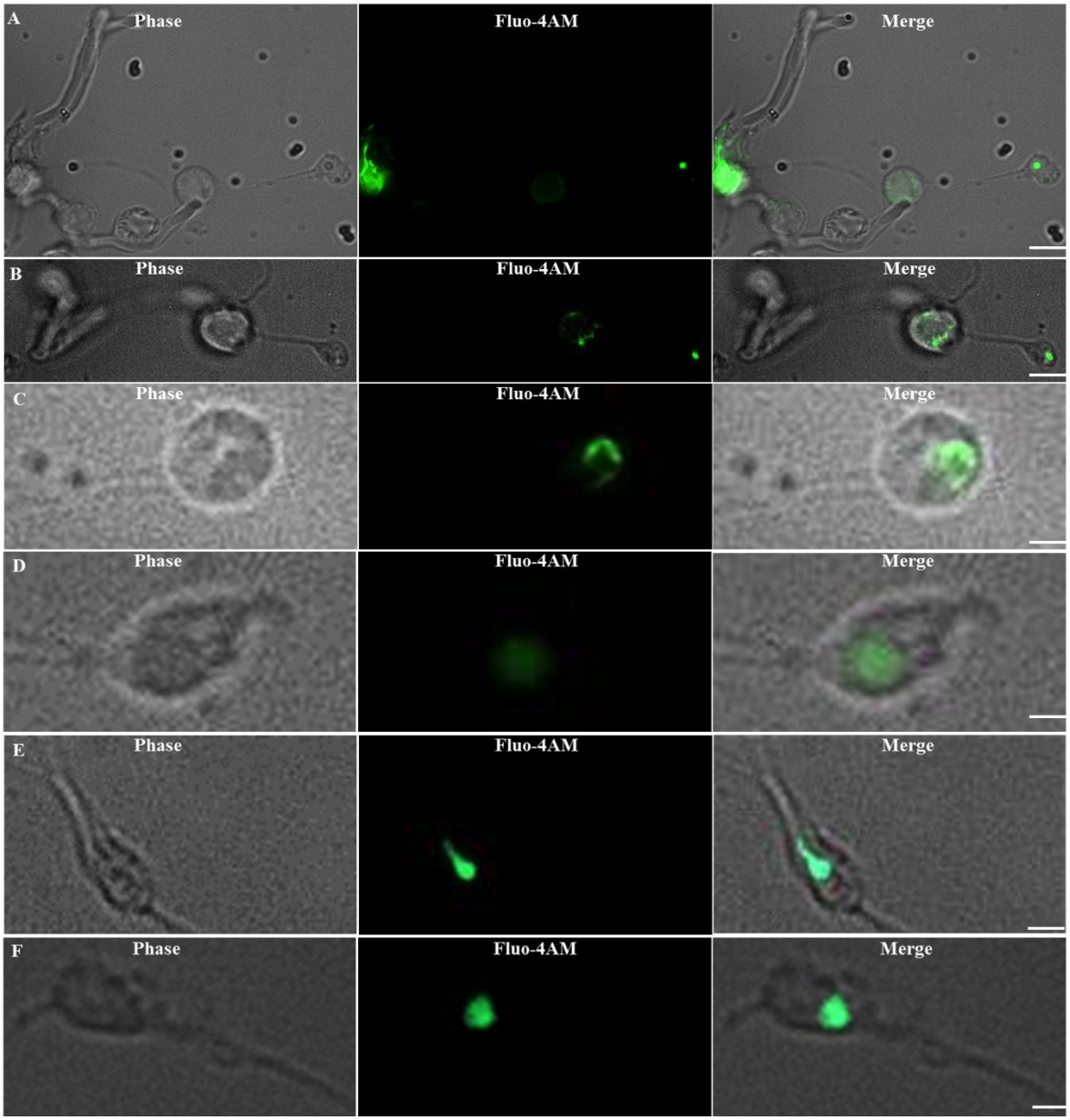

Figure ***33. Fluo-4Am uptake in papain treated rod photoreceptors. (A-F)*** *Fluo-4AM loaded isolated rod photoreceptors obtained by papain show intense labeled structure in the synaptic terminal. Scale bars: 1µm* ***(C-F)*** *and 5µm* ***(A & B).***

3.6.1 Characterization of Fluo-4AM-labeled structure by immunofluorescence with different marker antibodies

In the first step, I performed immunolabelling in the dye-loaded cells. I used antibody against RIBEYE to label the synaptic ribbon and to find whether the Fluo-4AM labeled structure is localized with ribbon. I found that the structure which is labelled with Fluo-4AM is not co-localized with synaptic ribbon. (Figure 34)

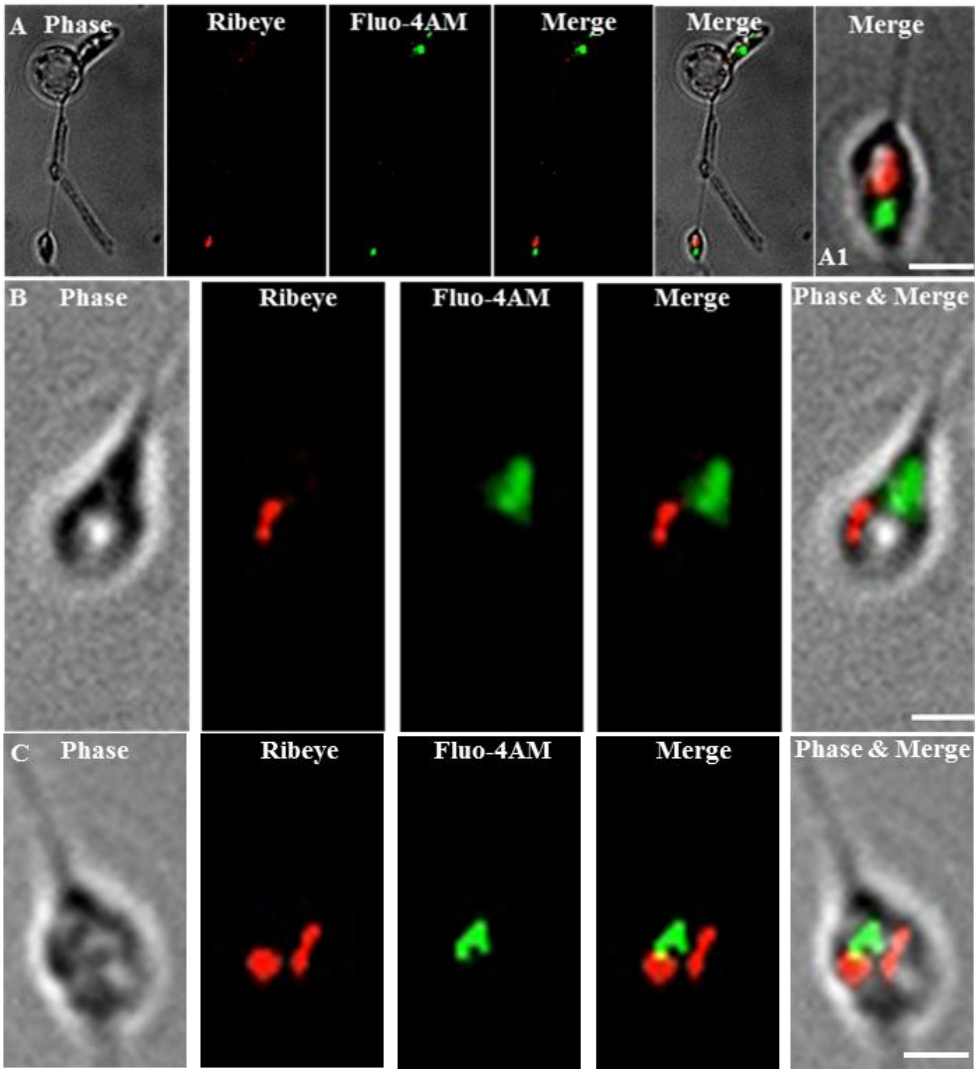

Figure ***34. Characterization of Fluo-4Am labeled structure in papain treated rod photoreceptors. (A-C)*** *Synaptic ribbon labeled with anti-RIBEYE (red) in synaptic terminal of the Fluo-4AM (green) loaded isolated rod photoreceptors Scale bars: 1µm* ***(A-C)***

In next experiment, I did double immunolabelling in the dye-loaded cells. I used antibody against RIBEYE to label the synaptic ribbon and SV2 to label synaptic vesicles. I found that the structure labelled with Fluo-4AM was not co-localized with

synaptic vesicles. (Figure 35)

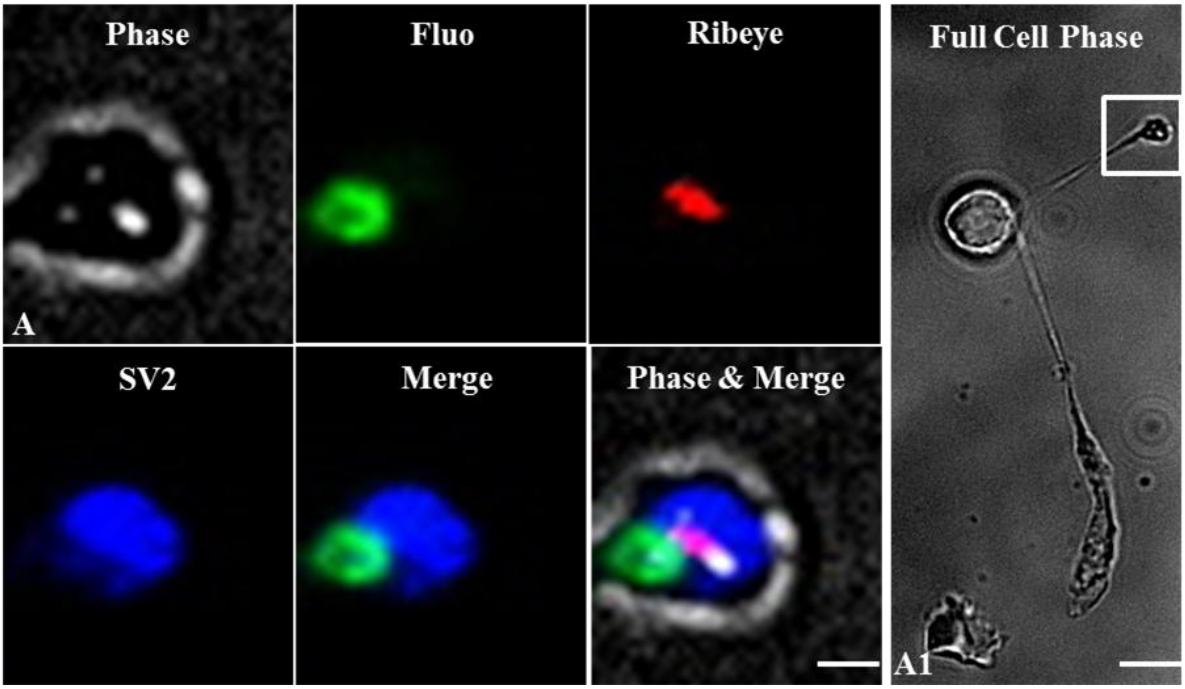

Figure ***35. Characterization of Fluo-4Am labeled structure in papain treated rod photoreceptors. (A)*** *Synaptic vesicles were labeled SV2 (blue) and ribbon labeled with RIBEYE (red) in synaptic terminal of the Fluo-4AM (green) loaded isolated rod photoreceptors Scale bars: 1µm* ***(A)*** *&* *5µm* ***(A1)***

In next experiment, I used early endosomal marker EEA1 (early endosomal Antigen 1) to characterize the localization of the Fluo-4AM labeled structure in the synaptic terminal of the cells. I found that the Fluo-4AM labeled structure is not a part of endosomal compartment. (Figure 36)

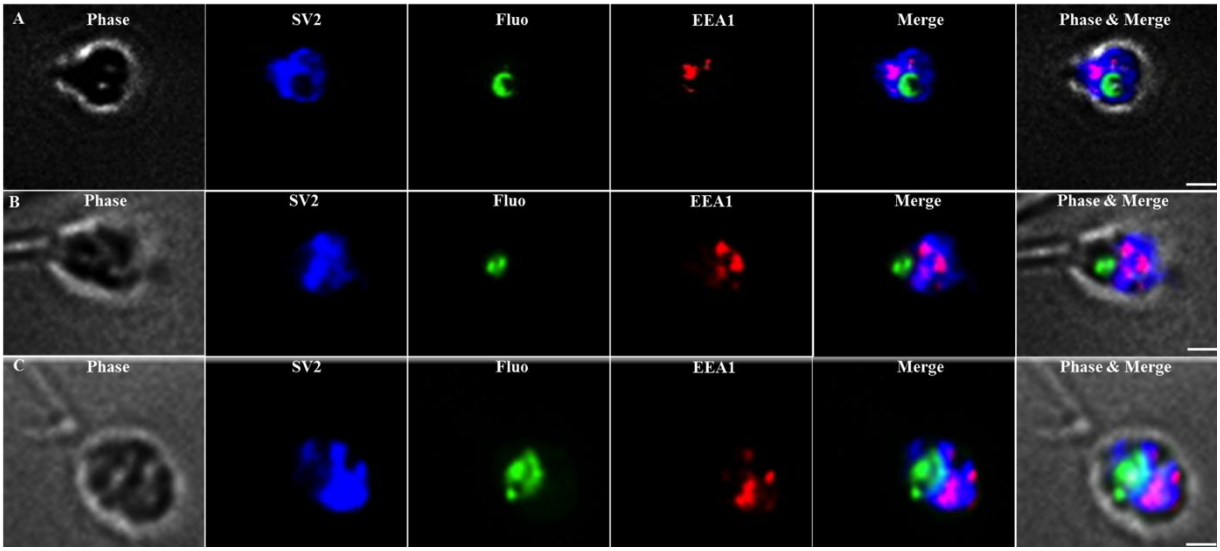

Figure ***36. Characterization of Fluo-4Am labeled structure in papain treated rod photoreceptors. (A-C)*** *Synaptic vesicles were labeled anti-SV2 (blue) and early endosomes were labeled with anti-EEA1 (red) in synaptic terminal of the Fluo-4AM (green) loaded isolated rod photoreceptors Scale bars: 1µm* ***(A-C)***

Further, I used anti- SERCA2 immunolabeling to characterize the localization of the Fluo-4AM labeled structure in the synaptic terminal of the cells. SERCA2 is an intracellular pump located in the endoplasmic reticulum. I found 80-90% co-localization of the signals of SERCA and Fluo-4AM. This indicated that Fluo-4AM labeled structure could be a part of endoplasmic reticulum. (Figure 37)

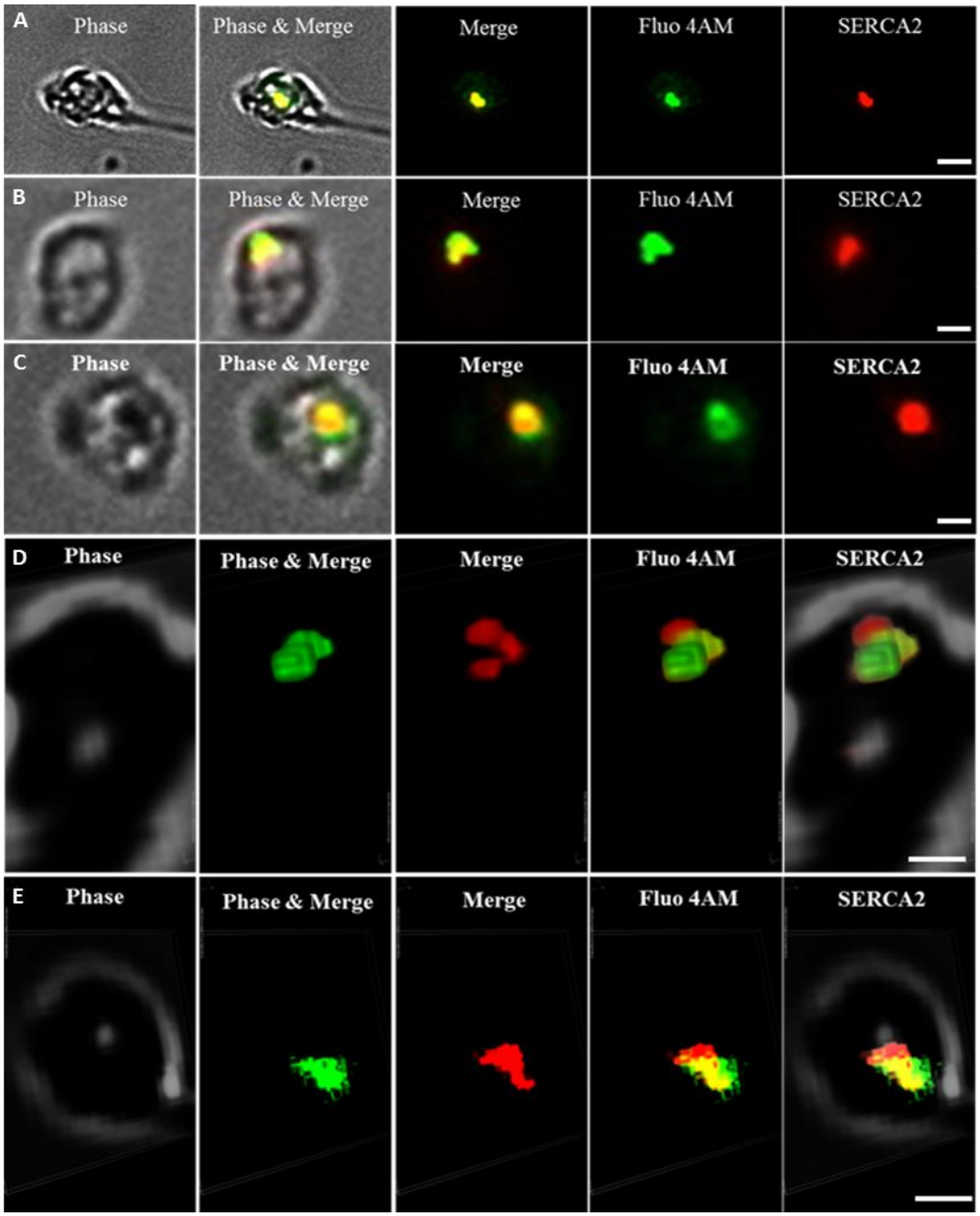

Figure *37.* ***Characterization of Fluo-4Am labeled structure in papain treated rod photoreceptors.*** ***(A-E)*** *shows SERCA 2 labelling (red) in synaptic terminal of the Fluo-4AM (green) loaded isolated rod photoreceptors.* ***(A-C)*** *were obtained by conventional imaging and* ***(D&E)*** *were obtained by confocal imaging and the volume. Scale bars: 1µm* ***(A-E)***

3.6.2 Confirmation of Fluo-4AM labeled structure as part of ER by using ER tracker dye

In this experiment, I sequentially incubated cells with ER tracker dye and Fluo-4AM as described in the material and methods. I found 90-95% co-localization with staining of ER tracker dye and Fluo-4AM labelled structure (Figure 38). This confirmed that Fluo-4AM labelled structure is ER-related.

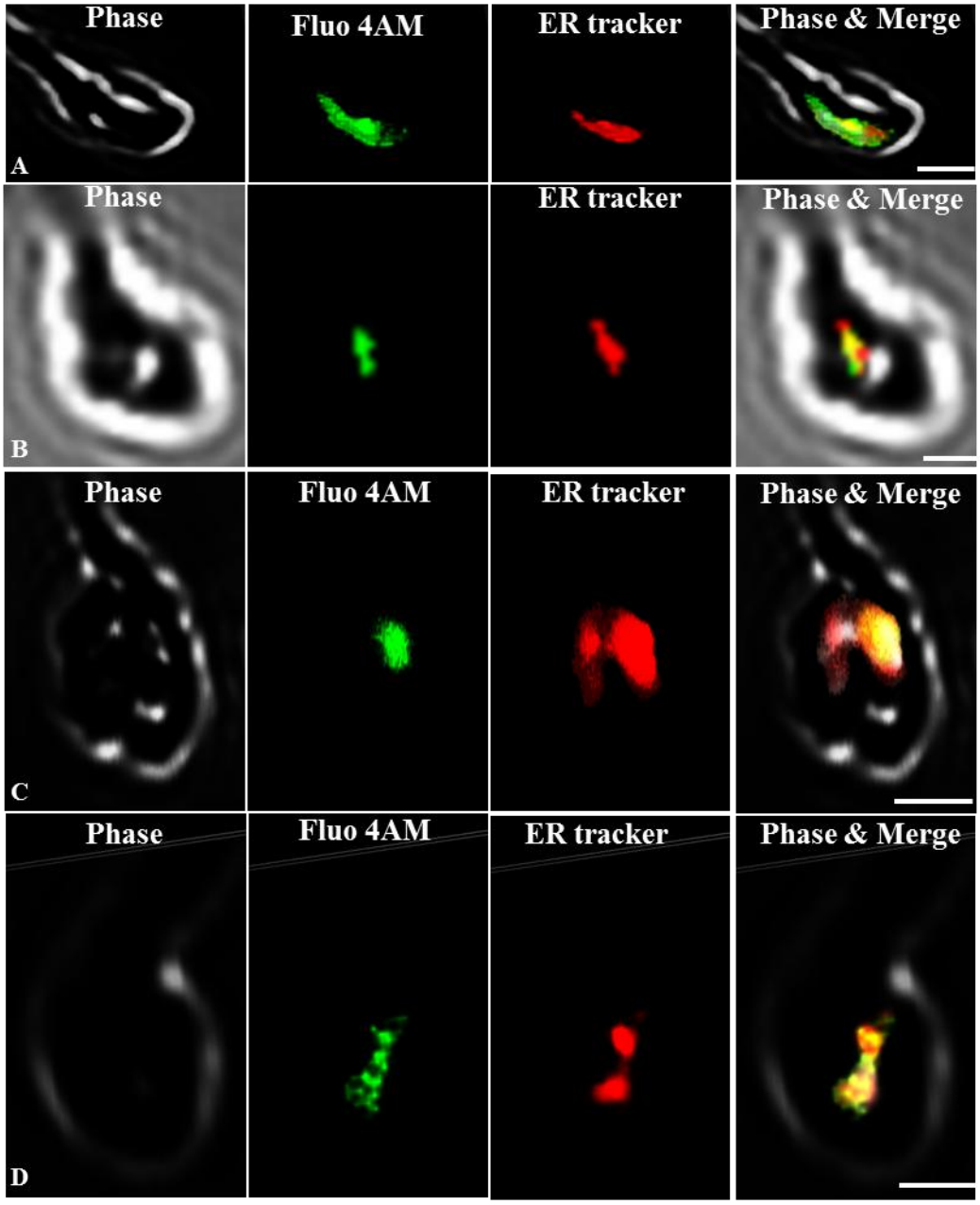

Figure ***38. Characterization of Fluo-4Am labeled structure in papain treated rod photoreceptors. (A-E)*** *show ER tracker labeling (red) in synaptic terminals of the Fluo-4AM (green) loaded isolated rod photoreceptors.* ***(A-D)*** *are volume view of confocal images. Scale bars: 5µm* ***(A-D)***

3.7 Intracellular Ca^{2+} stores and calcium release in the synaptic terminal of the papain dissociated rod photoreceptors from Ribeye-RFP mice.

In these experiments, I dissociated Ribeye-RFP mouse retina with papain to obtain isolated rod photoreceptor. The cells were incubated with Fluo-4AM as described in material and methods.

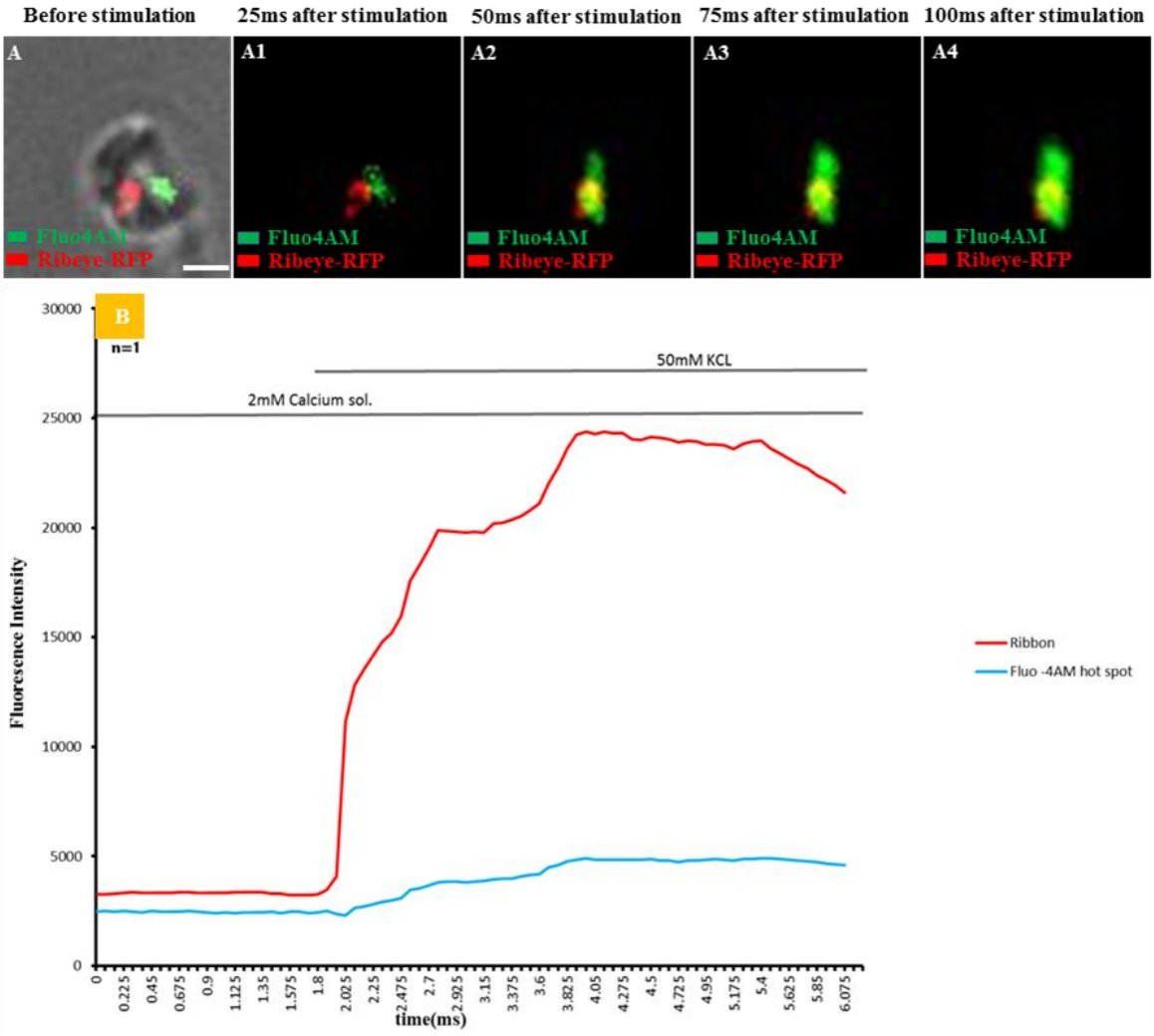

Figure ***39. Fluo4AM measurement of papain treated rod photoreceptors isolated from Ribeye-RFP mouse retina.*** *(A) Synaptic terminal labeled with Fluo-4AM (green) and containing fluorescent ribbon (red).* ***(A1-A4)*** *differnet time point during* Ca^{2+} *imaging****.(B)*** Ca^{2+} *imaging of synaptic terminal from a single represented isolated rod photoreceptor cell. Graph shows depolarization- evoked* Ca^{2+} *increase in the synaptic terminal of the terminal. Scale bars: 2µm*

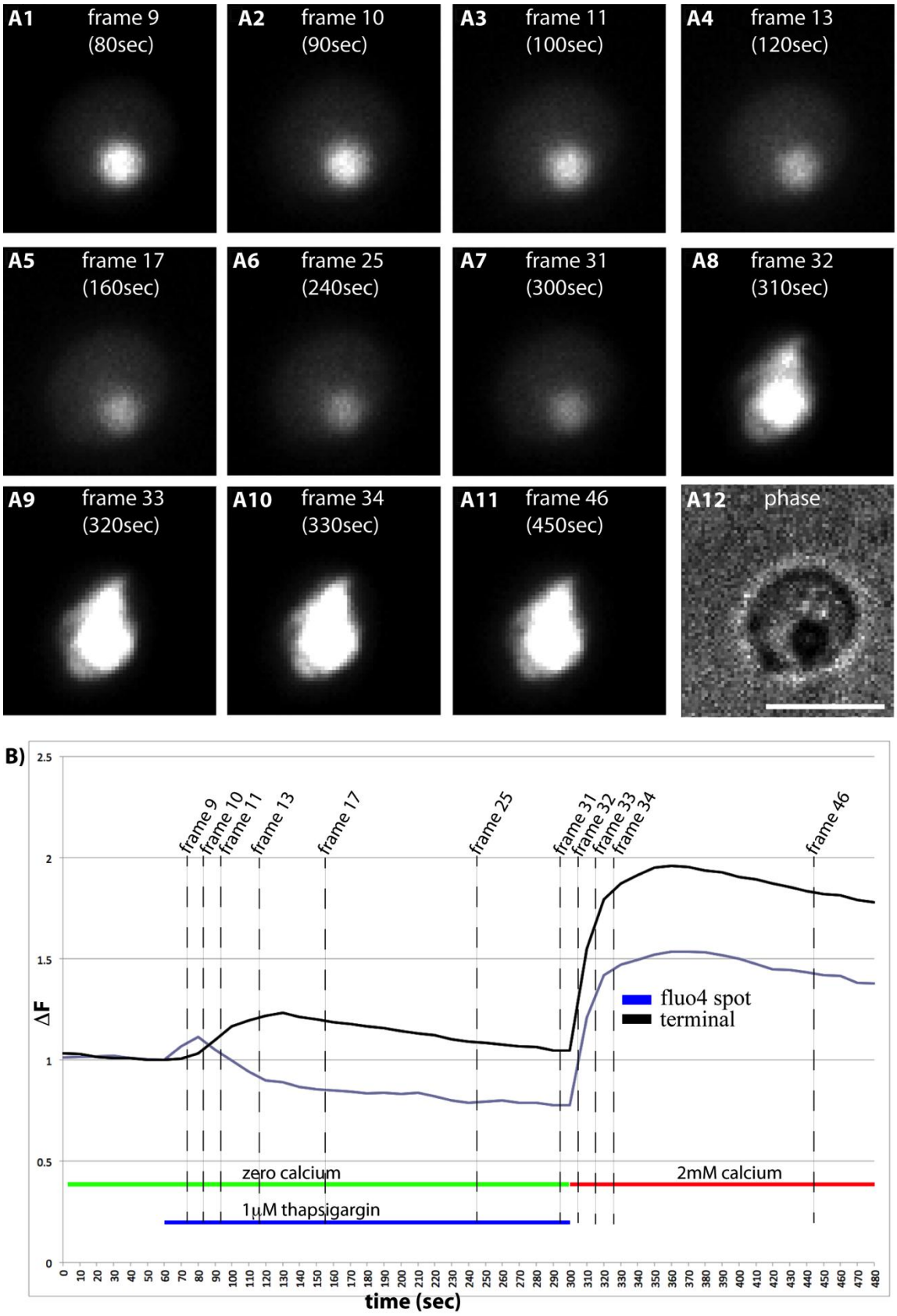

Figure *40.* *Depletion of Fluo-4AM hot spot and refilling.* *Rod photoreceptors were isolated from RIBEYE-RFP tagged mice by using papain. Graph from representative single cell shows that depletion of hot spot of Fluo4AM with Thapsigargin and refilling with 2mM Ca^{2+} .Scale bars:2μm*

In the first set of experiments, the Fluo-4 AM loaded cells were depolarized with high potassium solution to facilate Ca^{2+} entry through voltage gated channels. I found that there is more Ca^{2+} release by ER-related calcium source (hot spot of Fluo-4AM) in comparison to the Ca^{2+} entered through the voltage-gated channels (Figure 39). I have analyzed 20 isolated rod photoreceptors.

In the other set of experiments, the Fluo4AM loaded cells were first treated with thapsigargin to deplete the internal store of calcium and then 2mM calcium solution were added to refill the stores as shown in figure 40. I have analyzed 15 isolated rod photoreceptors.

3.8 Physiological evidence of more calcium release from internal stores in comparison to the calcium entering through calcium channels in the synaptic terminal of the papain dissociated rod photoreceptors.

Further, I did exocytosis assay with FM1-43 loaded cells. The rod photoreceptors were isolated from RIBEYE-RFP mice. In two independent experiments, cells were depolarized with high K^+ (10 isolated cells were analyzed) or internal stores were depleted with caffeine (10 isolated cells were analyzed). In control experiment (6 isolated cells were analyzed), I blocked Ca^{2+} channels with cobalt (Figure 41).

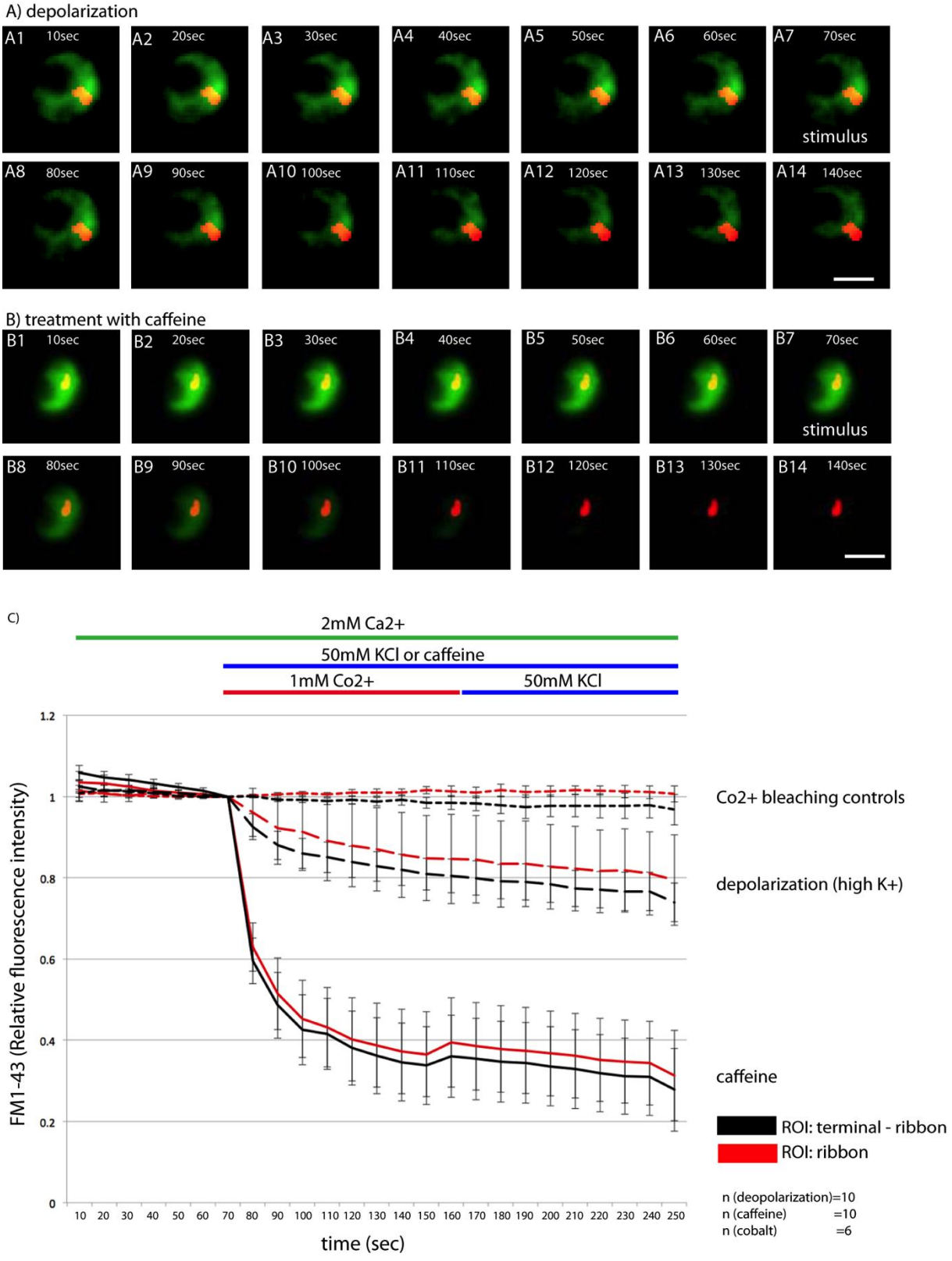

Figure *41.* ***Exocytosis measurements.*** *Rod photoreceptors were isolated from RIBEYE-RFP tagged mice by using papain. Synaptic terminal labeled with FM1-43 (green) and containing fluorescent ribbon (red). Average graph of all single cells. Scale bars: 2µm*

CHAPTER 4
DISCUSSION

In the sensory organ, eye, the innermost layer of photosensitive tissue consists of photoreceptor and bipolar cells which face the challenge to sense and transmit sensory stimuli over a broad range of stimulus intensities. To maintain high release rates these cells need a dynamically adjustable, efficient, and tightly coupled synaptic machinery. Ribbon synapses carry a specialized electron dense key structure, synaptic ribbon, which is immobilizing numerous synaptic vesicles next to presynaptic release sites (Schmitz, 2009; Sterling et al., 2005). Multiple functions have been proposed to synaptic ribbon including roles in exocytosis, endocytosis, and synaptic membrane trafficking. To understand molecular and functional organization of ribbon synapse of rod photoreceptor of mouse retina isolated cells are good choice in comparison of retinal slices. Retinal slices have limitations in term of feedback response of other neurons in comparison to solitary cells.

There are two main outcomes of the present study. First, solitary rod photoreceptors obtained by isolation methods are intact and physiologically active, providing a useful tool to analyze the structural and functional organization of ribbon synapse. Second, evidences of the presence of ER-related calcium source and their functional role at presynaptic terminal of rod photoreceptors of mouse retina.

4.1. Intact and physiologically active solitary mouse rod photoreceptors can be used as study tool.

As a prominent component of my work, initially I aimed to obtain isolated, intact rod photoreceptors from mouse retina. Therefore, the conditions to dissociate mouse retina were optimized by me. On the basis of experimental observation, it had been demonstrated that the cell density of isolated intact rod mouse photoreceptor depends up on the number of various factors such as concentration of the enzyme used for digestion, incubation time and temperature for digestion. Mostly two types of

enzymes, pronase and papain were used in various studies to isolate the cells from the mouse retina (Lolley et al, 1998). To isolate photoreceptor cells from retina of various species papain is commonly used (Krizaj et al., 1998; Steele et al., 2004). I compared pronase and papain to isolate the rod photorecptors from mouse retina. Suspension of dissociated retinal tissue contained a mixture of all retinal cells. However, the dissociation methods used in this study predominately yielded rod photoreceptors. Dissociation of the retinal tissue with pronase yielded photoreceptor cells having only soma and synaptic terminal. On the other hand, the retina digested with papain yielded a higher number of intact rod cells strongly adherent on Concavalin-A coated glass coverslips. It has been studied that the coating material of the glass coverslips plays an important role to adhere the specific cells on it (MacLeish et al., 1988).

In my experimental work, I used retina from different age group animals which could be freshly isolated or genetically manipulated (e.g. electroporated retina). I found that the concentration of papain and incubation time to digest retina is highly dependent on the age of the animal. During isolation of the cells from electroporated retina, I observed that the isolation process is needed to be modified and needed low concentration of the papain and short incubation time of the retina with the papain.

Isolated rod photoreceptors obtained from isolation methods were identified by using immunofluorescence technique demonstrating the presence of a single synaptic ribbon in the synaptic terminal. The electron micrograph of the solitary rod photoreceptors, proper localization of calcium channels at the active zone and synaptic proteins in the synaptic terminals of the cells reveal that the isolation processes were able to retain the integrity as similar to its counterpart in the intact retina.

It has been shown by morphological and physiological data that synaptic ribbon is important for continuous fusion of synaptic vesicles and for sustained release by providing a large pool of primed release vesicles (von Gersdorff 2001; Sterling et al., 2005; Heidelberger et al., 2005). Recent studies proposed that synaptic ribbon play an important role in endocytosis too. To avoid synaptic depression a balance of exocytosis and endocytosis is needed (Schweizer et al., 2006; Wu et al., 2007; Smith et al., 2008). I analyzed by experimental data of uptake assays that there is accumulation

of lysotracker dye and dextran specifically in the synaptic terminal of solitary rod photoreceptors obtained by pronase dissociation method. Lysotracker is a fluorescent acidotropic probe known to label acidic compartment of cells (e.g. endosomes or synaptic vesicles) (Becherer et al., 2003) and florescence-tagged dextran is a fluorescent marker of fluid phase endocytosis (Wenda et al., 1998). The control experimental data for Lysotracker uptake assay and immunoflorscence data where most of the synaptotagmin labels vesicles colocalised with the dextran labelled vesicles. This supported that the lysotracker and dextran uptake has done by the vesicle cycling at the synaptic terminal of the cells. These experiments indicated that the cells dissociated by pronase method are viable and physiologically active. Furthermore, the endocytic uptake of fluid phase marker sulforhodamine (Lichtman et al., 1985; Keifer et al., 1992; Teng et al., 1999; Takahashi et al., 2002; Euler et al., 2009; Nimmerjahn et al., 2004).and synaptic vesical marker FM1-43 (Rea et al., 2004; Betz et al., 1992, 1996; Cochilla et al., 1999) in the cells obtained by papain dissociation methods confirmed their viability and synaptic physiological activity. The control experiments with dynasore (Macia et al., 2006; Kirchhausen et al., 2008; van Hook et al., 2012) and cobalt (Chen et al., 2013) provided the supportive evidence to this finding.

I concluded from above findings that the cells obtained by the pronase and papain dissociation methods are viable and physiological active. However, the morphological appearance of the cells obtained by papain dissociation method is better in comparison with the pronase dissociation method. Papain dissociated cells were easy to identify. These experimental demonstrations suggested me to follow papain dissociation method for further experimental studied of my project.

Furthermore, I demonstrated that the solitary rod photoreceptors can be used as a useful tool to study ribbon associated endocytosis and presynaptic signaling (Wahl et al, 2013; Dembla et al., 2014; Katiyar et al., 2015).

4.2. Presynaptic intracellular Ca^{2+}-stores of the mouse rod photoreceptors.

It has been proposed that the presynaptic $[Ca^{2+}]_i$ in photoreceptor terminals is controlled by various mechanisms. These include $[Ca^{2+}]_i$ – influx through voltage-gated calcium channels and Ca^{2+} - release from the ER (e.g., Ca^{2+} -induced Ca^{2+}-release). In ribbon synapse of photoreceptors and hair cells, the role of Ca^{2+} stores is particularly prominent (Babai et al., 2010; Cadetti et al., 2006; Lelli et al, 2003; Suryanarayanan, 2006). In the present study, I found evidence for an additional relevant Ca^{2+} -source in mouse photoreceptor terminals. This intra-terminal Ca^{2+}-source is functional and distinct from Ca^{2+}-entry through VGCC at the plasma membrane. Present finding is relevant with the previous EM and X-ray diffraction studies showing the intracellular storage sites in the synaptic terminals which are mainly represented by smooth ER cisternae (Mercurio et al., 1982; Ungar et al., 1984; Peng et al., 1991; Babai et al., 2010).

Consistent with the presence of intracellular Ca^{2+} store in photoreceptor ribbon synapse, Parekh (2011) found that ER is a main intracellular store present in the terminals. It seems to be responsible for calcium-induced calcium-released (CICR) in presynaptic terminals (Verkhratsky, 2005). Further, Shoshan-Barmatz et al. (2005, 2007) found labeling of ryanodine receptor antibodies in the outer plexiform layer of the mammalian retina. It has also been judged by immuno-labelling with antibodies against ER components, e.g., SERCA-2 and SERCA-3, that ER is located close to the synaptic ribbon in the ribbon synapse. My results extended these findings by immune-fluorescent labeling for endoplasmic reticulum protein, SERCA-2. This SERCA protein co-localized with Ca^{2+} hot spot imaged with calcium indicator dye. Immune-florescent labeling for synaptic ribbon protein ribeye revealed the localization of ER as an intracellular calcium store in close proximity to the synaptic release site of the ribbon. Moreover, co-localization of ER-tracker dye and hot spot of calcium indicator dye provides supportive evidence to this finding.

Rod photoreceptors are specialized to operate at the lowest rate of light. Release of Ca^{2+} from intracellular stores is promoted by the constant depolarization of rods in

dark (Krizaj et al., 1999, 2003; Suryanarayanan et al., 2006; Cadetti et al., 2006). To maintain proper basal calcium level in the soma and terminal region of rod cells, CICR worked along with the other mechanisms including voltage-gated and store–operated Ca^{2+} channels (Corey et al., 1984; Szikra et al., 2008). The physiological experiments studied out using salamander retina demostrated that synaptic release from the rod terminal is enhanced by CICR which amplifying the effects of calcium entering through voltage-gated L-type Ca^{2+} channels. The same finding has been observed in mouse retina by using retina slices (Babai et al., 2010). In my studies, I analyzed in an improved way that the physiological signification of the intra-terminal ER-related Ca^{2+} -source by using solitary cells obtained by papain isolation method from the retina of RIBEYE-RFP transgenic mice. The RIBEYE-RFP-tag makes ribbons visible. Calcium imaging data of my work revealed that Ca^{2+} -signals obtained from characterized ER-related intracellular store are considerably bigger than Ca^{2+}- signals via influx of Ca^{2+} through VGCC. This intracellular store can be depleted by application of thapsigargin (Szikra et al., 2008). Exocytosis by using FM1-43 demonstrated that the intraterminal Ca^{2+} -stores could be released by depolarization probably via Ca^{2+} -release (CICR) and also by the application of caffeine.

In short, this experimental data provides a solitary intact system as a valuable tool to study ribbon synapse. This finding suggests that presynaptic terminal of rod photoreceptor contains ER-related calcium store which releases calcium through CICR and make a prominent contribution in synaptic release from rods that are tonically depolarized in darkness.

5. References

- Babai N, Bartoletti TM, Thoreson WB (2010) Calcium-induced calcium release contributes to synaptic release from mouse rod photoreceptors. *Neurosci 165(4):1447-56*
- Bagar T, Altenbach K, Read ND, and Bencina M (2009) Live-Cell Imaging and Measurement of Intracellular pH in Filamentous fungi Using a Genetically Encoded ratiometric probe. *Eukaryotic Cell. 703-712*
- Ball SL, Powers PA, Shin H-S, Morgans CW, Peachey NS, Gregg RG (2002) Role of the β2 subunit of voltage-dependent calcium channels in the retinal outer plexiform layer. *Invest Ophthalmol Vis Sci 43:1595–1603.*
- Bartoletti TM, Jackman SL, Babai N, Mercer AJ, Kramer RH, Thoreson WB (2011) Release from the cone ribbon synapse under bright light conditions can be controlled by the opening of few Ca^{2+} channels. *J. Neurophysiol. 106.*
- Bech-Hansen NT, Naylor MJ, Maybaum TA, Pearce WG, Koop B, Fishman GA, Mets M, Musarella MA, Boycott KM (1998) Loss-of-function mutations in a calcium-channel alpha1-subunit gene in Xp11.23 cause incomplete X-linked congenital stationary night blindness. *Nat Genet 19:264–267.*
- Becherer U, Moser T, Stuhmer W, Oheim M (2003). Calcium regulates exocytosis at the level of single vesicles. *Nat Neurosci 6: 846 -853.*
- Beck A., Nieden RZ, Schneider HP, and Deitmer JW (2004) Calcium release from intracellular stores in rodent astrocytes and neurons in situ. *Cell Calcium 35: 47-58.*
- Berridge MJ, Lipp P & Bootman MD (2000). The versatility and universality of calcium signalling. *Nat Rev Mol Cell Biol 1, 11–21.*
- Betz WJ, Mao F and Bewick GS (1992) Activity-dependent fluorescent staining and destaining of living vertebrate motor nerve terminals. *J.Neurosci.12,363-375*
- Betz S, Mao F and Smith CB (1996) Imaging exocytosis and endocytosis. Curr. *Opin.Neurobiol.6,365-371*

- Brandt A, Khimich D, Moser T (2005) Few Cav1.3 channels regulate the exocytosis of a synaptic vesicle at the hair cell ribbon synapse. *J. Neurosci.* 25 11577–11585
- Burae Z and Yang Y (2010) The β-subunit of Ca^{2+} channels. *Phsiol.Rev.90,1461-1506.*
- Burger PM, Mehl E, Cameron PL, Maycox PR, Baumert M, Lottspeich F, De Camilli P, Jahn R. Synaptic vesicles immunoisolated from rat cerebral cortex contain high levels of glutamate. *Neuron.1989; 3:715–720.*
- Cadetti L, Bryson EJ, Ciccone CA, Rabl K, Thoreson WB (2006).Calcium-induced calcium release in rod photoreceptor terminals boosts synaptic transmission during maintained depolarization. *Eur J Neurosci.23(11):2983-90.*
- Campbell AK (1983) Intracellular Calcium: Its Universal Role as Regulator*edited by Gutfreund H.London: Wiley,1983.*
- Carafolli E and Klee C (1999) Calcium as a Cellular Regulator. *Oxford, Univ. Press.*
- Catterall WA (2011) Voltage-gated calcium channels. *Cold Spring Harb. Perspect. Biol. 3 a00394710.*
- Catterall WA, Perez-Reyes E, Snutch T P, Striessnig J (2005) International union of pharmacology. XLVIII. Nomenclature and structure-function relationships of voltage-gated calcium channels. *Pharmacol. Rev. 57 411–425 10.1124/pr.57.4.5*
- Ceccarelli B, Hurlbut WP, Mauro A (1973) Turnover of transmitter and synaptic vesicles at the frog neuromuscular junction. *J Cell Biol 57:499–524*
- Chang GQ, Hao Y, Wong F (1993) Apoptosis: final common pathway of photoreceptor death in rd, rds, and rhodopsin mutant mice. *Neuron.11:595–605.*

- Chen M, van Hook M , Zenisek D, Thoreson W B (2013). Properties of ribbon and non-ribbon release from rod photoreceptors by visualizing individual synaptic vesicles. *J. Neurosci. 33 2071–2086 10.1523/JNEUROSCI.3426-12.2013*
- Choi SY, Jackman S, Thoreson WB, Kramer RH. (2008). Light regulation of Ca^{2+} in the cone photoreceptor synaptic terminal. *Vis Neurosci 25:693–700.*
- Clapham DE (2007) Calcium signaling. Cell. 131:1047–1058.
- Cochilla A.J., Angleson J.K., and Betz W.J. (1999) Monitoring secretory membrane with FM1-43 fluorescence. *Annu.Rev.Neurosci.22,1-10*
- Cooper NG, McLaughlin BJ (1983) Tracer uptake by photoreceptor synaptic terminals. I. Dark-mediated effects. *J Ultrastruct Res 84:252–267.*
- Corey DP, Dubinsky JM, Schwartz EA (1984) The calcium current in inner segment of rods from the salamander *(Ambystoma tigrimum)* retina. *J Physiol (Lond) 354:557-575*
- Crosson CF, Willis A, Potter D.E., (1990) Effect of the calcium anatagonist, nifedipine, on ischemic retinal dysfunction. J Ocul Pharmacol
- Dembla M, Wahl S, Katiyar R, Schmitz F (2014) ArGAP3 is a component of the the photoreceptor synaptic ribbon complex and forms a NAD(H)-regulated. Redox-sensitive complex with RIBEYE that is importnat for endocytosis. *J Neuroscience 34: 5245-5260*
- Doering, C.J., Peloquin, J. B., and McRory, J.E. (2007). The Ca(v)1.4 channel: more than meets the eye. *Channels(1) 1:3-10*
- Doonan F, Donovan M, Cotter TG (2005) Activation of multiple pathways during photoreceptor apoptosis in the rd mouse. *Invest Ophthalmol Vis Sci. 46:3530–3538.*
- Dowling JE, Werblin FS (1969). Organization of retina of the mudpuppy, Necturus maculosus. I. Synaptic structure. *J Neurophysiol 32: 315–338.*
- Dunlap K, Luebke JI, Turner TJ (1995) Exocytotic Ca2+ channels in mammalian central neurons. *Trends Neurosci 18:89–98.*

- Edward DP, Lam TT, Shahinfar S, Li J, Tso MO (1991) Amelioration of light-induced retinal degeneration by a calcium overload blocker Flunarizine. *Arch Ophthalmol; 109:554–562.*
- Euler T, Hausselt SE, Margolis DJ, Breuninger T, Castell X, Detwiler PB, Denk W (2009) Eyecup scope—optical recordings of light stimulus-evoked fluorescence signals in the retina. *Pflugers Arch 457:1393–1414.*
- Fox DA, Poblenz AT, He L, Harris JB, Medrano CJ (2003) Pharmacological strategies to block rod photoreceptor apoptosis caused by calcium overload: a mechanistic target-site approach to neuroprotection. *Eur J Ophthalmol. 13:S44–S56.*
- Fried RC, Blaustein MP (1978) Retrieval and recycling of synaptic vesicle membrane in pinched-off nerve terminals (synaptosomes). *J Cell Biol 78:685–700.*
- Fuchs PA (2005). Time and intensity coding at the hair cell's ribbon synapse. *J Physiol 566:7-12.*
- Ghosh KK, Bujan S, Haverkamp S, Feigenspan A, Wässle H (2004). Types of bipolar cells in the mouse retina. *J Comp Neurol 469:70–82.*
- Giner D, Lopez I, Villanueva J, Torres V, Viniegra S, and Gutierrez L M (2007) Vesicle movements are governed by the size and dynamics of F-actin cytoskeletal structures in bovine chromaffin cells. *Neuroscience 146, 659-669.*
- Glowatzki E., Fuchs P. (2002). Transmitter release at the hair cell ribbon synapse. Nat. Neurosci. *5 147–154.*
- Gray EG. Microtubules in synapses of the retina. *J Neurocytol (1976).5:361–370.*
- Gudlur A., Zhou Y., Hogan P. G. (2013). STIM–ORAI interactions that control the CRAC channel. Curr. Top. Membr. *71 33–58.*
- Haeseleer F., Imanishi Y., Maeda T., Possin D. E., Maeda A., Lee A., et al. (2004). Essential role of Ca2+-binding protein 4, a Cav1.4 channel regulator, in photoreceptor synaptic function. *Nat. Neurosci. 7 1079–1087 10.1038/nn1320*

- Hamer RD, Nicholas SC, Tranchina D, Lamb TD, Jarvinen JL (2005). Toward a unified model of vertebrate rod phototransduction. *Vis Neurosci 22: 417-436.*
- Hara MR, Snyder SH (2007) Cell signaling and neuronal death. *Annu Rev Pharmacol Toxicol 47:117–141.*
- Haverkamp S, Specht D, Majumdar S, Zaidi KF, Brandstätter JH, Wasco W, Wässle H, tom Dieck S (2008). Type 4 OFF cone bipolar cells of the mouse retina express calsenilin and contact cones as well as rods. *J Comp Neurol 507:1087-1101.*
- Heidelberger R, Thoreson WB, and Witkovsky P (2005). Synaptic transmission at retinal ribbon synapses. *Prog Retin Eye Res 24: 682-720.*
- Hemara-Wahanui A, Berjukow S, Hope CI, Dearden PK, Wu SB, Wilson-Wheeler J, Sharp DM, Lundon-Treweek P, Clover GM, Hoda JC, Striessnig J, Marksteiner R, Hering S, Maw MA (2005) A CACNA1F mutation identified in an X-linked retinal disorder shifts the voltage dependence of Cav1.4 channel activation. *Proc Natl Acad Sci USA.102:7553–7558.*
- Heuser J, Lennon AM (1973) Morphological evidence for exocytosis of acetylcholine during formation of synaptosomes from Torpedo electric organ. *J Physiol 1973; 233:39P–41P.*
- Hirano AA, Brandstätter JH, Morgans CW, Brecha NC (2011). SNAP25 expression in mammalian retinal horizontal cells. *J Comp Neurol 519: 972-88.*
- Hoda JC, Zaghetto F, Koschak A, Striessnig J (2005) Congenital stationary night blindness type 2 mutations S229P, G369D, L1068P, and W1440X alter channel gating or functional expression of Ca(v)1.4 Ltype Ca2+ channels. *J Neurosci 25:252–259.*
- Hoda JC, Zaghetto F, Singh A, Koschak A, Striessnig J (2006) Effects of congenital stationary night blindness type 2 mutations R508Q and L1364H on Cav1.4 L-type Ca2+ channel function an expression. *J Neurochem 96:1648–1658*

- Jackman SL, Choi SY, Thoreson WB, Rabl K, Bartoletti TM, Kramer RH (2009): Role of the synaptic ribbon in transmitting the cone light response. *Nature Neurosci. 12:303–310.*
- Johnson J, Tian N, Caywood MS, Reimer RJ, Edwards RH, Copenhagen DR. Vesicular neurotransmitter transporter expression in developing postnatal rodent retina: GABA and glycine precede glutamate. *J Neurosci. 2003a;23:518–529*
- Jokusch WJ, Praefcke GJ, McMahon HT, Lagnado L (2005): Clathrin-dependent and clathrin-independent retrieval of synaptic vesicles in retinal bipolar cells. *Neuron 46:869–878.*
- Juusola M, French AS, Uusitalo RO, Weckstrom M. (1996) Information processing by graded-potential transmission through tonically active synapses. *Trends Neurosci 19:292–297.*
- Influence of the b2-Subunit of L-Type Voltage-Gated Cav Channels on the Structural and Functional Development of Photoreceptor Ribbon Synapses (2015) Rashmi Katiyar, Petra Weissgerber, Elisabeth Roth, Janka Dörr, Vithiyanjali Sothilingam, Marina Garcia Garrido, Susanne C. Beck, Mathias W. Seeliger, Andreas Beck, Frank Schmitz, and Veit Flockerzi. *Invest Ophthalmol Vis Sci. 56:2312–2324.*
- Keifer J, Vyas D, Houk JC (1992) Sulforhodamine labelling of neural circuits engaged in motor pattern generation in the in vitro turtle brainstemcerebellum. *J Neurosci 12:3187–3199.*
- Kiel C, Vogt A, Campagna A, Chatr-aryamontri A, Swiatek-de Lange M, Beer M, Bolz S, Mack AF, Kinkl N, Cesareni G, Serrano L, Ueffing M (2011). Structural and functional protein network analyses predict novel signalling functions for rhodopsin. *Mol Syst Biol 7:551.*
- Kirchhausen T, Macia E, Pelish HE (2008) Use of dynasore, the small molecule inhibitor of dynamin, in the regulation of endocytosis. *Methods Enzymol 488:77–93.*

- Khimich D, Pujol R, tom Dieck S, Egner A, Gundelfinger ED, Moser T. (2005). Hair cell synaptic plasticity. *Biochem Soc Transactions 33:1345-9*
- Krizaj D., Bao I. X., Schmitz Y., Witkovsky P., Copenhagen D. R. (1999). Caffeine-sensitive stores regulate synaptic transmission from retinal rod photoreceptors. J. Neurosci. *19 7249–726*
- Krizaj D. (2003). Properties of exocytic response in vertebrate photoreceptors. J. Neurophysiol. *90 218–225*
- Krizaj D, Liu X, Copenhagen DR (2004) Expression of calcium transporters in the retina of the tiger salamander (Ambystoma tigrinum). *J Comp Neurol 475:463–480.*
- Kuba K (1994) Ca^{2+} -induced Ca^{2+} release in neurons. *Jpn. J. Physiol. 44,613-650*
- Kwok MC, Holopainen JM, Molday LL, Foster LJ, Molday RS (2008). Proteomics of photoreceptor outer segments identifies a subset of SNARE and Rab proteins implicated in membrane vesicle trafficking and fusion. *Mol Cell Proteomics 7:1053–1066.*
- Lelli A., Perin P., Martini M., Ciubotaru CD., Prigioni I., Rossi ML., and mammano F. (2003) Presynaptic Calcium Stores Modulate Afferent Release in Vestibular Hair Cells. *J Neurosci. 23(17) 6894-6903*
- Lenzi D, von Gersdorff H. (2001). Structure suggests function: the case for synaptic ribbons as exocytotic nanomachines. *Bioessays 23 831–840 10.1002/bies.1118*
- Lewis R. S. (2011). Store-operated calcium channels: new perspectives on mechanism and function. *Cold Spring Harb. Perspect. Biol.* 3 a003970 .
- Liang Y, Fotiadis D, Filipek S, Saperstein DA, Palczewski K, Engel A (2003). Organisation of the G protein-coupled receptors rhodopsin and opsin in native membranes. J Biol Chem 278: 21655–21662.
- Libby R. T., Lavallee C. R., Balkema G. W., Brunken W. J., Hunter D. D. (1999). Disruption of laminin beta2 chain production causes alterations in morphology and function in the CNS. *J. Neurosci. 19 9399–9411*

- Lichtman JW, Wilkinson RS, Rich MM (1985) Multiple innervation of tonic endplates revealed by activity-dependent uptake of fluorescent probes. *Nature 314:357–359.*
- Liu X., Kerov V., Haeseleer F., Majumder A., Artemyev N., Baker S. A., et al. (2013). Dysregulation of Cav1.4 channels disrupt the maturation of photoreceptor synaptic ribbons in congenital stationary night blindness type 2. *Channels* 24 7
- LoGiudice L, Matthews G (2007): Endocytosis at ribbon synapses. *Traffic 8:1123–1128.*
- LoGiudice L, Sterling P, Matthews G. Mobility and turnover of vesicles at the synaptic ribbon (2008). *J Neurosci. 28:3150–8.*
- Richard N. Lolley, Rehwa H. Lee,David G. Chase, and Elisabeth Racz (1986) Rod Photoreceptor Cells Dissociated From Mature Mice Retinas. *IVOS Vol. 27/3*
- Macia E, Ehrlich M, Massol R, Boucrot E, Brunner C, Kirchhausen T (2006) Dynasore, a cell-permeable inhibitor of dynamin. *Dev Cell 10:839–850.*
- MacLeish PR, Townes-Anderson E. (1988). Growth and synapse formation among major classes of adult salamander retinal neurons in-vitro. *Neuron 1: 751–760.*
- Masland RH (2001). The fundamental plan of the retina. *Nat Neurosci 4: 877-86.*
- Matthew,G., and Fuchs,P.(2010) The diverse roles of ribbon synpses in sensory neurotransmission. *Nat. Rev.Neurosci.11.812-822*
- Mercer A. J., Chen M., Thoreson W. B. (2011a). Lateral mobility of presynaptic L-type calcium channels at photoreceptor ribbon synapses. *J*. Neurosci. *31 4397–4406.*
- Mercer A. J., Rabl K., Riccardi G. E., Brecha N. C., Stella S. L., Jr., Thoreson W. B. (2011b). Location of release sites and calcium-activated chloride channels relative to calcium channels at the photoreceptor ribbon synapse. *J. Neurophysiol. 105 321–335.*

- Mercer AJ, Thoreson WB (2011): The dynamic architecture of photoreceptor ribbon synapses: cytoskeletal, extracellular matrix, and intramembrane proteins. *Vis Neurosci 28:453– 471.*
- Mercurio AM, Holtzman E (1982) Smooth endoplasmic reticulum and other agranular reticulum in frog retinal photoreceptors. *J Neurocytol 11:263–293.*
- Midorikawa M, Tsukamoto Y, Berglund K, Ishii M, Tachibana M (2007): Different roles of ribbon-associated and ribbon-free active zones in retinal bipolar cells. *Nat Neurosci 10:1268 –1276*
- Morgans CW (2000). Neurotransmitter release at ribbon synapses in the retina. *Immunol Cell Biol 78: 442-44690.*
- Morgans C. W., Bayley P. R., Oesch N., Ren G., Akileswaran L., Taylor W. R. (2005). Photoreceptor calcium channels: insight from night blindness. *Vis. Neurosci.* 22 561–568.
- Morgans JL, Dhingra A, Vardi N, Wong RO (2006). Axons and dendries originate from neuroepithelial like processes of retinal biploar cells. *Nat Neurosci. 9 : 85-92*
- Moser T, Brandt A, Lysakowski A (2006): Hair cell ribbon synapses. *Cell Tissue Res 326:347–359.*
- Nickell S, Park PS, Baumeister W, Palczewski K (2007). Three dimensional architecture of murine rod outer segments determined by cryoelectron tomography. *J Cell Biol 177: 917–25*.
- Nimmerjahn A, Kirchhoff F, Kerr JN, Helmchen F (2004) Sulforhodamine101 as a specific marker of astroglia in the neocortex in vivo. *Nat Methods1:31–37.*
- Nishimune H., Numata T., Chen J., Aoki Y., Wang Y., Starr M. P., et al. (2012). Active zone protein bassoon co-localizes with presynaptic calcium channels, modifies channel function, and recovers from aging related loss by exercise. *PLoS ONE 7:e38029 10.1371/journal.pone.0038029*
- Nishimune H., Sanes J. R., Carlson S. S. (2004). A synaptic laminin–calcium channel interaction organizes active zones in motor nerve terminals. *Nature 432 580–587 10.1038/nature03112*

- Nouvian R, Beutner D, Parsons TD, Moser T (2006). Structure and function of the hair cell ribbon synapse. *J Membr Biol 209: 153-65.*
- Paillart C, Li J, Matthews G, Sterling P (2003): Endocytosis and vesicle recycling at a ribbon synapse. *J Neurosci 23:4092– 4099.*
- Pang JJ, Abd-El-Barr MM, Gao F, Bramblett DE, Paul DL, Wu SM (2007). Relative contributions of rod and cone bipolar cell inputs to AII amacrine cell light responses in the mouse retina. *J Physiol 580: 397-410.*
- Pappas GD and Waxman SG (1972). Synaptic fine structure-morphological correlates of chemical and electronic transmission
- Parekh A. B. (2011). Decoding cytoplasmic Ca^{2+} oscillations. *Trends Biochem. Sci. 36 78–87.*
- Parekh AB., Putney JW Jr (2005). Store-operated calcium channels. *Physiol. Rev. 85, 757–810*
- Parsons TD, Sterling P (2003). Synaptic ribbon. Conveyor belt or safety belt? *Neuron 37: 379-382.*
- Pelassa I, Zhao C, Pasche M, Odermatt B, Lagnado L (2014) Synaptic vesicles are primed for fast clathrin-mediated endocytosis at the ribbon synapse. *Front Mol Neurosci 7: 91.*
- Peng Y. W., Sharp A. H., Snyder S. H., Yau K. W. (1991). Localization of the inositol 1,4,5-trisphosphate receptor in synaptic terminals in the vertebrate retina. *Neuron 6 525–531.*
- Penner R1, Neher E (1988) The role of calcium in stimulus-secretion coupling in excitable and non-excitable cells. *J Exp Biol.139:329-45*
- Picaud S, Hicks D, Forster V, Sahel J, Dreyfus H (1998)a. Adult human retinal neurons in culture: physiology of horizontal cells. *Invest Ophthalmol Vis Sci 39: 2637-2648.*
- Picaud S, Pattnaik B, Hicks D, Forster V, Fontaine V, Sahel J, Dreyfus H (1998)b.GABAA and GABAC receptors in adult porcine cones: evidence from a photoreceptor–glia co-culture model. *J Physiol. 513: 33-42.*

- Pierantoni, R.L., McCann, G.D. (1981). A quantitative study on synaptic ribbons in the photoreceptors of turtle and frog. In: Borsellino, A., Cervetto, L. (Eds.), Photoreceptors. *Plenum Press, New York, pp. 255–283.*
- Prescott ED, Zenisek D (2005). Recent progress towards understanding the synaptic ribbon. *Curr Opin Neurobiol 15: 431-6.*
- Purves, D., Augustine, G. J., Fitzpatrick, D., Katz, L. C., La Mantia, A. S., McNamara,J. O and Williams, SM(2001). Neuroscience. Second edition.
- Rao-Mirotznik R, Buchsbaum G, Sterling P (1998). Transmitter concentration at a three-dimensional synapse. *J Neurophysiol; 80:3163–3172.*
- Raviola E, Gilula NB. Intramembrane organization of specialized contacts in the outer plexiform layer of the retina. *J Cell Biol. 1975; 75:192–222.*
- Rea R, Li J, Dharia A, Levitan ES, Sterling P, Kramer RH (2004): Streamlined synaptic vesicle cycle in cone photoreceptor terminals. *Neuron 41:755–766*
- Rieke F., Schwartz E. A. (1996). Asynchronous transmitter release: control of exocytosis and endocytosis at the salamander rod synapse. *J. Physiol.* 493 1–8
- Royle SJ, Lagnado L. Endocytosis at the synaptic terminal. *J Physiol (Lond) 2003; 553:345–355.*
- Schacher S, Holtzman E, Hood DC (1976) Synaptic activity of frog retinal photoreceptors. A peroxidase uptake study. *J Cell Biol 70:178–192.*
- Schmitz F (2009). The making of synaptic ribbons: how they are built and what they do. *Neuroscientist 15: 611-24.*
- Schmitz F, Bechmann M, Drenckhahn D (1996). Purification of synaptic ribbons, structural components of the photoreceptor active zone complex. *J Neurosci 16: 7109-7116.*
- Schmitz F, Königstorfer A, Südhof TC (2000). RIBEYE, a component of synaptic ribbons: a protein's journey through evolution provides insight into synaptic ribbon function. *Neuron 28: 857-72.*
- Schmitz F, Natarajan S, Venkatesan JK, Wahl S, Schwarz K, Grabner CP (2012): EF-hand – mediated Ca^{2+}- and cGMP-signaling in photoreceptor presynaptic terminals. *Front Mol Neurosci 5:26.*

- Schmitz Y, Witkovsky P (1997)Dependence of photoreceptor glutamate release on a dihydropyridinesensitive calcium channel. *Neuroscience 78:1209–1216. [*
- Schweizer FE, Ryan TA (2006): The synaptic vesicle: cycle of exocytosis and endocytosis. *Curr Opin Neurobiol 16(3):298-304.*
- Shaltiel L., Paparizos C., Fenske S., Hassan S., Gruner C., Rötzer K., et al. (2012). Complex regulation of voltage-dependent activation and inactivation properties of retinal voltage-gated Cav1.4 L-type Ca^{2+} channels by Ca^{2+}-binding protein 4 (CaBP4). *J. Biol. Chem. 287 36312–36321.*
- Sharma AK, Rohrer B (2004) Calcium-induced calpain mediates apoptosis via caspase-3 in a mouse photoreceptor cell line. *J Biol Chem. 279:35564–35572.*
- Sheng Z, Choi SY, Dharia A, Li J, Sterling P, Kramer RH (2007): Synaptic Ca2+ in darkness is lower in rods than cones causing slower tonic release of vesicles. *J Neurosci 9; 27(19):5033-42.*
- Sherry DM, Wang MM, Frishman LJ. Differential distribution of vesicle associated membrane protein isoforms in the mouse retina. *Mol Vis. 2003b; 9:673–688.*
- Shoshan-Barmatz, V., Orr, I., Martin, C. & Vardi, N. (2005) Novel ryanodinebinding properties in mammalian retina. *Int. J. Biochem. Cell. Biol., 37,1681–1695.*
- Singer JH (2007). Multivesicular release and saturation of glutamatergic signalling at retinal ribbon synapses. *J Physiol 580: 23- 9.*
- Singer J. H., Lassová L., Vardi N., Singer J. S. (2004). Coordinated multivesicular release at a mammalian ribbon synapse. Nat. Neurosci. *7 826–833.*
- Singh,A., Hamedinger,D., Hoda,J.C., Gebhart,M., Koschak,A., Romanin,C.,and Striessnig,J.(2006). C-terminal modulator controls Ca^{2+} -dependent gating of Ca(v)1.4L-type Ca^{2+} channels. *Nat. Neurosci.9, 1108-1116.*
- Sjöstrand FS (1953): The ultrastructure of the outer segments of rods and cones of the eye as revealed by the electron microscope. *J Cell Physiol 42(1):15-44.*

- Smith SM, Renden R, von Gersdorff H (2008): Synaptic vesicle endocytosis: fast and slow modes of membrane retrieval. *Trends Neurosci 31:559 –568.*
- Snellman J, Mehta B, Babai N, Bartoletti TM, Akmentin W, Francis A, Matthews G, Thoreson WB, Zenisek D (2011): Acute destruction of the synaptic ribbon reveals a role for the ribbon in vesicle priming. *Nature Neurosci 14:1135–1141.*
- Soboloff J., Rothberg B. S., Madesh M., Gill D. L. (2012). STIM proteins: dynamic calcium signal transducers. *Nat. Rev. Mol. Cell Biol. 13 549–565*
- Ernest C. Steele, Jr.,1 Xiaoming Chen,1 P. Michael Iuvone,2 and Peter R. MacLeish1(2005) Imaging of Ca^{2+} Dynamics Within the Presynaptic Terminals of Salamander Rod Photoreceptors. *J. Neurophysiol 94:4544-4553*
- Sterling P (1998): The retina. In The Synaptic Organization of the Brain. Fourth Edition, G.Shepherd, ed. *New York: Oxford University Press*
- Sterling P, Matthews G (2005). Structure and function of ribbon synapses. *Trends Neurosci 28: 20-9.*
- Striessnig J., Bolz H. J., Koschak A. (2010). Channelopathies in CaV1.1, CaV1.3, and CaV1.4 voltage-gated L-type Ca^{2+}-channels. *Pflügers Arch. 460 361–374.*
- Suryanarayanan A., Slaughter M. M. (2006). Synaptic transmission mediated by internal calcium stores in rod photoreceptors. *J. Neurosci. 26 1759–1766.*
- Szikra T., Cusato K., Thoreson W. B., Barabas P., Bartoletti T. M., Krizaj D. (2008). Depletion of calcium stores regulates calcium influx and signal transmission in rod photoreceptors. *J. Physiol. 586 4859–4875.*
- Takahashi N, Kishimoto T, Nemoto T, Kadowaki T, Kasai H (2002) Fusion pore dynamics and insulin granule exocytosis in the pancreatic islet. *Science 297:1349 –1352.*
- Teng H, Cole JC, Roberts RL, Wilkinson RS (1999) Endocytic active zones:hot spots for endocytosis in vertebrate neuromuscular terminals. *J Neurosci 19:4855– 4866.*

- Thoreson WB (2007): Kinetics of synaptic transmission at ribbon synapses of rods and cones. *Mol Neurobiol 36(3):205-23.*
- Thoreson WB, Nitzan R, Miller RF(1997) Reducing extracellular Cl− suppresses dihydropyridinesensitive Ca^{2+} currents and synaptic transmission in amphibian photoreceptors. *J Neurophysiol 77:2175–2190.*
- Thoreson WB, Rabl K, Townes-Anderson E, Heidelberger R (2004): A highly Ca2+-sensitive pool of vesicles contributes to linearity at the rod photoreceptor ribbon synapse. *Neuron* 27; 42(4):595-605.
- tom Dieck S, Altrock WD, Kessels MM, Qualmann B, Regus H, Brauner D, Fejtová A, Bracko O, Gundelfinger ED, Brandstätter JH (2005). Molecular dissection of the photoreceptor ribbon synapse: physical interaction of Bassoon and RIBEYE is essential for the assembly of the ribbon complex. *J Cell Biol 168: 825-836.*
- tom Dieck S, Brandstätter JH (2006) : Ribbon synapses of the retina. *Cell Tissue Res 326: 339-46.*
- Townes-Anderson E, MacLeish PR, Raviola E. Rod cells dissociated from mature salamander retina: ultrastructure and uptake of horseradish peroxidase(1985). *J Cell Biol.100(1):175-88*
- Tse FW, Tse A, Hille, Horstmann H and Almers W (1997) Local Ca^{2+} release from internal stores controls exocytosis in pituitary gonadotrophs. *Neuron 18, 121-132*
- Tymianski M., Bernstein G.M., Abdel-Hamid K.M. , Sattler R., Velumian A., Carien P.L. , Razavi H and Jones O.T. (1996) A noval use for a carbodiimide compound for the fixation of fluorescent and non-fluorescent calcium indicators *in situ* following physiological experiments. *Cell Calcium 175-183*
- Ungar F, Irene P, Letizia J, and Holtzman E (1984) Uptake of Calcium by the Endoplasmic Reticulum Frog Photoreceptor. *The Jounal of Cell Bio. 1645-55*
- Van Hook M.J. and Thoreson WB (2012) Rapid synaptic Vesicle Endocytosis in Cone Photoreceptors of Salamander Retina. *J Neurosci. 18112-18123*

- Verkhratsky A. (2005). Physiology and pathophysiology of the calcium store in the endoplasmic reticulum of neurons. *Physiol. Rev. 85 201–279*
- Vígh J, Bánvölgyi T, Wilhelm M (2000). Amacrine cells of the anuran retina: morphology, chemical neuroanatomy, and physiology. *Microsc Res Tech 50:373-83.*
- Von Gersdorff H, (2001). Synaptic ribbons: versatile signal transducers. Neuron 29: 7-10.
- Von Gersdorff H, Vardi E, Matthews G, Sterling P (1996). Evidence that vesicles on the synaptic ribbon of retinal bipolar neurons can be rapidly released. *Neuron 16: 1221-7.*
- Wahl S, Katiyar R, Schmitz F (2013) A Local Preiactive Zone Endocytic Machinery at Photoreceptor Synapses in Close Vicinity to Synaptic Ribbons. *J Neurosci 33: 10278-10300*
- Wässle (2004): Parallel processing in the mammalian retina. Nature reviews Neuroscience 5(10):747-57.
- Wenda Shurety, Nancy L. Stewart, and Jennifer L. Stow (1998) Fluid-Phase Markers in the Basolateral Endocytic Pathway Accumulate in Response to the Actin Assembly-promoting Drug Jasplakinolide. *Mol Biol Cell. Apr; 9(4): 957–975*
- Wilkinson MF, Barnes S (1996) The dihydropyridine-sensitive calcium channel subtype in cone photoreceptors. *J Gen Physiol 197:621–630*
- Woodruff ML, Wang Z, Chung HY, Redmond TM, Fain GL, Lem J (2003) Spontaneous activity of opsin apoprotein is a cause of Leber congenital amaurosis. *Nat Genet. 35:158–164.*
- Wu LG, Ryan TA, Lagnado L (2007): Modes of vesicle retrieval at ribbon synapses, calyx-type synapses and small central synapses. *J Neurosci* 27: 11793–11802.
- Wycisk K. A., Budde B., Feil S., Skosyrski S., Buzzi F., Neidhardt J., et al. (2006). Structural and functional abnormalities of retinal ribbon synapses due to cacna2d4 mutations. *Invest. Ophthalmol. Vis. Sci.* 47 3523–3530.

- Young RW (1967). The renewal of photoreceptor cell outer segments. J. Cell Biol. 33: 61–72.
- Young RW, Bok D (1969). Participation of the retinal pigment epithelium in the rod outer segment renewal process. J. Cell Biol 42: 392–403.
- Zenisek D, Steyer JA, Almers W (2000): Transport, capture and exocytosis of single synaptic vesicles at active zones. *Nature* 105:4922– 4927.
- Zenisek D. (2008). Vesicle association and exocytosis at ribbon and extraribbon sites in retinal bipolar cell presynaptic terminals. *Proc. Natl. Acad. Sci. U.S.A.* 105 4922–4927.
- Zanazzi G, Matthews G (2009): The molecular architecture of ribbon presynaptic terminals. *Mol Neurobiol* 39(2):130-48.
- Zenisek D, Steyer JA, Almers W (2000): Transport, capture and exocytosis of single synaptic vesicles at active zones. *Nature* 105:4922– 4927.

6. List of Abbreviations

1^{st}	First
2^{nd}	Second
3^{rd}	Third
µg	microgram
µl	microliter
µM	micromolar.
Ab	Antibody
bc	Bipolar cell
BSA	Bovine serum albumin
°C	Celsius
Ca^{2+}	Calcium-ion
CICR	Calcium induce calcium release
C-terminal	Carboxy-terminal
Cy5	Cyanine5
DMEM	Dulbecco's Modified Eagle's medium
EDAC	1-ethyl-3(3-dimethylaminoproply)-carbodiimide
EGF	External growth factor
EGTA	ethylene glycol tetraacetic acid
EM	Electron Microscopy
ER	Endoplasmic recticulum

ECS	Extracellular solution
FCS	Fetal calf serum
FM1-43	N-(3-Triethylammoniumpropyl)-4-(4-(Dibutylamino).
GCL	Ganglion cell layer
hc	Horizontal cells
Hrs	hours
INL	Inner nuclear layer
IPL	Inner plexiform layer
IS	Inner Segment
kDa	Kilo Dalton
LA	Live acquisation
LCS	Low Calcium solution
mbar	millibar
mg	miligram
min	minutes
ml	mililiter
mono	monoclonal
MW	Molecular weight
ng	nanogram
nm	nanometer

NPG	N-propyl gallate
OPL	Outer plexiform layer
ONL	Outer nuclear layer
OS	Outer segments
Pa	Pascal
PBS	Phosphate Buffered Saline
PFA	Paraformaldehyde
Poly	polyclonal
PR	Photoreceptor
RPE	Retinal pigment epithelium
RRP	readily releasable pool
Pr	Presynaptic terminal
Po	postsynaptic dendrite
Pm	extra synaptic plasma membrane
RB	Rod bipolar cell
Ribeye-FP	Ribeye fluorescent protein
ROI	Region of interest
RS	Resting solution
RT	Room temperature
SERCA	Sarcoplasmic/endoplasmic reticulum calcium ATPase

SR	Synaptic ribbon
SR101	sulforhodamine
SOC	Store operated channels
SOCE	Store operated channels entry
SR-SIM	Super-resolution structured illumination microscopy
SRP	Slowly releasable pool
SV	Synaptic vesicles
SV2	Synaptic vesicle protein 2
TIRF	Total Internal Reflection Fluorescence Microscopy
VGCC	Voltage gated Calcium Channel

7. List of figures

Figure 1:	Diagrammatic view of the adult human eye.	16
Figure 2:	(left) Cross-section through an immunolabeled mature mouse transgenic retina showing lamination of cell bodies and synaptic terminals. (right) Schematic representation of main retinal neurons.	19
Figure 3:	(A) Schematic diagramme of photoreceptor ribbon synapses. (B) Representation of molecular structure of retinal ribbon synapse.	23
Figure 4:	Ultrastucture of photoreceptor ribbon synapses.	25
Figure 5:	Schematic structure of RIBEYE	26
Figure 6:	Isolation of mouse retina.	42
Figure 7:	Pronase dissociated retinal cells.	52
Figure 8:	Pronase treated retinal cells.	53
Figure 9:	Papain treated retinal cells.	54
Figure 10:	Ultrastructure of papain isolated rod photoreceptors.	55
Figure 11:	Immunofluorescence labeling of acutely dissociated rod photoreceptor by pronase.	57
Figure 12:	Immunofluorescence labeling of acutely dissociated rod photoreceptor by pronase.	58
Figure 13:	Immunofluorescence labeling of acutely dissociated rod photoreceptor by pronase.	59
Figure 14:	Immunofluorescence labeling of acutely dissociated rod photoreceptor by pronase.	60
Figure 15:	Immunofluorescence labeling of acutely dissociated rod photoreceptor by pronase.	61

Figure 16:	Immunofluorescence labeling of acutely dissociated rod photoreceptor by pronase.	62
Figure 17:	Dextran uptake assay in pronase treated rod photoreceptors.	63
Figure 18:	Immunofluorescence labeling of dextran loaded cells.	64
Figure 19:	Lysotracker uptake in rod photoreceptors obtained by pronase isolation method.	65
Figure 20:	Lysotracker uptake in sodium azide treated rod photoreceptors obtained by pronase isolation method.	66
Figure 21:	Long incubation of sulforhodamine (SR101) in papain treated rod photoreceptors.	67
Figure 22:	Short pulse of sulforhodamine (SR101) in papain treated rod photoreceptors.	67
Figure 23:	Ribbon-associated endocytosis and localization of the SR101.	68
Figure 24:	Localization of Dynamin in synaptic terminal of isolated rod photoreceptors.	69
Figure 25:	Sulforhodamin uptake assay in Tulp1 Knockout mice and in litte control mice.	70
Figure 26:	Endocytosis in papain treated rod photoreceptors.	72
Figure 27:	Focal endocytic uptake of FM1-43.	73
Figure 28:	FM1-43 uptake in electroporated retina.	74
Figure 29:	Localization of endocytosed vesicles in papain treated rod photoreceptors.	75
Figure 30:	Fura-2AM measurement of papain treated rod photoreceptors.	76
Figure 31:	Ratiometric Ca^{2+} imaging from Fura-2AM loaded synaptic terminal isolated rod photoreceptors of wild type and ecβ2 KO.	77
Figure 32:	Localization of endogenous RIBEYE with transgenically exp RIBEYE with RFP- tag in papain treated rod photoreceptors.	78

Figure 33: Fluo-4Am uptake in papain treated rod photoreceptors. 79

Figure 34: Characterization of Fluo-4Am labeled structure in papain treated ro 80
photoreceptors.

Figure 35: Characterization of Fluo-4Am labeled structure in papain treated 81
rod photoreceptors.

Figure 36: Characterization of Fluo-4Am labeled structure in papain treated 81
rod photoreceptors.

Figure 37: Characterization of Fluo-4Am labeled structure in papain treated 82
rod photoreceptors.

Figure 38: Characterization of Fluo-4Am labeled structure in papain treated 83
rod photoreceptors.

Figure 39: Fluo4AM measurement of papain treated rod photoreceptors is 84
from Ribeye-RFP mouse retina.

Figure 40: Depletion of Fluo-4AM hot spot and refilling. 85

Figure 41: Exocytosis measurements. 87

10.Publications

1. Influence of the β2-subunit of L-type voltage-gated Cav channels on the structural and functional development of photoreceptor ribbon synapses.
   Katiyar R*, Weissgerber P*, Roth E*, Dörr J, Sothilingam V, Garcia Garrido M, Beck SC, Seeliger M, Beck A, Schmitz F§, Flockerzi V§.
   Invest Ophthalmol Vis Sci. 2015
   (*,§ equal contributions)

2. ArfGAP3 is a component of the photoreceptor synaptic ribbon complex and forms a NAD(H)-regulated, redox-sensitive complex with RIBEYE that is important for endocytosis.
   Mayur Dembla, Silke Wahl*, **Rashmi Katiyar***, and Frank Schmitz
   The Journal of Neuroscience,April 9, 2014.
   (* equal contributions)

3. A Local, Periactive Zone Endocytic Machinery at Photoreceptor Synapses in Close Vicinity to Synaptic Ribbons.
   Silke Wahl, **Rashmi Katiyar** and Frank Schmitz
   The Journal of Neuroscience, 2013 June 19.

4. The RP14 diseace protein Tulp1 is essential for peri-active zone endocytosis in photoreceptor synapses. (in submission)
   Silke Wahl*, Venkat Giri Magupalli*, Mayur Dembla$, **Rashmi Katiyar$**, Louise Koblitz, Karin Schwarz, Kannan Alpadi, Elmar Krauser, Jens Rettig, Ching-Hwa Sung, Andy Golderg and Frank Schmitz
   (*,$ equal contribution)

5. Synaptic trafficking in mouse rod photoreceptor is prominently regulated by

presynaptic Ca^{2+}-stores. (In preparation)

Rashmi Katiyar[*], Ulf Matti[*], Andreas Beck, Karin Schwarz and Frank Schmitz